KONINKLIJK NEDERLANDS METEOROLOGISCH INSTITUUT

MEDEDELINGEN EN VERHANDELINGEN

64

Dr H. M. DE JONG

THEORETICAL ASPECTS OF AERONAVIGATION AND ITS APPLICATION IN AVIATION METEOROLOGY

1956

STAATSDRUKKERIJ- EN UITGEVERIJBEDRIJF/'S-GRAVENHAGE

PUBLICATIENUMMER: KNMI 102-64

UDC: 551 . 509 . 317:
551 . 557:
629 . 13:

PREFACE

Problems of current interest, related to the navigation of ships in stationary fields of flow are discussed in this volume. Parts I, II, III and IV deal with theoretical investigations each concerned with a special type of navigation, as defined in part I. In part V the theory has been applied to the navigation of aircraft.

Under the title "Single heading and shortest time navigation", the parts I—IV were accepted as a doctor's thesis by the Philosophical Faculty of the University of Utrecht. Professor Dr. H. FREUDENTHAL acted as promotor; his interest in Dr. DE JONG's work is kindly acknowledged.

The remaining part is a summary of working methods, developed and applied by the author at Schiphol Airport. The close cooperation and the assistance of many authorities of the Royal Dutch Airlines, K.L.M., is highly appreciated. Special thanks are due to Mr. F. C. BIK, Captain of K.L.M., who with enthusiasm and ingenuity contributed to the development of various ideas.

Dr. W. BLEEKER, head of Scientific Research stimulated the study and discussed various phases of the project with the author.

The Director in Chief

C. J. WARNERS.

CONTENTS

PART I

GENERAL CONSIDERATIONS

Introduction

In this part a general treatment is presented of the motion of a ship in a stationary two-dimensional aero- or hydrodynamic field of flow. Properties of the motion are derived, which because of their navigational aspects form the basis of a special system of navigation, viz. aeronavigation.

Since many of these properties are of great practical interest both for navigation at sea and in the air the word ship will be used as a collective for all kinds of aircraft, ships, missiles etc.

Throughout the assumption is made that the internal forces (engines) are in equilibrium with the frictional and gravitational forces as well as all other forces operating on the ship so as to ensure a constant speed with respect to the surrounding medium. Furthermore it is assumed that the structure of the ship is such that the internal forces operate along the main axis of the ship.

With respect to the surrounding medium such a ship will move in the direction of the main axis. With respect to a fixed coordinate-system however the ship will deviate from the direction of the main axis and follow a course determined by the resultant motion of the ship and the flow.

In general the true velocity c of the ship surpasses the velocity of the flow, but the hypothetical case in which c is smaller than the velocity of the flow will not be excluded.

1. The stationary field of flow

The two-dimensional aerodynamic flow will be described in local, i.e. Eulerian, coordinates. At an arbitrary point P within the field of flow the intensity and direction of the flow are defined by the vector $\vec{u}$. The velocity components u_1 and u_2 are functions of the coordinates x_1 and x_2. So the equations for the stationary field of flow can be written:

$$u_1 = f(x_1, x_2),$$
$$u_2 = g(x_1, x_2)$$

where the functions f and g are arbitrary one-valued bounded functions of x_1 and x_2.

Depending on the properties of these functions singularities and discontinuities may exist in the flow. For instance any point, where f and g vanish simultaneously, may be a vortex point, a col, a source point etc. Unless stated otherwise the functions f and g are assumed to be continuous.

Because a vector is defined by direction and magnitude two sets of lines can be

introduced of equal vector direction and vector magnitude respectively, which together define the field of flow unambiguously. The lines of equal vector direction are called *isogones* or *isoklines* and the lines of equal vector magnitude *isotachs*.

In aeronavigation the isotachs are of special importance. The isotach $u = + \sqrt{f^2 + g^2} = c$, or $\frac{c}{u} = \varepsilon = 1$, where c is the true velocity of the ship and ε the velocity parameter, will be called the *limiting* isotach.

The limiting isotach devides the field of flow in a number of connected regions, in which the velocity of the flow is either greater or smaller than c. In stationary flow stream-lines and trajectories coincide. In general the flow will be neither non-divergent nor irrotational. If, however, the flow is non-divergent, then a stream-function ψ may be defined, such that

$$u_1 = \frac{\partial \psi}{\partial x_2}, \qquad u_2 = -\frac{\partial \psi}{\partial x_1}. \tag{I, 1}$$

The lines $\psi =$ constant represent the stream-lines of the flow.

If the flow is irrotational, then a velocity-potential φ may be introduced, such that

$$u_1 = \frac{\partial \varphi}{\partial x_1}, \qquad u_2 = \frac{\partial \varphi}{\partial x_2}. \tag{I, 2}$$

Finally, if the field is both non-divergent and irrotational, both the stream-function ψ and the velocity-potential φ exist.

Then

$$u_1 = \frac{\partial \psi}{\partial x_2} = \frac{\partial \varphi}{\partial x_1}, \qquad u_2 = -\frac{\partial \psi}{\partial x_1} = \frac{\partial \varphi}{\partial x_2}. \tag{I, 3}$$

These relations for ψ and φ are the differential equations of Cauchy-Riemann. Both ψ and φ satisfy the differential equation of Laplace:

$$\triangle \psi \equiv \frac{\partial^2 \psi}{\partial x_1^2} + \frac{\partial^2 \psi}{\partial x_2^2} = 0, \qquad \triangle \varphi \equiv \frac{\partial^2 \varphi}{\partial x_1^2} + \frac{\partial^2 \varphi}{\partial x_2^2} = 0. \tag{I, 4}$$

The lines $\psi =$ constant and the lines $\varphi =$ constant are perpendicular to each other.

2. The steering equations

When a ship moves in a field of flow, it will deviate from its proper course with respect to an observer in a fixed system, in other words, the axis of the ship does not coincide with the direction, in which it moves with respect to the fixed system. The motion of the ship with respect to the fixed system is given by the vector sum of the true velocity vector $\vec{c}$, which indicates direction and velocity c of the ship relative to the surrounding medium and the stream vector $\vec{u}$. The equations of motion of the ship with respect to this fixed system are:

$$w_1 = \frac{dx_1}{dt} = u_1 + c\cos\xi$$
$$w_2 = \frac{dx_2}{dt} = u_2 + c\sin\xi \qquad \text{(I, 5)}$$

or in vector notation: $\vec{w} = \vec{u} + \vec{c}$ (I, 6)

where $\vec{w}$ (w_1, w_2) is the speed vector of the ship with respect to the fixed system. ξ is the angle between the axis of the ship and the positive x_1-axis. This angle will be called the *heading*.

If the flow pattern is governed for instance by a deep cyclone, rotational fields of flow may be used as a first approximation of the real flow and in that case it is advisable to introduce polar coordinates.

The equations in polar coordinates r, α can be derived from the equations in rectangular coordinates by means of a polar transformation. It is, however, simpler to derive these equations directly by means of a vector diagram (fig. I, 1).

$$r\frac{d\alpha}{dt} = u_\alpha + c\sin(\xi - \alpha),$$
$$\frac{dr}{dt} = u_r + c\cos(\xi - \alpha). \qquad \text{(I, 7)}$$

The equations (I, 5) and (I, 6) uniquely determine a vector field for $\vec{w}$ except at the points where ξ is indefinite and at the points where $\vec{w}$ is a zero vector, i.e. at the points where simultaneously

$$u_1 + c\cos\xi = 0 \text{ and } u_2 + c\sin\xi = 0.$$

These points lie on the limiting isotach, for $u_1^2 + u_2^2 = u^2 = c^2$, or $\frac{c}{u} = \varepsilon = 1$ (u and c positive).

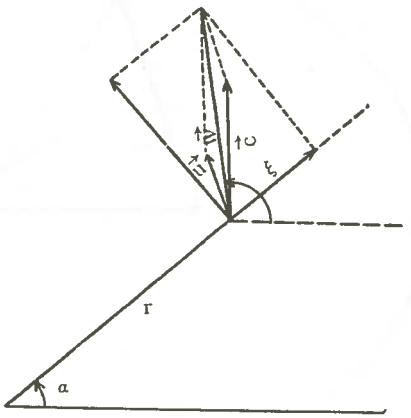

Fig. I, 1.

Points where $\vec{w}$ is either indefinite or a zero vector are singular points of the system.

Supposing the field of flow $\vec{u}$ is known, then, according to the equations I,5 or I,7 three main groups of problems may be distinguished:

1. If the heading ξ is given as a function of x_1 and x_2 the equations I,5 and I,7 may be integrated and the solutions $x_1 = x_1(t)$ and $x_2 = x_2(t)$ represent the trajectories along which the ship will travel with the given heading. For practical reasons the trajectories will be called *pressure-pattern trajectories*, particularly in view of the application to aerology where standard pressure-surface topographies determine the structure of the flow.
2. If on the other hand a curve is prescribed along which the ship has to be manoeuvred, the heading ξ can be derived from I,5 or I,7 at every point of the trajectory. In this sense the equations may be considered as *steering* equations. If along the curve

$$\frac{dx_2}{dx_1} = p\,(x_1, x_2),$$

$$\text{then} \quad \frac{dx_2}{dt} = p\,(x_1, x_2)\,\frac{dx_1}{dt}.$$

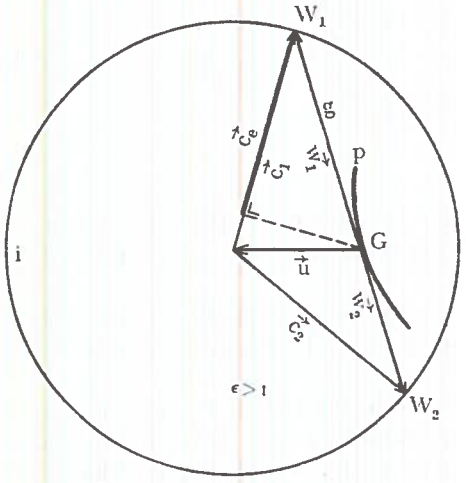

Fig. I, 2,a.

This relation yields a goniometric equation for ξ, which at any point is satisfied by two values of ξ (ξ may be imaginary). *If the values of ξ are real, the ship can be manoeuvred along the curve in two distinct ways.*

3. Finally it is possible that a functional relation exists between a beforehand unknown heading $\xi\ (x_1, x_2)$ and an unknown trajectory. Then by means of the equations I,5 or I,7 and this functional relation both heading and trajectory may be calculated.

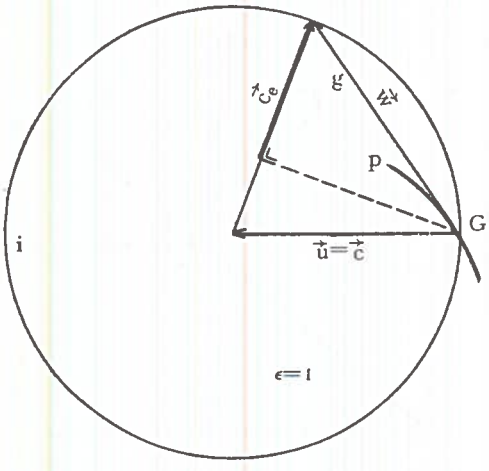

Fig. I, 2,b.

To this group of problems belongs the "variation problem of aeronavigation" This is the problem dealing with the pressure-pattern trajectories between two given points P and Q, for which the time of travel is an extreme.

Apart from these groups of problems other groups of problems arise, when the field of flow itself is unknown. For instance it may be required to let a ship

travel with a given heading along a prescribed trajectory and the problem will be to find out, what the structure of the field of flow must be to satisfy this requirement.

In part IV a detailed analysis of such a problem is given.

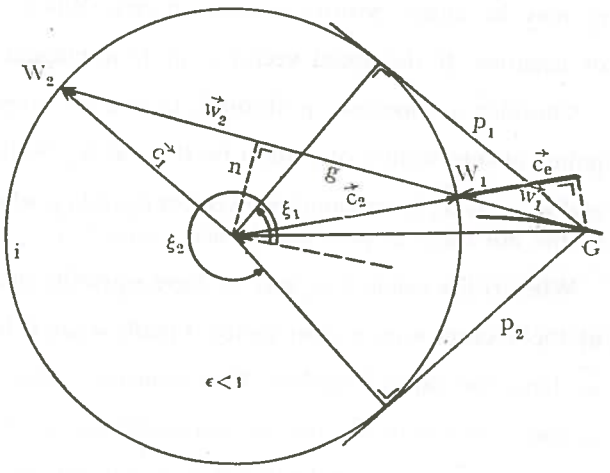

Fig. I, 2,c.

3. The indicatrix. Regions of limited and unlimited manoeuvrability

In an arbitrary field of flow there are limits to the manoeuvrability of a ship with a given true velocity c. In particular when this velocity is smaller than the velocity of the flow the ship cannot be directed along every prescribed curve.

In order to investigate what possibilities may occur the concept of the indicatrix of Carathéodory will be introduced. Let a circle i with radius c be drawn around the terminal point of the stream vector $\vec{u}$. Then the vector connecting the terminal point of $\vec{c}$ with the starting point of $\vec{u}$ is the sum vector $\vec{w}$, the speed vector of the ship with respect to the fixed system (fig. I, 2, *a*, *b*, *c*). The circle i with radius c will be called *indicatrix* and the associated starting point of the stream vector $\vec{u}$ the corresponding *base point G*. This nomenclature is justified because this circle can be shown to be the indicatrix of the variation problem of aeronavigation (cf. part III).

When $\varepsilon > 1$ the base point lies inside the indicatrix (fig. I, 2, a).
When $\varepsilon < 1$ the base point lies outside the indicatrix (fig. I, 2, c).
When $\varepsilon = 1$ the base point lies on the indicatrix (fig. I, 2, b).

Let the vector $\vec{u}$ be projected upon $\vec{c}$. Then the sum vector of $\vec{c}$ and the component of $\vec{u}$ along $\vec{c}$ will be called the *vector of the effective true velocity* $\vec{c}_e$.

The *effective true velocity* itself will be defined, not as the length of its vector, but by the relation:

$$c_e = c + \frac{1}{c}\vec{c} \,.\, \vec{u} = c + u_1 \cos\xi + u_2 \sin\xi \qquad \text{(I, 8)}$$

Thus the length of the vector $\vec{c}_e$ is equal to the absolute value of c_e.

It follows from fig. I, 2 that c_e is always positive, when $\varepsilon > 1$. If $\varepsilon = 1$, then

c_e may be either positive or equal to zero. When $\varepsilon < 1$, c_e may be either positive or negative. If the speed vector $\vec{w}$ at G is tangent to i, then $c_e = 0$.

Consider a trajectory p through G and its tangent g at G (fig. I, 2, c). Let the points of intersection of g and i be W_1 and W_2. With the tangent vectors $\vec{w}_1 = \overrightarrow{GW_1}$ and $\vec{w}_2 = \overrightarrow{GW_2}$ correspond two vectors $\vec{c}_1$ and $\vec{c}_2$, which are symmetrical with respect to the normal n of p at G (*symmetry property*).

When G lies inside i, $\vec{w}_1$ and $\vec{w}_2$ have opposite directions. When G lies on i, one of the vectors $\vec{w}$ is a zero vector. Finally when G lies outside i, the vectors $\vec{w}_1$ and $\vec{w}_2$ have the same direction. They coincide, when w is tangent to i. In this case $\vec{c}_1$ and $\vec{c}_2$ also coincide and are perpendicular to the speed vector $\vec{w}$. If $\vec{c}$ is made to rotate about the terminal point of $\vec{u}$, $\vec{w}$ will not always rotate through the complete angular interval $(0 - 2\pi)$. For if the base point lies outside the indicatrix, $\vec{w}$ can only rotate through an angle determined by the tangents from the base point to the indicatrix. The angle between these tangents will be called the *limiting angle*. The line elements coinciding with the extreme positions of the vector $\vec{w}$ will be called the *anomalous line elements*. From an arbitrary point P within the field of flow a ship can only move into the limiting angle; this point can be *reached* only from the opposite angle. At P the manoeuvrability is now said to be limited. Since the position of the base point with respect to the indicatrix depends only on the velocity parameter ε and since the lines $u =$ constant or, because of the constancy of c, the lines $\varepsilon =$ constant, represent the isotachs the following regions may be distinguished in the field of flow. In the regions, where $\varepsilon > 1$ the base point lies inside the indicatrix and the manoeuvrability is unlimited. In the regions where $\varepsilon < 1$ the base point lies outside the indicatrix and consequently the manoeuvrability will be limited. In the regions where $\varepsilon = 1$ the manoeuvrability is also limited. *Regions with $\varepsilon > 1$ are called regions of unlimited manoeuvrability. Regions with $\varepsilon \leqslant 1$ are called regions of limited manoeuvrability.*

Both regions $\varepsilon > 1$ and $\varepsilon < 1$ are bounded by the limiting isotach $\varepsilon = 1$, or by regions where $\varepsilon = 1$.

It follows that three different types of field of flow can now be defined. If in a field of flow ε is everywhere > 1, i.e., if the true velocity is everywhere greater than the velocity of the flow, then the manoeuvrability will be unlimited throughout the field. If on the other hand ε is everywhere either $= 1$ or < 1 or $\leqslant 1$, then the manoeuvrability will be limited throughout the field. If ε varies in the field between values > 1 and $\leqslant 1$, then the field will contain both regions of limited and regions of unlimited manoeuvrability.

At any point in the field of flow the anomalous line elements may be drawn and curves constructed, which at every point contain such a line element, in the same

way as stream-lines are constructed from the line elements along the stream direction. These *limiting curves* can be found by integration of the steering equation subject to the *condition that the effective true velocity* $c_e = 0$.

Line elements lying inside the limiting angle are to be called *regular* and those lying inside the supplementary angles *singular* line elements, according to C a r a t h é o d o r y. *Admissible* trajectories therefore only consist of regular or anomalous line elements.

In a region of unlimited manoeuvrability all curves are admissible trajectories because all line elements are regular. On the other hand in a region of limited manoeuvrability any arbitrary curve may consist of sections which are either admissible or inadmissible. Any such section is bounded by two successive tangent points of the curve with limiting curves, provided the tangent point is not a point of inflection on the curve. Limiting curves consist of anomalous line elements, except at the points where $\varepsilon = 1$, and are admissible trajectories.

Between the admissible trajectories in both regions $\varepsilon \leqslant 1$ and $\varepsilon > 1$ a gradual difference exists. For according to the theory of the indicatrix there are two ways of manoeuvring along any admissible trajectory. In regions of limited manoeuvrability both manoeuvres are in the same direction, but in regions of unlimited manoeuvrability they are in opposite directions.

However there is only one way of manoeuvring along the limiting curves. Similarly only one manoeuvre is possible for the case $\varepsilon = 1$, for the total speed $w = 0$ with the second manoeuvre.

4. Limiting curves. Manoeuvrable strips

Along a limiting curve $c_e = 0$ or according to I, 8:

$$c + u_1 \cos \xi + u_2 \sin \xi = 0. \qquad \text{(I, 9)}$$

Multiplying the equations I, 5 with $\cos \xi$ and $\sin \xi$ respectively and adding them together one obtains:

$$\cos \xi \frac{dx_1}{dt} + \sin \xi \frac{dx_2}{dt} = 0 \qquad \text{(I, 10)}$$

or in vector notation: $\vec{c} \cdot \vec{w} = 0.$

This equation expresses the fact that, when manoeuvring along a limiting curve, the true velocity vector is always normal to the curve.

After squaring I, 9:

$$(c^2 - u_1^2) \cos^2 \xi - 2u_1 u_2 \cos \xi \sin \xi + (c^2 - u_2^2) \sin^2 \xi = 0$$

and eliminating the heading ξ by means of I, 10 one gets:

$$\left(c^2 - u_1^2\right) \left(\frac{dx_2}{dt}\right)^2 + 2u_1 u_2 \frac{dx_2}{dt} \cdot \frac{dx_1}{dt} + \left(c^2 - u_2^2\right) \left(\frac{dx_1}{dt}\right)^2 = 0 \qquad \text{(I, 11)}$$

If everywhere $\frac{dx_1}{dt} \neq 0$, this equation reduces to the differential equation for the limiting curves:

$$\left(c^2 - u_1^2\right)\left(\frac{dx_2}{dx_1}\right)^2 + 2u_1u_2\frac{dx_2}{dx_1} + c^2 - u_2^2 = 0 \qquad \text{(I, 12)}$$

The discriminant is

$$\begin{aligned}\triangle &= 4u_1^2u_2^2 - 4\,(c^2 - u_1^2)\,(c^2 - u_2^2)\\ &= 4\varepsilon^2u^2\,(u_1^2 + u_2^2 - c^2) \qquad \varepsilon = \frac{c}{u}\\ &= 4\varepsilon^2u^4\,(1 - \varepsilon^2)\end{aligned}$$

In the field of flow there are two sets of limiting curves. These are real if $\triangle > 0$ or $\varepsilon < 1$, i.e. in regions of limited manoeuvrability. In regions where $\varepsilon = 1$ both sets coincide. In regions of unlimited manoeuvrability, where $\varepsilon > 1$, both sets are imaginary.

It is obvious that in a given field of flow not all curves through two given points P and Q can be admissible trajectories, unless the entire field is a region of unlimited manoeuvrability. The admissible trajectories through P and Q are contained within a certain *strip*. However not every curve within this strip will be an admissible trajectory. Such strips will be called *manoeuvrable* strips. If Q is lying in the neighbourhood of P the strips are bounded by the limiting curves through P and Q.

A complete description of the manoeuvrable strips in the different types of field of flow is not possible without a penetrating mathematical analysis. Here the discussion will be confined to one special case and some examples.

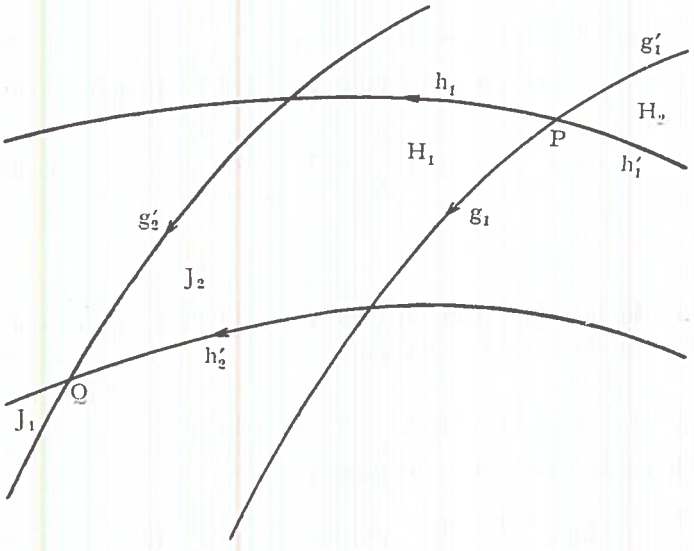

Fig. I, 3.

Consider a field of flow of limited manoeuvrability, $\varepsilon < 1$. Suppose that the two sets of limiting curves in the whole field of flow form two fields of curves, each curve of one set intersecting a curve of the other set in one point only.

Let through a given point P be drawn the two limiting curves g and h (see fig. I, 3). The arcs g_1 and h_1 form the boundary of a sector-shaped area

H_1. The admissible trajectories with P as starting point are contained in H_1. The trajectories with P as terminal point are contained within the complementary manoeuvrable sector H_2, bounded by the arcs g_1' and h_1'. Let Q be a point in sector H_1. Through Q the limiting curves g_2' and h_2' have been drawn, which form the boundary of the complementary sector J_2. All trajectories with P as starting-point and Q as terminal point, for instance the trajectory consisting of g_1 and h_2', are contained within the common section of H_1 and J_2, bounded by g_1, h_1, g_2' and h_2'. This section will be called a manoeuvrable strip ($P\,Q$). If Q is lying in H_2, P can be reached from Q and a manoeuvrable strip ($Q\,P$) exists, being the common section of J_1 and H_2. If Q is lying outside H_1 and H_2, P cannot be reached from Q and vice versa Q cannot be reached from P. The regions outside H_1 and H_2 will be called the prohibited regions associated with P. Since according to the properties of the limiting curves the sectors H_1 and H_2 have no common section H_{12}, it is impossible in this case that for a chosen pair of points $P\,Q$ manoeuvrable strips ($P\,Q$) and ($Q\,P$) exist simultaneously. The case of a double strip may occur, but an example shows that these strips can be very complicated. Sometimes the concept of R i e m a n n surfaces may be usefully applied.

Examples.

1. Let a uniform rectilinear field of flow be defined by:

$$u_1 = u \qquad u \text{ const.}$$
$$u_2 = 0.$$

The differential equation for the limiting curves becomes (See I, 12):

$$(c^2 - u^2)\left(\frac{dx_2}{dx_1}\right)^2 + c^2 = 0,$$

$$\frac{dx_2}{dx_1} = \pm \frac{\epsilon}{\sqrt{1-\epsilon^2}}, \quad \epsilon = \frac{c}{u}.$$

The solutions are:

$$x_2 = \pm \frac{\epsilon}{\sqrt{1-\epsilon^2}} x_1 + \text{const.}$$

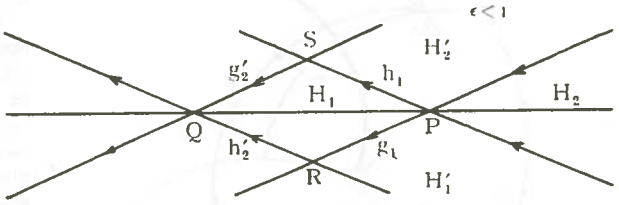

Fig. I, 4.

These are straight lines which intersect the x_1-axis at an angle equal to arc tan $\pm \frac{\epsilon}{\sqrt{1-\epsilon^2}}$.

Take a point P in a field of flow with $\epsilon < 1$ and draw the limiting curves g_1 and h_1 through P (fig. I, 4). The manoeuvrable sectors associated with P are H_1 and H_2. The sectors H_1' and H_2' are the prohibited regions associated with P. For a point Q in H_1 with limiting curves g_2' and h_2' there exists a manoeuvrable strip ($P\,Q$) consisting of the parallelogram $PRQS$. Similarly there exist manoeuvrable strips ($Q\,P$) for points Q in H_2. There are however no regions such that manoeuvrable strips ($P\,Q$) and ($Q\,P$) exist simultaneously for any point Q.

2. Solid rotational field of flow.

From I, 7 and the condition $c_c = 0$ the differential equation for the limiting curves in polar coordinates can be derived in the same way as I, 12:

$$(c^2 - u_a^2)\left(\frac{dr}{d\alpha}\right)^2 + 2ru_r\,u_a\frac{dr}{d\alpha} + r^2(c^2 - u_r^2) = 0. \qquad \text{(I, 13)}$$

The solid rotation is defined by: $u_r = 0$

$$u_\alpha = kr, \qquad k \text{ const.}$$

The equation for the limiting curves now becomes:

$$(c^2 - k^2r^2)\left(\frac{dr}{d\alpha}\right)^2 + r^2c^2 = 0.$$

or

$$\frac{dr}{d\alpha} = \pm \frac{rc}{\sqrt{k^2r^2 - c^2}} = \pm \frac{ar}{\sqrt{r^2 - a^2}},$$

where $a = \frac{c}{k}$ is the radius of the limiting isotach circle about the centre of the flow.

The solutions are:

$$\alpha = \pm \frac{\sqrt{r^2 - a^2}}{a} + \text{bg cos}\,\frac{a}{r} + \text{const.}$$

Apparently the limiting curves in a solid rotational field of flow are the *involutes* of the limiting isotach circle τ with radius $r = a = \frac{c}{k}$. On this circle the involutes possess a cusp. Through P (fig. I, 5) two limiting curves g_1 and h_1 have been drawn. g_1 has a cusp K on τ. Similarly the involutes g_2' and h_2' have been drawn through a point Q outside τ, i.e. in the region of limited manoeuvrability. It is obvious that Q can be reached from P along admissible trajectories, some of which may intersect the limiting curves. In fig. I, 5 for instance Q can be reached along the trajectory γ_1 but also along the trajectory γ_2 which intersects both g_1 and g_2'.

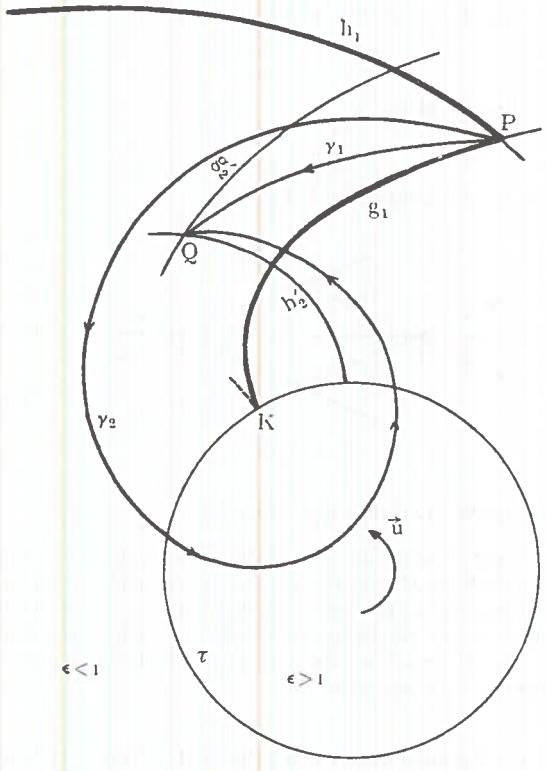

Fig. I, 5.

Therefore the structure of the manoeuvrable sector H_1 is rather complicated. However this structure can be understood by interpreting the navigation as occurring in a *Riemann surface*. One takes n superimposed planes each slit along the involute arcs g_1 and h_1. One binds the edge of one cut to the opposite edge of the cut of the next sheet and binds the remaining edge of the latter to the opposite edge of the cut of the third sheet, etc. Thus one obtains for $n \to \infty$ a Riemann surface of an infinite number of sheets with the point K as branch-point. The sector H_1 consisting of this Riemann surface covers the whole plane, so that each point within the plane can be reached. For instance in fig. I, 5 the ship can be manoeuvred along the track γ_2 in the top sheet and next by passing the cut along g_1 arrive at Q in the second sheet. The track γ_1 lies wholly in the top sheet. Manoeuvrable strips (PQ) and (QP) can be found by considering the Riemann surfaces of P and Q and their common sections.

5. Systems of navigation

Consider a field of pressure-pattern trajectories p in a field of flow, such that one and only one trajectory passes through any point in the field. The true velocity vector $\vec{c}$ is uniquely determined at every point. The vectors $\vec{c}\,(x_1, x_2)$ therefore form a field which may be interpreted as a "pseudo" field of flow in which the stream velocity is constant and equal to the true velocity c. In this field "pseudo" stream-lines v may be drawn in the usual manner. Conversely a vector field $\vec{c}\,(x_1, x_2)$ or a "pseudo" field of flow with stream-lines v uniquely defines a field of trajectories and thereby a *system of navigation* All fields obtained by a translation or a rotation of a given field $\vec{c}\,(x_1, x_2)$ will be considered as defining one and the same system of navigation. Therefore a system of navigation as defined above gives rise to a triply infinite set of pressure-pattern trajectories. By imposing certain conditions on the displacement of the vector field $\vec{c}\,(x_1, x_2)$ the triply infinite set of trajectories can be reduced to a singly infinite set by means of which problems like the construction of the trajectory through two given points can be solved.

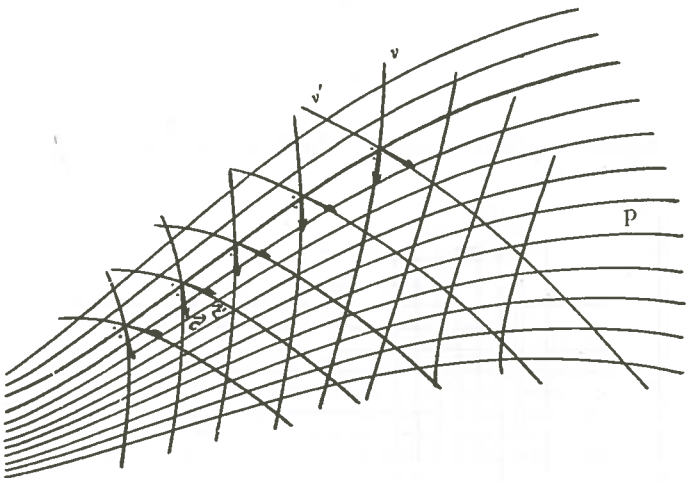

Fig. I, 6.

If the trajectories have been given, but without time parameter, then according to I, 3 there will be *two* vectors $\vec{c}$ and $\vec{c}'$ at any point, each for a different manoeuvre along the same trajectory. Therefore also two sets of "pseudo" stream-lines v and v' exist. According to the symmetry property of the vectors $\vec{c}$ and $\vec{c}'$, cf. I, 3 the trajectories are bisecting curves of the stream-lines v and v' (fig. I, 6).

If a "pseudo" field of flow $\vec{c}\,(x_1,x_2)$ with $|\vec{c}\,| =$ constant has been given, the associated system of navigation is characterized by the property that at every point in the field the vector $\vec{c}$ is tangent to the "pseudo" stream-line v through that point. Because of this such a system of navigation will be called a *tangential system of navigation.*

It is clear that there is an infinity of systems of navigation because the vector field $\vec{c}\,(x_1, x_2)$ can be freely chosen. However by imposing certain restrictions on this vector field special systems of navigation can be introduced, including some well-known systems that are used in practice.

1. *Stream navigation.*

If the "pseudo" field of flow $\vec{c}\,(x_1, x_2)$ with components $\vec{c_1}\,(x_1, x_2)$ and $\vec{c_2}\,(x_1, x_2)$ possesses a stream-function ψ', in other words if

$$c_1 = c \cos \xi = \frac{\partial \psi'}{\partial x_2}, \qquad c_2 = c \sin \xi = -\frac{\partial \psi'}{\partial x_1}, \qquad |\operatorname{grad} \psi'| = c \tag{I, 14}$$

a type of navigation results, which will be called *stream navigation.*

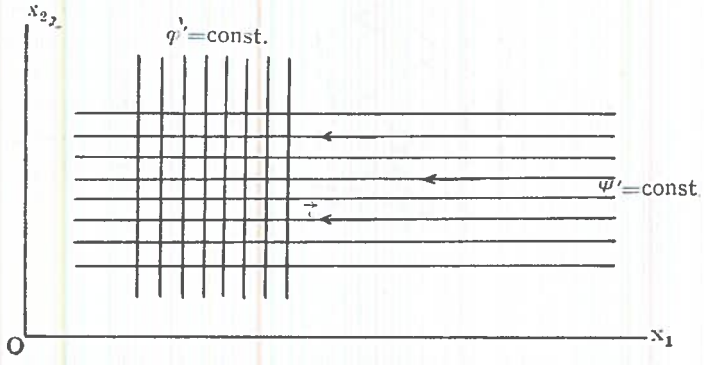

Fig. I, 7.

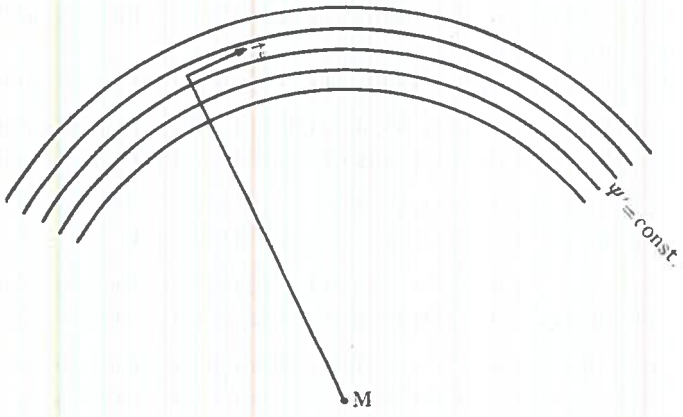

Fig. I, 8.

Examples.

$\psi' = cx_2 + C$, C constant. The vector field simply consists of parallel vectors and the "pseudo" stream-lines are parallel straight lines (fig. I, 7). The heading is constant throughout the field. This system is identical with the well-known system of *single-heading navigation.* With this system there exists only a singly infinite set of fields of "single-heading trajectories" because only a rotation of the vector field gives rise to different vector configurations $\vec{c}\,(x_1, x_2)$.

$\psi' = c\sqrt{x_1^2 + x_2^2} + C$, C constant. Here the "pseudo" field of flow is a field of rotation and the axis of the ship is always normal to the radius vector from the ship to the centre of the field M. This point M, where the vector c becomes indefinite, must be eliminated from the field (fig. I, 8).

The "pseudo" field of rotation admits a doubly infinite set of fields of pressure-pattern trajectories, because only translations give rise to a doubly infinite set of vector configurations.

2. *Potential navigation.*

Potential navigation is by definition the type of navigation which arises if the "pseudo" field of flow $\vec{c}\,(x_1, x_2)$ with components $\vec{c}_1\,(x_1, x_2)$ and $\vec{c}_2\,(x_1, x_2)$ possesses a potential φ', in other words, if

$$c_1 = c\cos\xi = \frac{\partial\varphi'}{\partial x_1}, \qquad c_2 = c\sin\xi = -\frac{\partial\varphi'}{\partial x_2}. \qquad |\operatorname{grad}\varphi'| = c \tag{I, 15}$$

The "pseudo" stream-lines are the orthogonal trajectories of potential lines $\varphi' =$ constant.

Examples.

$\varphi' = cx_1 + C$, C constant. The potential lines form a set of parallel straight lines and the "pseudo" field of flow is again a field of translation. The system of navigation is that of single-heading navigation (fig. I, 7).

$\varphi' = c\sqrt{x_1^2 + x_2^2} + C$, C constant. The potential lines form a family of concentric circles centred on O (fig. I, 9). The vector field $\vec{c}$ consists of vectors $\vec{c}$ directed towards O. (O itself must be eliminated from the field). This system of navigation is also called *point navigation*. The set of fields of trajectories belonging to this system is doubly infinite since only translations produce different vector configurations.

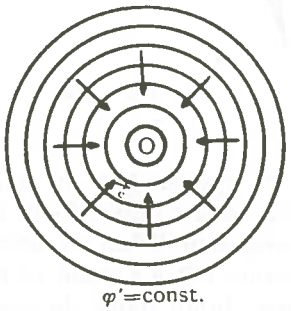

Fig. I, 9.

If the "pseudo" field of flow possesses both a potential and a stream-function, i.e. if

$$c_1 = c\cos\xi = \frac{\partial\psi'}{\partial x_2} = \frac{\partial\varphi'}{\partial x_1}, \qquad c_2 = c\sin\xi = -\frac{\partial\psi'}{\partial x_1} = \frac{\partial\varphi'}{\partial x_2}, \qquad |\operatorname{grad}\psi'| = |\operatorname{grad}\varphi'| = c$$

no new system is introduced since the only solution yields the system of single-heading navigation (fig. I, 7).

3. *Evolute navigation.*

Consider a "pseudo" field of flow $\vec{c}\,(x_1, x_2)$ with $|c|$ = constant, in which the "pseudo" stream-lines r are straight lines. If sufficiently prolonged these straight lines envelop a curve hence-forward called *steering curve* and indicated by the letter S (fig. I, 10). If p is the trajectory through P the figure resembles the figure of an evolute of a curve, in this case of the trajectory p. Because of this similarity

the corresponding system of navigation is called *evolute navigation*. However, if the steering curve is an elementary curve, for instance a circle (fig. I, 11) or an ellipse it is preferable to speak of *circle navigation* or *ellipse navigation* respectively. A straight line as steering curve has no meaning, unless the field of flow contains a straight stream-line along which the ship happens to travel.

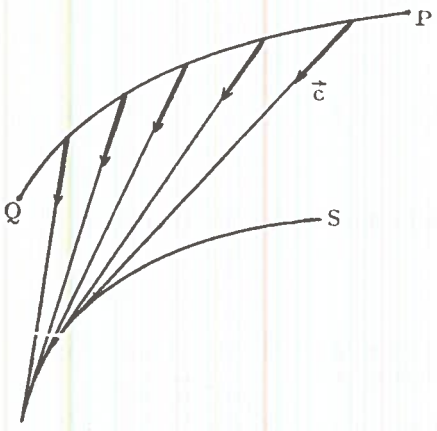

Fig. I, 10.

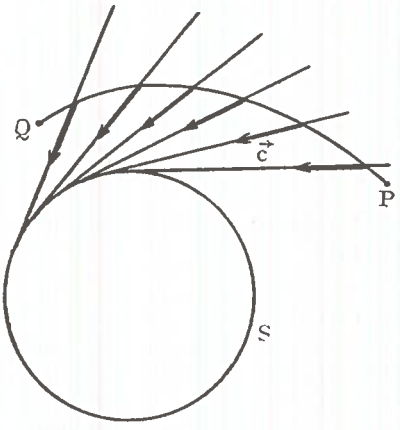

Fig. I, 11.

A special type of evolute navigation is obtained, when the steering curve degenerates into a point, the steering point. This system is again a system of point navigation. When the steering point coincides with the terminal point Q of the trajectory PQ, a method of navigation obtains, popularly called dog-heading navigation. In air traffic the steering point is identical with a radio beacon. The axis of the ship is now always directed towards the radio beacon at the terminal point. If the steering point is at infinity the navigation is again a single-heading navigation.

In general there exists a steering curve corresponding with the navigation along a given pressure-pattern trajectory. Consider an arbitrary trajectory p through P, whose tangent varies continuously along the trajectory (fig. I, 12). Let A be a point on p and a a straight line through A and along the vector $\vec{c}$. When A moves along p the straight lines a envelop a curve S, which is the steering curve associated with p. If on the other hand the steering curve S is given in the field of flow the trajectory p through P can be followed by making $\vec{c}$ coincide at every point with the tangent to S.

According to I, 3 two manoeuvres along p are possible, so two straight lines a and a' may be drawn through A. For every trajectory therefore two *complementary* steering curves S and S' are found. The trajectory p itself is, according to the symmetry property of I, 3 a bisecting curve of the families of straight lines a and a'.

If p happens to be a limiting curve both families a and a' coincide and so do the steering curves S and S'. Moreover the steering curve S will also be the locus of the centres of curvature of the trajectory and therefore the evolute of the limiting curve.

If the trajectory p is situated in a region where $\varepsilon = 1$, then only one steering curve exists since the other one has degenerated because the associated speed vector $\vec{w}$ is zero.

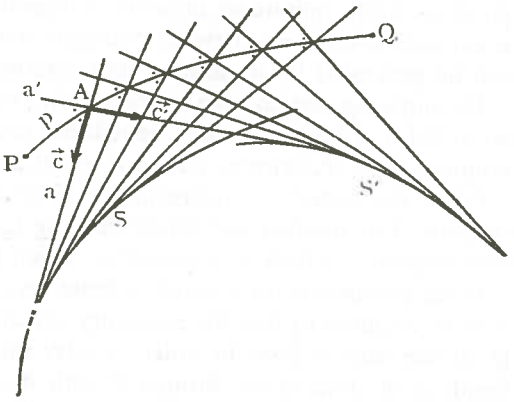

Fig. 1, 12.

It is not always possible to define a system of evolute-heading navigation by choosing a steering curve, so that everywhere the true velocity vector $\vec{c}$ is uniquely determined. It is conceivable that at a point of the field different tangents to the steering curve can be drawn. If the steering curve is the boundary of a convex region and the "pseudo" stream-lines consist of the straight half lines which envelop the steering curve and if $\vec{c}$ is pointing to the tangent point, the field $\vec{c}\,(x_1, x_2)$ is always unique. The choice of an arbitrary steering curve requires special arrangements to define uniquely a field $\vec{c}\,(x_1, x_2)$.

6. Construction of pressure-pattern trajectories

If the method of navigation has been defined by the heading $\xi\,(x_1, x_2)$ the steering equations I, 5 must be solved in order to find the trajectories. This cannot always be done analytically so that often the trajectories can be determined only approximately by means of graphical and numerical methods of integration.

At every point in the field of flow the equations I, 5 define a sum vector $\vec{w}$. The trajectories are identical with the "stream"lines of the field $\vec{w}$. These "stream"lines may be drawn by free-hand extrapolation.

Trajectories through two given points P and Q.

If the method of navigation is defined by a unique "pseudo"field $\vec{c}\,(x_1, x_2)$ there exists a corresponding field of trajectories in the field of flow. According to the definition of a field only one trajectory passes through any point P in the field of flow. If subsequently the "pseudo"field is displaced as a whole by means of a solid rotation and/or translation the system of navigation remains the same according to I, 5. If all translations and rotations of the rigid field of $\vec{c}$ are allowed, a corres-

ponding triply infinite set of fields of trajectories is hereby introduced. For instance, when using the system of evolute navigation a triply infinite set of fields of trajectories can be generated by translation and rotation of the steering curve.

By imposing certain restrictions on the translation and rotation the triply infinite set of fields of trajectories can be reduced to a singly infinite set. In that case a singly infinite set of trajectories passes through any point P in the field of flow.

Often the system of navigation itself reduces already the number of degrees of freedom. For instance with single-heading navigation only a rotation of the "pseudo" field generates a field of trajectories, which therefore is only singly infinite.

If the conditions for a singly infinite set of fields of trajectories are given it may now be required to find the trajectory which passes through two given points P and Q in the field of flow. In order to solve this boundary-value problem consider the family p of trajectories through P with P as starting point and also the family q of trajectories through Q with Q as terminal point, both families being associated with the given configurations of vectorfields $\vec{c}\,(x_1, x_2)$ (fig. I, 13).

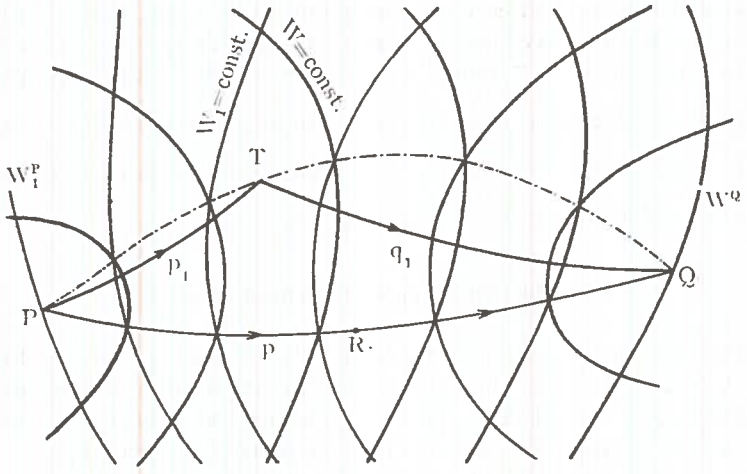

Fig. I, 13.

If there exists a trajectory p of the set p which passes through Q, then this trajectory is a common trajectory of both sets p and q, which corresponds with one fixed "pseudo" field $\vec{c}\,(x_1, x_2)$.

Let next a *time function* W be defined, such that at any point P_1 on a trajectory p, W is equal to the time of travel of the ship from P to P_1 along p. The lines $W =$ constant will be called *time fronts*. The figure consisting of all trajectories through P and the set of curves $W =$ const. is said to be *complete* in analogy with the same figure consisting of extremals and transversals, which occurs in variation theory and is called "the complete figure" after C a r a t h é o d o r y. In the same manner a time function W_1 may be defined, such that at any point Q_1 on a trajectory q,

W_1 is equal to the time of travel of the ship from Q_1 to Q along q. In order to distinguish both types of time fronts for a given point P the time fronts $W = \text{const.}$ will be called *post-time fronts* and the time fronts $W_1 = \text{const.}$ *pre-time fronts.*

The figure consisting of the trajectories q and the pre-time fronts $W_1 = \text{constant}$ is now also complete and is called *complementary* complete figure.

Consider next the trajectory p passing through both P and Q. For an arbitrary point R on p the sum of the values of the time functions W and W_1 is constant and equal to the values of W^Q at Q and of W_1^P at P.

Consider next an arbitrary trajectory p_1 through P and a point T on p_1. Let q_1 be the trajectory of the family q, which passes through T. The trajectory PTQ now consists of a trajectory PT corresponding with a certain vector configuration $\vec{c}'\,(x_1, x_2)$ and a trajectory TQ corresponding with another configuration $\vec{c}''\,(x_1, x_2)$ of the same system of navigation. Therefore the trajectory consisting of two different trajectories associated with two different vector configurations $\vec{c}'\,(x_1, x_2)$ and $\vec{c}''\,(x_1, x_2)$ of the same system of navigation is called a "*composite pressure-pattern trajectory*" with T as "*composite point*".

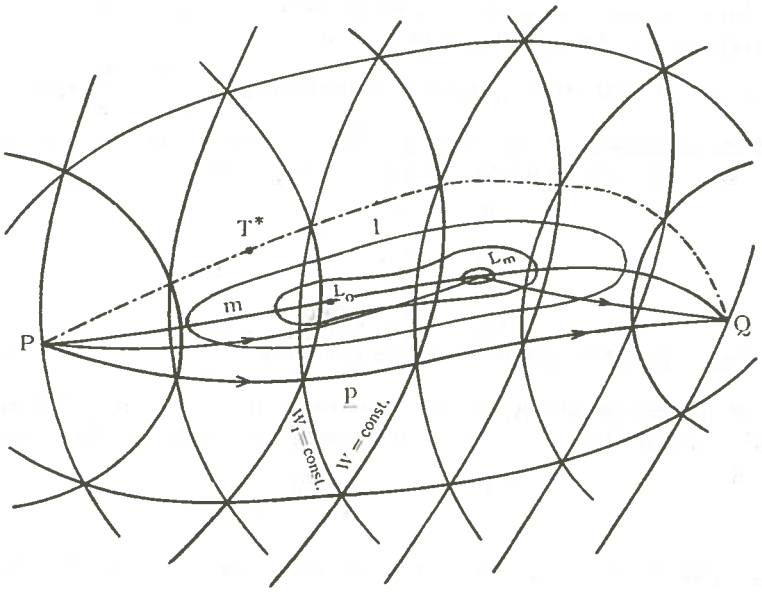

Fig. I, 14.

Along the composite trajectory the time of navigation is equal to $W^T + W_1^T$. Those points T for which $W^T + W_1^T = W^Q = W_1^P$ will be called T^*. If both sets of time fronts have been drawn one can find the locus of points T^*, for which $W + W_1$

$=$ const. $= W^P = W_1^P$. It is obvious that this locus contains the points of the common trajectory p through P and Q.

The trajectory through two given points P and Q associated with a certain method of navigation is a section of the locus of the points of intersection of post-time fronts $W =$ constant and pre-time fronts $W_1 =$ constant, for which the sum of the values of W and W_1 is constant and equal to the value of W at Q or the value of W_1 at P. The value $W^Q = W_1^P$ is the time of navigation along the trajectory. The remaining section of the locus consists of composite points for which the time of navigation along composite trajectories is equal to the time of navigation along the trajectory through P and Q itself.

In fig. I, 14 curves have been drawn through the points of intersection of the lines $W =$ constant and $W_1 =$ constant, for which the sum of the values of W and W_1 is constant, but not equal to W^Q or W_1^P. These curves 1 are loci of composite points, for which the time of navigation along composite pressure-pattern trajectories is constant and equal to the sum $W + W_1$. These curves therefore possess a property corresponding with the property of an ellipse, where the sum of the distances from a point on the ellipse to the foci is constant. So the curves 1 may be called "focal" curves with foci P and Q. The set of curves 1 may be regarded as a confocal set. Among these there are curves, for which the time of navigation along composite pressure-pattern trajectories is shorter then the time of navigation along the pressure-pattern trajectory p through P and Q.

If $W\ (x_1,\ x_2)$ and $W_1\,(x_1,\ x_2)$ are continuous and $\frac{\partial W}{\partial x_1}$, $\frac{\partial W}{\partial x_2}$ resp. $\frac{\partial W_1}{\partial x_1}$, $\frac{\partial W_1}{\partial x_2}$ exist and are continuous in the whole field (except in P and Q), the stationary points of $W' = W + W_1$ are found by solving simultaneously

$$\frac{\partial W}{\partial x_1} + \frac{\partial W_1}{\partial x_1} = 0,$$

$$\frac{\partial W}{\partial x_2} + \frac{\partial W_1}{\partial x_2} = 0.$$

Those points therefore will be found on the curve $\frac{\partial\,(W, W_1)}{\partial\,(x_1, x_2)} = 0$, which is the locus m of tangent points of the pre-time fronts $W_1 =$ const. and the post-time fronts $W =$ const. The character of the stationary points will be determined by the sign of

$$\frac{\partial^2 W'}{\partial x_1^{\,2}} \cdot \frac{\partial^2 W'}{\partial x_2^{\,2}} - \left(\frac{\partial^2 W'}{\partial x_1 \partial x_2}\right)^2.$$

On the curve m the time function W' is defined by $W' = W + W_1$. The function W' may have several isolated minima for instance at the points L_0, L_1, $L_2 \ldots$ Let L_m be the point, where W' has an absolute minimum. Then this point is the composite point for the composite pressure-pattern trajectory, which, with the given method of navigation, gives an absolute minimum for the time of navigation with respect to all other composite pressure pattern trajectories through P and Q and the pressure-pattern trajectory p through P and Q itself.

In part III, which deals with the variation problem, a similar figure will be found, but there the time fronts $W =$ constant and $W_1 =$ constant, for which $W + W_1 = W^Q = W_1^P$ are tangent to each other and the curve connecting their points of contact is the *extremal* through P and Q.

If Q is made to coincide with P one considers the trajectories with P as starting point and as terminal point. Fot both sets of trajectories again the sets of time fronts $W =$ constant and $W_1 =$ constant can be drawn. The curves 1 passing through the points of intersection of the sets of time fronts $W =$ constant and $W_1 =$ constant are now loci of composite points R for composite pressure pattern trajectories PRP along which the time of navigation is constant and equal to $W + W_1$. If for instance in aviation the range of various types of aircraft is determined by a maximum time of navigation, the curves 1 are the boundaries of regions, within which these aircrafts using the given method of navigation can operate from and back to their base.

7. Some special construction methods

In practice it is important to have a quick and elegant construction method and a very quick one exists, if both the given field of flow and the "pseudo" field possess a stream-function. In this case the addition method of Maxwell for superposed vector fields can be applied. Let the field of flow have a stream-function ψ:

$$u_1 = \frac{\partial \psi}{\partial x_2}$$

$$u_2 = -\frac{\partial \psi}{\partial x_1}$$

and similarly the "pseudo"field of $\vec{c}$ a stream-function ψ':

$$c_1 = \frac{\partial \psi'}{\partial x_2}$$

$$c_2 = -\frac{\partial \psi'}{\partial x_1}.$$

If both fields are superposed, then according to the steering equations the sum vector

$$\vec{w}(w_1, w_2) = \vec{u} + \vec{c},$$

or

$$w_1 = \frac{\partial (\psi + \psi')}{\partial x_2},$$

and

$$w_2 = -\frac{\partial (\psi + \psi')}{\partial x_1}. \qquad \text{(I, 16)}$$

It follows that $\psi + \psi'$ is the stream-function of the sum field $\vec{w}(x_1, x_2)$.
The stream-lines $\psi + \psi' =$ constant therefore represent the trajectories.

Therefore if stream-lines of both fields of flow are drawn at unit intervals, the trajectories will be found by connecting the points of intersection of the ψ and ψ'-lines, for which $\psi + \psi'$ is constant. The stream-lines of the sum field have also unit intervals and the speed of a ship in the field of flow with respect to a fixed system is determined by the magnitude of the gradient of $\psi + \psi'$ in the sum field, according to the formula:

$$w^2 = \left\{\frac{\partial(\psi + \psi')}{\partial x_2}\right\}^2 + \left\{\frac{\partial(\psi + \psi')}{\partial x_1}\right\}^2 = \{\text{grad. } (\psi + \psi')\}^2.$$

The same addition method may be applied, if both the given field of flow and the "pseudo" field possess a velocity-potential, in other words, if potential-navigation methods are used.

Let the field of flow have a velocity-potential φ:

$$u_1 = \frac{\partial \varphi}{\partial x_1},$$

$$u_2 = \frac{\partial \varphi}{\partial x_2},$$

and similarly the "pseudo" field $\vec{c}\,(c_1, c_2)$ a velocity-potential φ':

$$c_1 = \frac{\partial \varphi'}{\partial x_1},$$

$$c_2 = \frac{\partial \varphi'}{\partial x_2}.$$

If now both fields are superposed, then according to I, 6 the sum vector $\vec{w}\,(w_1, w_2)$ becomes:

$$\begin{aligned} &\vec{w} = \vec{u} + \vec{c}, \\ &w_1 = \frac{\partial(\varphi + \varphi')}{\partial x_1}, \\ &w_2 = \frac{\partial(\varphi + \varphi')}{\partial x_2}, \\ &w^2 = \left\{\frac{\partial(\varphi + \varphi')}{\partial x_1}\right\}^2 + \left\{\frac{\partial(\varphi + \varphi')}{\partial x_2}\right\}^2 = \{\text{grad}\,(\varphi + \varphi')\}^2. \end{aligned} \qquad \text{(I, 17)}$$

It follows that $\varphi + \varphi'$ is the velocity-potential of the sum field. So if the iso-potential lines $\varphi + \varphi' =$ constant are drawn, the trajectories are the orthogonal trajectories of these potential lines and the speed $\vec{w}$ along those trajectories is determined by the magnitude of the gradient of $\varphi + \varphi'$ in the sum field.

If the stream-navigation method is used in a field of flow with a stream-function

and if the triply infinite set of "pseudo" fields can be reduced to a singly infinite set, the trajectory through two arbitrary points P and Q can be found by applying the addition method of M a x w e l l in such a manner that the sums of the values ψ and ψ' at P and at Q are equal. So the given "pseudo" field is displaced and/or rotated in the prescribed manner until $\psi^P + \psi'^P = \psi^Q + \psi'^Q$.

The curve joining the points of intersection of stream-lines for which the sum $\psi + \psi' = \psi^P + \psi'^P$, *is the trajectory.* It may occur that more than one trajectory is found for the given navigation method.

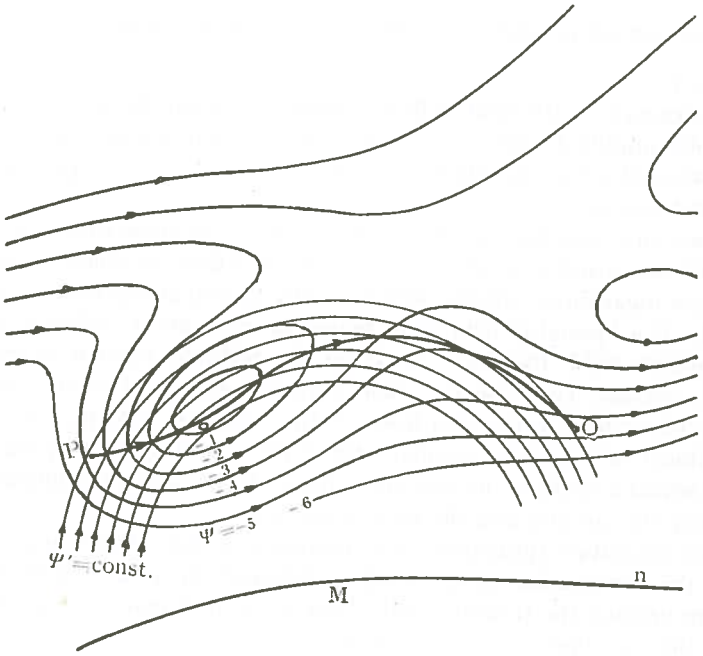

Fig. I, 15.

The method may be demonstrated for a tangential navigation system with a "pseudo" field given by the stream-function $\psi' = c\sqrt{x_1^2 + x_2^2}$ (fig. I, 15). The "pseudo"-stream-lines are concentric circles. The field of flow is given by an arbitrary stream-function ψ. In this field two points P and Q are given. In fig. I, 15 stream-lines of both fields have been drawn at unit intervals. Since the "pseudo" field is rotational-symmetric a singly or doubly infinite set of "pseudo" fields can be formed by means of translations only.

To reduce the number of "pseudo" fields the translations must be restricted, for instance by moving the centre M of the circles along a prescribed curve n. The trajectory is now found by moving M along n, untill $\psi^P + \psi'^P = \psi^Q + \psi'^Q$. The "sum line" $\psi + \psi' = \psi^P + \psi'^P$, is the trajectory asked for.

There may be several points on n for which the condition is satisfied, so that several trajectories through P and Q are found with the given method of navigation.

Notes.

Because of the symmetry of the addition method of M a x w e l l the interpretation of the method may be reversed in those cases, where the stream velocity u of the given field of flow is constant.

So if u = constant = $|$ grad ψ $|$ and c = constant = $|$ grad ψ' $|$ the sum lines $\psi + \psi'$ = constant can also be interpreted as the trajectories in a field of flow $\vec{c}\ (x_1, x_2)$ corresponding with a method of navigation defined by the "pseudo" field $\vec{u}\ (x_1, x_2)$.

Often the structure of the field of flow is such, that it can be regarded as the sum of two or more simplified fields of flow each with a stream-function. Such a field may also be constructed using the addition method of M a x w e l l, provided certain conditions are satisfied (1).

For instance an irrotational circular motion may be combined with a non-divergent recti linear motion from a source to yield a field of flow, in which streamlines and trajectories are logarithmic spirals, which all end in coinciding centers of the constituent fields. If a "pseudo" field for a tangential navigation system is superposed on this composite field, the order in which the addition method is applied may be arbitrarily chosen. The "pseudo" field may first be added to the circular field and the recti linear field to the sum field. Or the "pseudo" field may be added first to the recti linear field and the circular field to the sum field. Finally the "pseudo" field may be added directly to the field consisting of logarithmic streamlines, obtained by superposing the circular and the recti linear fields.

If potential navigation (potential φ') is applied to a field of flow with a velocity-potential φ, the construction of a trajectory through two given points P and Q is not so simple because the trajectory asked for is the orthogonal trajectory through P and Q of the sum lines $\varphi + \varphi'$ = constant.

8. A theorem for the time of navigation

According to I, 16 the sum lines $\bar{\psi} = \psi + \psi'$ = constant represent the trajectories associated with a stream navigation in a field of flow with a stream-function. The time of navigation T may then be obtained by measuring an area.

The speed w of the ship with respect to a fixed coordinate system is determined by the gradient of $\bar{\psi}$:

$$w = |\ \text{grad}\ \bar{\psi}\ | .$$

The time of navigation along a trajectory is given by:

$$T = \int_P^Q \frac{ds}{w} = \lim_{\Delta s \to 0} \Sigma \frac{\Delta s}{w}$$

where $\triangle s$ is a line element on the pressure-pattern trajectory $\overline{\psi}$ = constant. Consider next two adjacent sum lines or, in other words, two adjacent pressure-pattern trajectories $\overline{\psi}$ and $\overline{\psi} - \triangle\overline{\psi}$ (fig. I, 16) and let a point S be given on the trajectory $\overline{\psi}$. At this point the normal is drawn to the trajectory $\overline{\psi} - \triangle\overline{\psi}$. Putting the length of the normal equal to $\triangle n$ one may write:

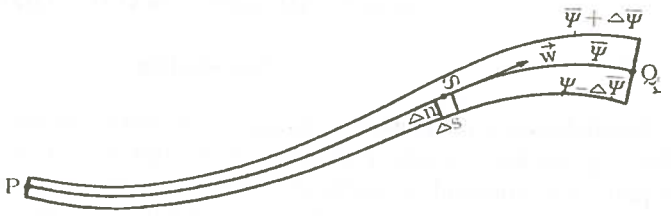

Fig. I, 16.

$$T = \lim_{\substack{\triangle s \to 0 \\ \triangle\overline{\psi} \to 0}} \Sigma \frac{\triangle s \,.\, \triangle n}{\triangle\overline{\psi}},$$

or, if the summation is carried out for a constant value of $\triangle\overline{\psi}$, T becomes:

$$T = \lim_{\substack{\triangle s \to 0 \\ \triangle\overline{\psi} \to 0}} \frac{1}{\triangle\overline{\psi}} \Sigma \, \triangle s \,.\, \triangle n$$

$$= \lim_{\substack{\triangle s \to 0 \\ \triangle\overline{\psi} \to 0}} \frac{1}{\triangle\overline{\psi}} \Sigma \, \triangle O$$

where $\triangle O$ is a surface element between the trajectories $\overline{\psi}$ and $\overline{\psi} - \triangle\overline{\psi}$

or $$\boxed{T = \lim_{\triangle\overline{\psi} \to 0} \frac{1}{\triangle\overline{\psi}} \,.\, O.}$$

Here O is the area of the strip bounded by the lines $\overline{\psi}$ = constant and $\overline{\psi} - \triangle\overline{\psi}$ = constant and the normals through P and Q.

So if the value of $\triangle\overline{\psi}$ is chosen sufficiently small the time of navigation T is approximately equal to the area of this strip divided by $\triangle\overline{\psi}$:

$$T \backsim \frac{1}{\triangle\overline{\psi}} \,.\, O. \qquad \text{(I, 18)}$$

If for instance $\triangle\overline{\psi} = 1$, the time of navigation is approximately equal to the area of the strip between the pressure-pattern trajectories $\overline{\psi}$ and $\overline{\psi} - 1$:

$$T \backsim O. \qquad \text{(I, 19)}$$

Similarly it may be shown that the time of navigation is approximately equal to the area of the strip between the trajectories $\overline{\psi}$ and $\overline{\psi} + \triangle\overline{\psi}$, divided by $\triangle\overline{\psi}$. The areas of both strips may be measured and the mean of the values taken. Or the area of the strip between the trajectories $\overline{\psi} - \triangle\overline{\psi}$ and $\overline{\psi} + \triangle\overline{\psi}$ may be measured and divided by two. Examples are given in part II.

PART II

SINGLE-HEADING NAVIGATION

Introduction

Single-heading navigation is certainly one of the simplest methods of navigation. The ship remains always parallel to itself and is carried freely by the flow. The heading ξ is constant throughout the manoeuvre. In part I, 5 it was shown that single-heading navigation could be classified both as *stream navigation* and as *potential navigation*. The pseudo field $\vec{c}\,(x_1, x_2)$ consists of parallel equidistant straight lines as stream-lines, $\psi' =$ constant. The parallel equidistant straight lines orthogonal to these are isopotential lines $\varphi' =$ constant (see fig. I, 7). It has also been shown that single-heading navigation is a special case of *evolute navigation* or rather of *point navigation* with the steering point at infinity.

Since a translation of the field $\vec{c}\,(x_1, x_2)$ leaves it completely unchanged, the method of single-heading navigation is defined by the given $\vec{c}$ field and the configurations which result from a *rotation* of the $\vec{c}$ field. The single-heading trajectory passing through the starting point P and the terminal point Q is therefore unambiguously defined for a given heading ξ. It is, however, possible that several single-heading trajectories pass through P and Q, but for different values of the constant heading.

Apart from its simple steering principle single-heading navigation has in practice also other advantages and is therefore in many cases to be preferred to other methods of navigation. For instance in aviation, the lateral drift may often become so large that zones of bad flying weather are avoided. Generally also the time of navigation along the single-heading trajectory is shorter than the time of navigation along the geometrically shortest route, i.e. the chord PQ, which subtends the single-heading trajectory PQ. Another advantage is that, both if the field of flow is slowly changing with time and if the actual flow pattern differs slightly from the forecast flow pattern, the radius within which the ship approaches the terminal point Q, remains small, a constant heading appropriate to the forecast flow pattern being used.

Furthermore single-heading navigation is important for the planning of even better routes, for instance of the trajectory along which the time of navigation is a minimum (part IV).

In the present part the most important properties of single-heading navigation in stationary fields of flow are dealt with on the basis of stream navigation.

1. Single-heading navigation in stationary fields of flow

The description of the methods of navigation, given in part I, can be repeated almost literally. For every point in the field of flow a complete and a complementary

complete figure of single-heading trajectories and time fronts can be drawn. If a single-heading trajectory exists from a given point P to another point Q, this trajectory is a section of the locus of the points of intersection of time fronts W = constant of the complete figure of P and W_1 = constant of the complementary complete figure of Q for which the sum of the values of W and W_1 is constant and equal to the value of W at Q or the value of W_1 at P. The value $W^Q = W_1{}^P$ is the time of navigation along the trajectory. The remaining section of the locus consists of composite points for which the time of navigation along composite single-heading trajectories is equal to the time of navigation along the single-heading trajectory through P and Q itself.

Here also focal curves exist and points for which the time of navigation along composite single-heading trajectories from P to Q is an absolute minimum.

The description of the complete figure for single-heading trajectories will however not be carried further, since in this chapter only fields of flow with a stream-function will be considered.

2. Single-heading navigation in stationary fields of flow with a stream-function

Fields of flow with a stream-function $\psi(x_1, x_2)$ are most important in practice. In aerology for instance the field of flow in a pressure surface in a narrow strip about a latitude circle in middle latitudes can be fairly accurately described by means of the stream-function $\psi = -\frac{g}{2\omega \sin \varphi_m} z$, where g is the acceleration of gravity, ω the angular velocity of the rotating earth, φ_m the latitude (assumed constant) and z the height of the pressure surface. The theory developed in I, 7 can be directly applied if the single-heading navigation is conceived as a stream navigation with a stream-function $\psi'(x_1, x_2)$, $|\operatorname{grad} \psi'| = c$.

I. Single-heading trajectories.

If the x_1-axis is taken parallel to the pseudo stream-lines $\psi' =$ constant, ψ' becomes (apart from an additive constant) $\psi' = \pm c\, x_2$. According to I, 16 the equation of the single-heading trajectories is:

$$\psi + \psi' = \text{constant or}$$

$$\psi(x_1, x_2) \pm c x_2 = A,\ A \text{ constant} \qquad \text{(II, 1)}$$

The trajectories can be constructed by means of the addition method of Maxwell. If both fields ψ and ψ' have been normalized in the same manner, then the lines connecting the points of intersection of stream-lines, for which $\psi + \psi'$ = constant, are single-heading trajectories.

II. Single-heading trajectories through two given points P and Q. Formula for the drift.

Since the single-heading navigation is determined by the ψ' field and the configuration resulting from a rotation of this field, the single-heading trajectory from a

given point P to another point Q can be found by turning the ψ' field until the sum of the values of the stream-functions at P and Q are equal. When $\psi^P + \psi'^P = \psi^Q + \psi'^Q$, the single-heading trajectory is the sum line connecting the points for which

$$\psi + \psi' = \psi^P + \psi'^P = \psi^Q + \psi'^Q \qquad \text{(II, 2)}$$

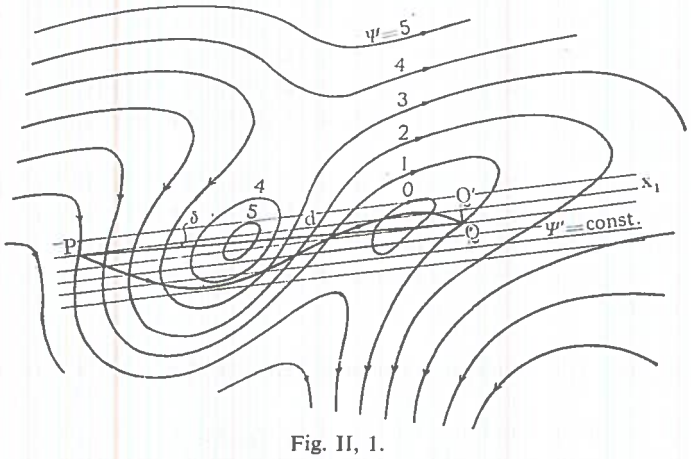

Fig. II, 1.

Consider now figure II, 1. The orientation of the pseudo field for a single-heading navigation is determined by condition II, 2. Let the coordinate system be adjusted to the pseudo field, such that the positive x_1-axis coincides with the pseudo stream vector $\vec{c}$. The stream-function ψ' of the pseudo field is then given by $\psi' = cx_2$.

Draw the perpendicular from Q to the pseudo stream-line through P and let the base-point of this perpendicular be Q'. Then $\sin \delta = \dfrac{QQ'}{PQ} = \dfrac{x_2}{d}$, where δ is the angle between the pseudo stream-lines and the chord PQ and d the distance from P to Q. From II, 2 it follows that:

$$x_2 = \frac{1}{c}(\psi'^Q - \psi'^P) = \frac{1}{c}(\psi^P - \psi^Q).$$

$$\text{So:} \quad \boxed{\sin \delta = \frac{1}{cd}(\psi^P - \psi^Q).} \qquad \text{(II, 3)}$$

The drift angle δ therefore can be calculated from the difference between the values of the stream-function ψ of the given field of flow at the starting point and at the terminal of the trajectory.

Substituting $\psi = -\dfrac{g}{2\omega \sin \varphi_m} z$ in II, 3 one gets

$$\sin \delta = \frac{g}{2\omega \sin \varphi_m} \cdot \frac{z^Q - z^P}{cd}.$$

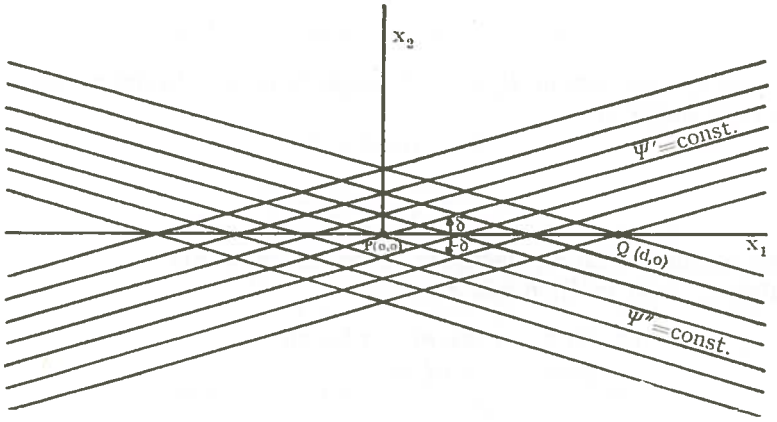

Fig. II, 2.

This is the well-known formula of Bellamy for aeronavigation (2). Applying II, 3 to the single-heading trajectory from Q to P one has:

$$\sin \delta' = \frac{1}{cd}(\psi^Q - \psi^P) = -\sin \delta, \qquad \text{or } \delta' = -\delta \text{ (see fig. II, 2).} \qquad \text{(II, 4)}$$

III. Concentration points.

In a field of flow with a stream-function ψ the following property holds:

The single-heading trajectories through two given points P and Q for different true velocities c of the ship intersect each other at the same points R_i. The points R_i lie on the chord PQ.

Consider fig. II, 2. If the x_1-axis is taken along the chord PQ, the stream-function ψ' for single-heading trajectories from P to Q can be written:

$$\psi' = -c\,(x_2 \cos \delta - x_1 \sin \delta),$$

where δ is the drift angle.

Applying the addition method of Maxwell one obtains the following expression for the single-heading trajectories from P to Q:

$$-c\,(x_2 \cos \delta - x_1 \sin \delta) + \psi\,(x_1, x_2) = A,$$

where ψ is the stream-function of the given field of flow and A is constant. Substituting the coordinates of $P\,(o, o)$ in this expression one finds that $A = \psi\,(o, o)$.

So
$$-c\,(x_2 \cos \delta - x_1 \sin \delta) + \psi\,(x_1, x_2) = \psi\,(o, o). \qquad \text{(II, 5)}$$

The stream-function ψ'' for single-heading trajectories from Q to P with drift angle $\delta' = -\delta$ becomes:

$$\psi'' = c\,(x_2 \cos \delta + x_1 \sin \delta).$$

Applying the addition methode of Maxwell one obtains for the single-heading trajectories from Q to P:

$$c\,(x_2 \cos \delta + x_1 \sin \delta) + \psi\,(x_1, x_2) = B.$$

Substituting the coordinates of $P\,(o,o)$ in this expression one finds that $B = \psi\,(o, o)$.

So $$c\,(x_2 \cos\delta + x_1 \sin\delta) + \psi\,(x_1, x_2) = \psi\,(o, o). \qquad \text{(II, 6)}$$

The points of intersection R_i of both single-heading trajectories are found by equating II, 5 and II, 6:

$$2c\,x_2 \cos\delta = 0.$$

So if $$\delta \neq \frac{\pi}{2}: \qquad x_2 = 0.$$

The points of intersection R_i therefore lie on the chord PQ.
Substituting $x_2 = 0$ in II, 6 one has:

$$cx_1 \sin\delta + \psi\,(x_1, o) = \psi\,(o, o),$$

or $$cx_1 \frac{\psi\,(o, o) - \psi\,(d, o)}{cd} + \psi\,(x_1, o) = \psi\,(o, o),$$

or $$d\,\psi\,(x_1, o) + (x_1 - d)\,\psi\,(o, o) - x_1\,\psi\,(d, o) = 0. \qquad \text{(II, 7)}$$

This is an equation for x_1, the solutions of which give the points R_i. It may be noted that the equation II, 7 for the points of intersection R_i is independent of the true velocity c. Therefore in a given field of flow all single-heading trajectories from a given point P to a given point Q and vice versa intersect each other at fixed points R_i on the straight line PQ, whatever the value of the true velocity c. The existence of such "points of concentration" may be of considerable importance for air traffic control in aviation (see fig. II, 3).

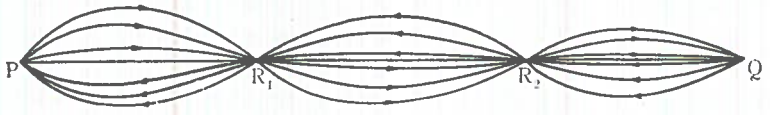

Fig, II, 3.

If $\psi\,(d, o) = \psi\,(o, o)$, equation II, 7 reduces to:

$$\psi\,(x_1, o) = \psi\,(o, o).$$

The points of concentration on PQ are then found at those points, where the value of ψ is equal to the value at the starting point or terminal point. In other words the points of cencentration are the points of intersection of the stream-line $\psi = \psi\,(o, o)$ and the straight line PQ. They can be found immediately in the field of flow without constructing a single-heading trajectory. The number of points of intersection of the streamline $\psi = \psi\,(o, o)$ with PQ, P and Q not inclusive, is, according to a algebraic theorem, at the most *one less than the number of zero-points between P and Q of the differential quotient* $\frac{d\,\psi\,(x_1, o)}{dx_1}$ *i.e. the number of maxima and minima on the stream-line* $\psi = \psi\,(o, o)$ *relative to the chord PQ.*

The points P and Q are also concentration points. The points R_i and P and Q are interchangeable, for if the starting point and terminal point coincide with points R_i then P and Q become concentration points for the set of single-heading trajectories

through those two points. If two or more concentration points coincide, the single-heading trajectories are tangent to each other at these points (fig. II, 4).

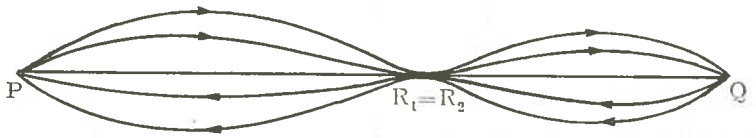

Fig. II, 4.

IV. Single-heading trajectory through a singular point.

In fields of flow with a stream-function $\psi\ (x_1, x_2)$ singular points may occur, where $\frac{\partial \psi}{\partial x_1}$ and $\frac{\partial \psi}{\partial x_2}$ vanish simultaneously. In aerology for instance singular points occur where the height z of the chosen standard pressure surface has a maximum, minimum or stationary value, corresponding to the centres of anti-cyclones, depressions and cols.

For a critical value c_k of the true velocity the trajectory PQ will pass through a centre L.

In figure II, 5 the orientation of the pseudofield $\vec{c_k}$ is such that PS is the pseudo streamline through P. PS is also the x_1-axis of a coordinate system. Draw through Q a line QT parallel to PS and drop the perpendicular LM, which intersects QT at N. Now according to II, 1, the single-heading trajectory is given by $\psi + c\,x_2 = A$, A constant along the trajectory. Since the single-heading trajectory must pass through $P\ (o, o)$ it follows that

$$A = \psi^P,$$

or

$$\psi + cx_2 = \psi^P.$$

The point L must also lie on the single-heading trajectory:

$$\psi^L + c_k \bar{x}_2 = \psi^P,$$

where $\bar{x}_2$ is the ordinate of L : $\bar{x}_2 = ML$.
So

$$ML = \frac{\psi^P - \psi^L}{c_k}.$$

Furthermore if δ_k is the drift angle QPS then $MN = d \sin \delta_k$.

According to II, 3:

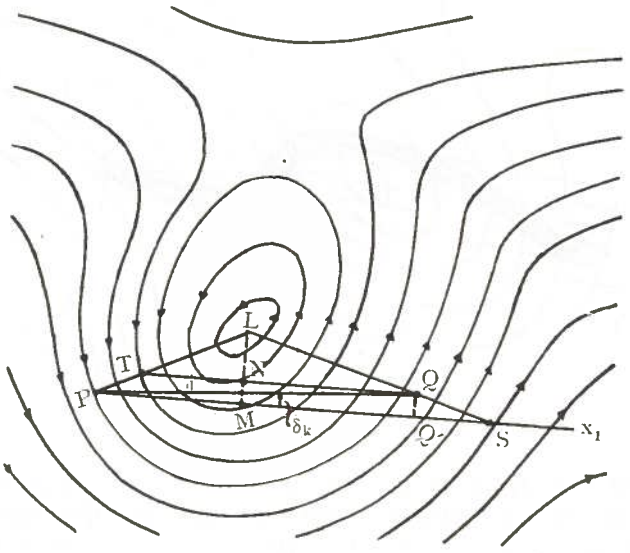

Fig. II, 5.

$$MN = \frac{\psi^P - \psi^Q}{c_k},$$

and

$$\frac{MN}{ML} = \frac{\psi^P - \psi^Q}{\psi^P - \psi^L}. \qquad \text{(II, 8)}$$

The value of this ratio depends only on the values of the stream-function ψ at the starting point, the terminal point and the singular point.

Since $\frac{MN}{ML} = \frac{QS}{LS}$ the point S on QL can be determined. Then ML is also known and it follows that:

$$c_k = \frac{\psi^P - \psi^L}{ML}. \qquad \text{(II, 9)}$$

V. The time of navigation.

If the addition method of Maxwell is applied, the time of navigation $T_{s.h.}$ may be obtained according to part I, 7 by measuring or calculating the area of a strip between two neighbouring sum lines $\bar{\psi} = \psi + \psi'$ and $\bar{\psi} + \triangle\bar{\psi}$

$$T_{s.h.} = \lim_{\triangle\bar{\psi}\to 0} \frac{1}{\triangle\bar{\psi}} \cdot O_{\triangle\bar{\psi}} \qquad \text{(II, 10)}$$

where $O_{\triangle\bar{\psi}}$ is the area enclosed by the single-heading trajectories $\bar{\psi}$ and $\bar{\psi} + \triangle\bar{\psi}$ and the normals from P and Q to the trajectory $\bar{\psi} + \triangle\bar{\psi}$ (see also fig. II, 6).

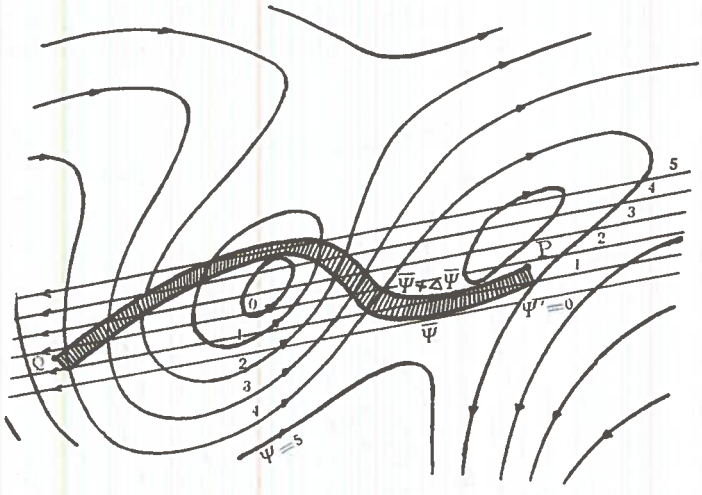

Fig. II, 6.

VI. Symmetry property.

Because of the symmetry of the addition method of Maxwell the single-heading trajectories in a *uniform* field of flow can also be interpreted as pressure-pattern trajectories of a stream navigation in a uniform recti linear field of flow. If for instance the stream velocity of the given uniform field is equal to u and the true velocity of the ship equal to c, the single-heading trajectories are also trajectories for a ship with a true velocity u in a uniform recti linear field with stream velocity c.

Examples.

Single-heading navigation in uniform circular flow.

The stream-function ψ is: $\psi = u\sqrt{x_1^2 + x_2^2}$, with u constant. In polar coordinates: $\psi = ur$,

$$u_\alpha = u \qquad u_r = 0.$$

According to formula II, 1 the equation for the single-heading trajectories is

$$u\sqrt{x_1^2 + x_2^2} + cx_2 = \overline{\psi},$$

where $\overline{\psi}$ is a parameter, or in polar coordinates:

$$r = \frac{\overline{\psi}}{u + c \sin \alpha}. \qquad \text{(II, 11)}$$

This may be written:

$$r = \frac{\frac{\overline{\psi}}{u}}{1 + \epsilon \cos\left(\frac{\pi}{2} - \alpha\right)}, \quad \epsilon = \frac{c}{u},$$

where ϵ is the velocity parameter defined in part I, 1. The solution now consists of a singly infinite set of conics with $\frac{\overline{\psi}}{u}$ as parameter, the centre of the circular flow as focus and an eccentricity given by $\epsilon = \frac{c}{u}$. The trajectories also form a set of similar curves with the origin as centre of similitude.

The following cases may be distinguished:

a) Uniform circular flow with unlimited manoeuvrability ($\epsilon > 1$). Here the single-heading trajectories are hyperboles.

b) Uniform circular flow with limited manoeuvrability ($\epsilon < 1$). The single-heading trajectories are ellipses.

c) Uniform circular flow with $\epsilon = 1$. The single-heading trajectories are paraboles.

In the first case the common asymptotic directions through the origin, defined by $\sin \alpha = -\frac{1}{\epsilon}$, are also integral curves of II, 11 and are obtained, when $\overline{\psi} = 0$.

According to II, 2 the trajectories can be constructed by means of the addition method. This has been shown in fig. II, 7 for case a.

The time of navigation can be computed by means of II, 10. First the equation of two neighbouring trajectories must be found. The trajectory $\overline{\psi}$ is given by $r = \frac{\overline{\psi}}{u + c \sin \alpha}$ and the trajectory $\overline{\psi} + \Delta\overline{\psi}$ by $r' = \frac{\overline{\psi} + \Delta\overline{\psi}}{u + c \sin \alpha}$.

For a sufficiently small value of $\Delta\overline{\psi}$ the area $O_{\Delta\overline{\psi}}$ of the strip between these sum lines is approximately equal to the difference between the areas of the sectors $OP'Q'$ and OPQ (fig. II, 7).

$$O_{\nabla\overline{\psi}} = \tfrac{1}{2}\int_P^Q (r'^2 - r^2)\, d\alpha = \tfrac{1}{2}\int_P^Q \left\{\frac{(\overline{\psi} + \Delta\overline{\psi})^2}{(u + c \sin \alpha)^2} - \frac{\overline{\psi}^2}{(u + c \sin \alpha)^2}\right\} d\alpha$$

$$= \tfrac{1}{2}\int_P^Q \left\{\frac{2\overline{\psi}\,\Delta\overline{\psi}}{(u + c \sin \alpha)^2} + \frac{(\Delta\overline{\psi})^2}{(u + c \sin \alpha)^2}\right\} d\alpha.$$

According to II, 10 the time of navigation is:

$$T_{s.h.} = \lim_{\Delta\overline{\psi} \to 0} \frac{1}{\Delta\overline{\psi}} \left\{ \Delta\overline{\psi} \int_P^Q \frac{\overline{\psi}}{(u + c \sin \alpha)^2}\, d\alpha + \tfrac{1}{2}(\Delta\overline{\psi})^2 \int_P^Q \frac{d\alpha}{(u + c \sin \alpha)^2} \right\}.$$

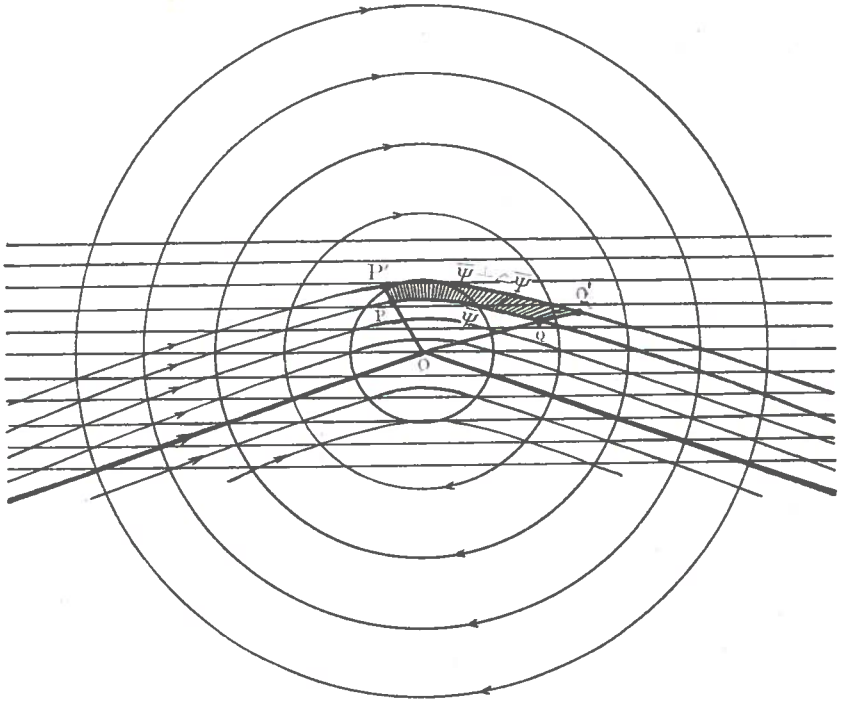

Fig. II, 7.

When taking the limit for $\Delta\bar{\psi} \to 0$ this reduces to:

$$T_{s.h.} = \int_P^Q \frac{\bar{\psi}}{(u + c \sin \alpha)^2} d\alpha = \int_P^Q \frac{r}{u + c \sin \alpha} d\alpha$$

$$= \int_P^Q \frac{r^2}{\bar{\psi}} d\alpha = \frac{2}{\bar{\psi}} \times \text{area of sector } OPQ \text{ (see fig. II, 7).}$$

So $T_{s.h.} = \frac{2}{\bar{\psi}} \times$ area OPQ.

Applying the symmetry property to a single-heading navigation in a field of uniform circular flow the following results are obtained (cf. II, 2; VI).

a′ In a uniform rectilinear field of limited manoeuvrability the pressure-pattern trajectories associated with a circular stream navigation are hyperboles.

b′ In a uniform rectilinear field of unlimited manoeuvrability the pressure-pattern trajectories associated with a circular stream navigation are ellipses.

c′ In a uniform rectilinear field, where $u = c$, the pressure-pattern trajectories associated with a circular stream navigation are paraboles.

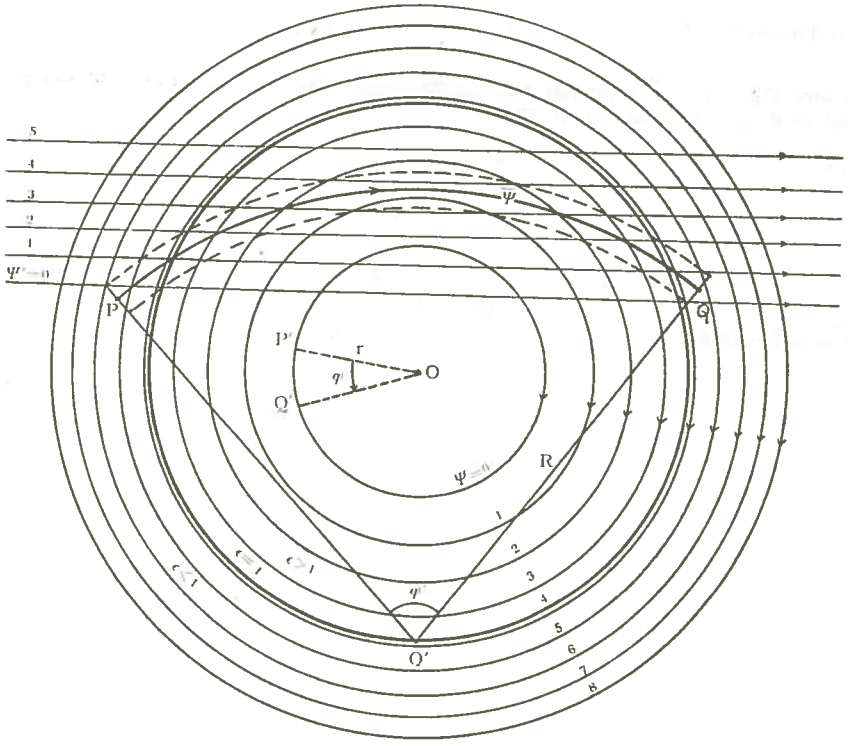

Fig. II, 8.

Solid rotational flow.

The stream-function ψ is: $\psi = \frac{k}{2}(x_1^2 + x_2^2)$. The single-heading trajectories according to II, 1 are given by $\frac{k}{2}(x_1^2 + x_2^2) + cx_2 = A$ with A constant, or in polar coordinates:

$$r^2 + 2ar \sin \alpha + \overline{\psi} = 0. \ \overline{\psi} \text{ a parameter, } a = \frac{c}{k}.$$

This represents a set of concentric circles with its centre M on the limiting isotach $r = a$. For any other heading the solution remains formally unchanged and the figure has only to be rotated through an angle about O. The doubly infinite set of single-heading trajectories consists of all the circles centred on the limiting isotach, $r = a$ ($\epsilon = 1$).

Here also the single-heading trajectories can be constructed by means of the addition method of Maxwell (fig. II, 8). The symmetry property however cannot be applied because the field is not uniform. Although the time of navigation can also be calculated directly by integrating along the trajectory, it will be seen that for circles centred on the limiting isotach the time of navigation is self-evident. For the sum field of a solid rotation and a simple translation is again a solid rotation centred on the limiting isotach and with the same velocity as the original field. Since the figure of the single-heading trajectories is identical with that of the given field of flow, the stream-function of the sum field $\overline{\psi} = \psi + \psi'$ has the same form as ψ. Now $\psi = \frac{k}{2} \cdot r^2$, so in the sum field $\overline{\psi} = \frac{k}{2} R^2$, where R is the distance measured from the centre of the sum field.

According to II, 10: $$T_{s.h.} = \lim_{\Delta\overline{\psi}\to 0} \frac{1}{\Delta\overline{\psi}} O_{\Delta\overline{\psi}}.$$

The area $O_{\Delta\overline{\psi}}$ of a strip between two neighbouring "single-heading circles" $\overline{\psi}$ and $\overline{\psi} + \Delta\overline{\psi}$ is equal to $R \,.\, \varphi' \,.\, \Delta R$. (see fig. II, 8).

Since $$\Delta\overline{\psi} = kR\ \Delta R,$$

$$O_{\Delta\overline{\psi}} = \frac{\varphi'}{k} \,.\, \Delta\overline{\psi}.$$

So: $$T_{s.h.} = \lim_{\nabla\overline{\psi}\to 0} \frac{1}{\Delta\overline{\psi}} \,.\, \frac{\varphi'}{k} \,.\, \Delta\overline{\psi} = \frac{\varphi'}{k}.$$

which is self-evident.

PART III

THE VARIATION PROBLEM IN AERONAVIGATION

Introduction

The problem of finding the path which minimizes the time of travel of a body travelling with a constant true velocity from a point P to a point Q in a moving fluid arises in different forms of several branches of physics. One of the best-known problems is found in the theory of light, where according to the Law of Fermat the path of a ray of light is a minimizing extremal with respect to all adjacent paths. This law is based on the minimizing property of the path of a ray with respect to the integral $\int_P^Q n \, . \, ds$, where n is the refractive index of the medium under consideration. If n is constant throughout the medium the rays are all rectilinear, but if n is a function of the space coordinates, i.e. if the medium is non-homogeneous, they are curved. If a discontinuity exists in the medium, for instance at the boundary surface of two media with different refractive indices, the rays will be refracted. This refraction is governed by the Law of Snellius: $n \sin i =$ constant, or the numerical aperture, which is the product of the refractive index and the sine of the angle of refraction i, is constant along the path of a ray. If the boundary surface is impermeable to light the rays will be reflected according to the law of reflection: the angle of incidence is equal to the angle of reflection.

If the refractive index n is a function not only of the space coordinates, but also of the direction of a ray of light, in other words if the medium is neither homogeneous nor isotropic, the analogy with the variation problem of aeronavigation is complete. For this is the problem of finding an arc, which minimizes the line intregal $\int_P^Q \frac{ds}{w}$, where w is the total speed of the ship, which depends both on the position of the ship and on its heading. Non-isotropic media in which the velocity of light depends on the direction hardly occur in nature. A special case is that of crystals with double refraction.

The analogy between the Law of Fermat and the variation problem of aeronavigation was pointed out by Frank (3).

The laws of refraction and reflection also occur in aeronavigation though in a modified form. Also the principle of Huygens described in his "Traité de la lumière" (1690) is found again in aeronavigation. The figure of rays of light and wave fronts is shown to correspond with the *complete figure of time fronts and extremals.*

Although the problem of aeronavigation was first studied by Giblett, who

worked out a method of constructing extremals (4), Zermelo (5) was the first to for mulate the problem as a problem of the calculus of variation, in a lecture at Prague, titled: "Ueber der Navigation in der Luft als Problem der Variationsrechnung". The solution of the problem, now known as the "Navigation equation of Zermelo" applies to non-stationary plane currents. In his text-book "Variationsrechnung und partielle Differentialgleichungen" Carathéodory gives a solution of the same problem, but now for stationary ocean currents (6). This solution is derived by means of a Hamilton function.

Since the present problem belongs to the simplest class of problems of the calculus of variations, the navigation equation of Zermelo is derived in this chapter using the Euler-Lagrange differential equation. A second interpretation of the problem is given by means of the theory of Hamilton-Jacobi, and the theory of the indicatrix and the complete figure of Carathéodory in order to illustrate the connection between this problem and the principle of Huygens.

In the present treatment the principles of the calculus of variations are applied without proof.

1. The navigation equation of Zermelo

The variation problem may be formulated as follows:
Given two points P and Q in a plane stationary field of flow, to find the pressure-pattern trajectory along which a ship will travel from P to Q in the shortest possible time.

Since the solution of the problem so formulated has to satisfy certain boundary conditions at P and at Q it is for the present not certain that such a pressure-pattern trajectory exists.

The flow will again be defined by means of a vector field $\vec{u}\,(u_1, u_2)$ where u_1 and u_2 are the flow-distribution functions $\vec{u_1}\,(x_1, x_2)$ and $\vec{u_2}\,(x_1, x_2)$. The true velocity vector $\vec{c}\,(c\cos\xi, c\sin\xi)$ has a constant magnitude.

The sum field is again a vector field $\vec{w}\,(w_1, w_2)$ with $\vec{w} = \vec{u} + \vec{c}$.

In general the integral for the time of navigation has the form:

$$T = \int F\,(x_1, x_2, \dot{x}_1, \dot{x}_2)\,dt$$

where F must be a positive homogeneous function of the first order.

Supposing that everywhere $\dot{x}_1 > o$ one may write for T:

$$T = \int f(x_1, x_2, p)\,dx_1, \tag{III,1}$$

where according to I, 5:

$$p = \frac{w_2}{w_1} = \frac{\dot{x}_2}{\dot{x}_1} = \frac{u_2 + c\sin\xi}{u_1 + c\cos\xi}, \quad p = \frac{dx_2}{dx_1} \tag{III, 2}$$

According to I, 5: $$f = \frac{1}{w_1} = \frac{1}{u_1 + c\cos\xi},$$

and $T = \int \frac{dx_1}{u_1 + c\cos\xi}$, where ξ is related to u_1, u_2 and p by the steering equation.

It is supposed that f_{x_2}, f_p and f_{pp} exist and are continuous. Primarily is is supposed that $\vec{u}(x_1, x_2)$ is defined and continuous with continuous derivatives in the whole field of flow. The present variation problem differs from the classical problems in so far as the variation of p is bounded in an interval $p_1 \leqslant p \leqslant p_2$ where p_1 and p_2 correspond to the tangents to the indicatrix through its base point (see fig. I, 2c). Besides p is determined implicitely by ξ. With each value of p correspond two values of ξ, except for $p = p_1$ and $p = p_2$ with only one value $\xi = \xi_1$ and $\xi = \xi_2$ respectively which satisfy the relation $c_e = c + u_1 \cos \xi + u_2 \sin \xi = 0$. So, if ξ varies in the interval $\xi_1 \leqslant \xi \leqslant \xi_2$ for which $c_e \geqslant o$ or ξ varies in the interval $\xi_2 \leqslant \xi \leqslant \xi_1$, for which $c_e \leqslant o$, p varies in the interval $p_1 \leqslant p \leqslant p_2$. Now f_p and f_{pp} have c_e in the numerator. See III, 5 and III, 13. Therefore $c_e = 0$ must be excluded.

From the above considerations it is clear that the problem can be solved seperately for the case that everywhere along the trajectories $c_e > o$ with $\xi_1 < \xi < \xi_2$ and for the case that everywhere along the trajectories $c_e < o$ with $\xi_2 < \xi < \xi_1$. However, it will be shown that for $c_e > o$ only minimizing extremals can exist and for $c_e < o$ only maximizing extremals (see III. 2). Now supposing e is a minimizing extremal through the points P and Q with time of navigation T_e, while γ is an admissable trajectory through P and Q in the neighbourhood of e (with everywhere $c_e > o$) and time of navigation T_γ, then $T_\gamma > T_e$. Along γ a second manoeuvre is possible with everywhere $c_e < o$ and time of navigation T_γ'. Since for this manoeuvre along γ at every point the total speed $w = |\vec{u} + \vec{c}|$ is smaller than the speed for the first manoeuvre along γ, it follows that always $T_\gamma' > T_\gamma > T_e$. Therefore e is also a minimizing extremal for all trajectories in the vicinity of e, along which $c_e < o$ ($\xi_2 < \xi < \xi_1$). A similar result is found for maximizing extremals. Summarizing one finds that the extremal e is a maximizing or minimizing extremal for all trajectories in its vicinity, along which either $c_e < o$, or $c_e > o$.

The problem remains unsolved if along the trajectories the sign of c_e changes, in other words if the trajectories contain anomalous line elements ($o < \xi \leqslant 2\pi$).

In order to get an extreme value for the time of navigation T the first requirement is that the trajectory is an extremal, in other words the trajectory must be a solution of the Euler-Lagrange differential equation:

$$f_{x_1} - \frac{d}{dx_1} f_p = 0. \qquad \text{(III, 3)}$$

Writing III, 2 in the form $p = \frac{w_2}{w_1}$ and taking x_1, x_2 and p as independent variables, partial differentiation with respect to these variables leads to the following expressions:

$$\begin{aligned} 0 &= w_1 \frac{\partial w_2}{\partial x_1} - w_2 \frac{\partial w_1}{\partial x_1}, \\ 0 &= w_1 \frac{\partial w_2}{\partial x_2} - w_2 \frac{\partial w_1}{\partial x_2}, \\ 1 &= \frac{c\,(w_1 \cos \xi + w_2 \sin \xi)}{w_1^2} \frac{\partial \xi}{\partial p}. \end{aligned} \qquad \text{(III, 4)}$$

Now according to I, 8 and I, 5 the effective true velocity is:

$$c_e = c + u_1 \cos\xi + u_2 \sin\xi = (c\cos\xi + u_1)\cos\xi + (c\sin\xi + u_2)\sin\xi = \\ = w_1 \cos\xi + w_2 \sin\xi.$$

From the last relation of III, 4 it follows that:

$$\frac{\partial\xi}{\partial p} = \frac{{w_1}^2}{cc_e}.$$

The two terms of the Euler-Lagrange differential equation III, 3 become:

$$f_p = -\frac{1}{{w_1}^2}\frac{\partial w_1}{\partial p} = \frac{c}{{w_1}^2}\sin\xi\frac{\partial\xi}{\partial p} = \frac{\sin\xi}{c_e}, \qquad \text{(III, 5)}$$

$$f_{x_2} = -\frac{1}{{w_1}^2}\frac{\partial w_1}{\partial x_2}.$$

Substituting these terms in the Euler-Lagrange differential equation one gets,

$$-\frac{1}{{w_1}^2}\frac{\partial w_1}{\partial x_2} - \frac{d}{dx_1}\frac{\sin\xi}{c_e} = 0,$$

or

$$\frac{1}{w_1}\frac{\partial w_1}{\partial x_2} - \frac{d}{dt}\left(\frac{1}{w_1\operatorname{cotan}\xi + w_2}\right) = 0, \qquad \text{(III, 6)}$$

$$\frac{1}{w_1}\frac{\partial w_1}{\partial x_2} - \frac{\sin\xi\cos\xi}{{c_e}^2}\left(w_1\frac{\partial w_1}{\partial x_1} + w_2\frac{\partial w_1}{\partial x_2}\right) - \frac{\sin^2\xi}{{c_e}^2}\left(w_1\frac{\partial w_2}{\partial x_1} + w_2\frac{\partial w_2}{\partial x_2}\right) + \frac{w_1}{{c_e}^2}\frac{d\xi}{dt} = 0.$$

Using the second relation of III, 4 and substituting for $\frac{\partial w_2}{\partial x_2}$:

$$\frac{d\xi}{dt} = \sin\xi\cos\xi\frac{\partial w_1}{\partial x_1} + \sin^2\xi\frac{\partial w_2}{\partial x_1} - \left(\frac{{c_e}^2 - w_1 w_2\sin\xi\cos\xi - {w_2}^2\sin^2\xi}{{w_1}^2}\right)\frac{\partial w_1}{\partial x_2},$$

$$\frac{d\xi}{dt} = \sin\xi\cos\xi\frac{\partial w_1}{\partial x_1} + \sin^2\xi\frac{\partial w_2}{\partial x_1} - \cos^2\xi\frac{\partial w_1}{\partial x_2} - \frac{w_2}{w_1}\sin\xi\cos\xi\frac{\partial w_1}{\partial x_2}.$$

Using the second relation of III, 4 again, the equation finally becomes:

$$\frac{d\xi}{dt} = \frac{\partial w_2}{\partial x_1}\sin^2\xi + \left(\frac{\partial w_1}{\partial x_1} - \frac{\partial w_2}{\partial x_2}\right)\sin\xi\cos\xi - \frac{\partial w_1}{\partial x_2}\cos^2\xi. \qquad \text{(III, 7)}$$

Now differentiate the components $w_1 = u_1 + c\cos\xi$ and $w_2 = u_2 + c\sin\xi$ partially with respect to x_1 and x_2:

$$\frac{\partial w_1}{\partial x_1} = \frac{\partial u_1}{\partial x_1} - c\sin\xi\frac{\partial\xi}{\partial x_1},$$

$$\frac{\partial w_1}{\partial x_2} = \frac{\partial u_1}{\partial x_2} - c\sin\xi\frac{\partial\xi}{\partial x_2},$$

$$\frac{\partial w_2}{\partial x_1} = \frac{\partial u_2}{\partial x_1} + c\cos\xi\,\frac{\partial \xi}{\partial x_1},$$

$$\frac{\partial w_2}{\partial x_2} = \frac{\partial u_2}{\partial x_2} + c\cos\xi\,\frac{\partial \xi}{\partial x_2}.$$

Substitution of these terms in equation III, 7, finally leads to the well-known *navigation equation of Zermelo*:

$$\boxed{\frac{d\xi}{dt} = \frac{\partial u_2}{\partial x_1}\sin^2\xi + \left(\frac{\partial u_1}{\partial x_1} - \frac{\partial u_2}{\partial x_2}\right)\sin\xi\cos\xi - \frac{\partial u_1}{\partial x_2}\cos^2\xi} \qquad \text{(III, 8)}$$

The extremals of the variation problem are determined by this equation and the steering equation.

If at a given point the coordinate system is so chosen that the x_1-axis coincides with the direction of navigation, then the navigation equation reduces to

$$\frac{d\xi}{dt} = -\frac{\partial u_1}{\partial x_2} \qquad \text{(III, 9)}$$

for $\sin\xi = o$, $\cos\xi = 1$.

According to III, 7 the navigation equation also reduces to

$$\frac{d\xi}{dt} = -\frac{\partial w_1}{\partial x_2}$$

where w_1 is identical with the effective true velocity.

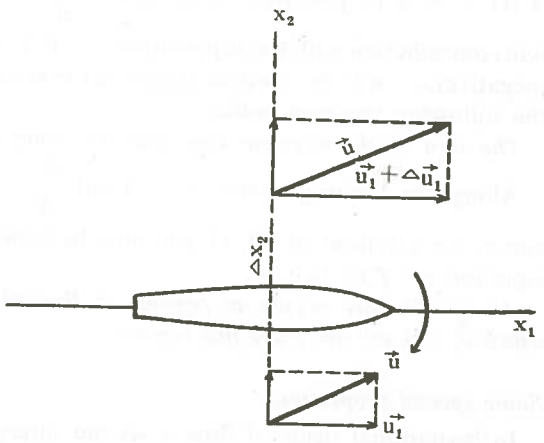

Fig. III, 1.

This result may be interpreted as follows: *Along an extremal the ship must be navigated in such a manner that the change of the heading per unit time is equal to the shear of the effective true velocity or to the shear of the flow component in the direction of the main axis. The ship must be steered in such a manner that its axis turns towards the direction in which the tail component decreases or the head component increases* (fig. III, 1).

If both sides of the navigation equation III, 4 are divided by $\cos^2\xi$, this equation may be written in the form:

$$\frac{d\tan\xi}{dt} = \frac{\partial u_2}{\partial x_1}\tan^2\xi + \left(\frac{\partial u_1}{\partial x_1} - \frac{\partial u_2}{\partial x_2}\right)\tan\xi - \frac{\partial u_1}{\partial x_2}. \qquad \text{(III, 10)}$$

In addition to the navigation equation of Zermelo, which contains an expression for the rate of change with time of the heading along the extremal, one

can also derive an expression for the rate of change of the effective true velocity c_e along the extremal.

After a calculation similar to the one required for the derivation of the navigation equation, an expression is obtained for this rate of change with time of c_e along an extremal. This calculation will not be reproduced here, but the result is given below:

$$\frac{dc_e}{dt} = c_e \left\{ \frac{\partial u_1}{\partial x_1} \cos^2 \xi + \left(\frac{\partial u_1}{\partial x_2} + \frac{\partial u_2}{\partial x_1} \right) \sin \xi \cos \xi + \frac{\partial u_2}{\partial x_2} \sin^2 \xi \right\}. \quad \text{(III, 11)}$$

The equation states that the sign of c_e does not change along the extremal. For one can write $\frac{dc_e}{dt} = A(t)c_e$, where the coefficient A of c_e is a function of t only along the extremal. Suppose in a t-interval (o, t_1) $c_e \geqslant o$. Since $A(t)$ is bounded: $A(t) > -k$ (k positive). That means $\frac{dc_e}{dt} \geqslant -kc_e$ or $c_e \geqslant c_e(o)e^{-kt} > 0$. This is in contradiction with the supposition $c_e \geqslant 0$. If at a point of the extremal c_e is positive (negative), c_e will be positive (negative) everywhere along the extremal. Therefore the following theorem holds:

The sign of the effective true velocity along an extremal is permanent.

Along the limiting curves $c_e \equiv 0$ and $\frac{dc_e}{dt} \equiv 0$. This means, that the limiting curves are solutions of III, 11 and may be considered as solutions of the navigation equation of Zermelo.

As $c_e < 0$ only occurs in regions of limited manoeuvrability the extremals along which $c_e < 0$ will not leave this region.

Some special properties.

In irrotational fields of flow a second interpretation of the navigation equation is possible. Since $\frac{\partial u_1}{\partial x_2} = \frac{\partial u_2}{\partial x_1}$, the simplified navigation equation of Zermelo III, 9 may be written:

$$\frac{d\xi}{dt} = -\frac{\partial u_2}{\partial x_1}.$$

In words: In irrotational fields of flow the rate of change of the heading with time along an extremal is equal to the shear of the flow component at right angles to the main axis.

If the right hand side of the equation III, 11 is identically equal to zero, c_e will be constant along every extremal. The identity $\frac{dc_e}{dt} \equiv 0$ occurs, when all the coëfficients on the right hand side are identically equal to zero, so $\frac{\partial u_1}{\partial x_1} = \frac{\partial u_2}{\partial x_2} \equiv 0$ and $\frac{\partial u_1}{\partial x_2} + \frac{\partial u_2}{\partial x_1} \equiv 0$.

It follows from the first two relations that u_1 and u_2 are independent of x_1 and x_2 respectively, so one may write:

$$u_1 = F(x_2) + l,$$
$$u_2 = G(x_1) + m, \text{ where } l \text{ and } m \text{ are constants.}$$

The third ralation requires that

$$F'(x_2) = -G'(x_1).$$

This can only be achieved if both derivatives $F'(x_2)$ and $-G'(x_1)$ are equal to one and the same constant k:

$$F'(x_2) = -G'(x_1) = k.$$

The solution for the field of flow is therefore:

$$u_1 = kx_2 + l,$$
$$u_2 = -kx_1 + m. \qquad \text{(III, 12)}$$

The field of flow $\vec{u}(u_1, u_2)$ in which the effective true velocity along the extremals is constant, therefore consists of the superposition of a translation $u_1 = l$, $u_2 = m$ and a solid rotation $u_1 = kx_2$, $u_2 = -kx_1$ with angular velocity k. As such a superposition is equivalent to a simple displacement of the field of rotation one finally finds:

Both in a field of solid rotation and in a uniform rectilinear field of flow the effective true velocity is constant along every extremal.

In the trivial case in which no field of flow $\vec{u}$ exists the navigation equation of Zermelo reduces to the indentity:

$$\frac{d\xi}{dt} \equiv 0.$$

or ξ is constant along an extremal. Substituting for ξ in the steering equation one has:

$$\frac{dx_2}{dx_1} = \tan \xi = \text{const.},$$

the solution of which consists of straight lines making an angle ξ with the x_1-axis. This solution applies to the problem of finding the trajectories along which a body moving at a constant true velocity c will travel in the shortest possible time from a point P to a point Q. It also expresses the principle of Fermat for homogeneous isotropic media, where the true velocity is identical with the velocity of light.

2. The Legendre condition

Minimizing and Maximizing extremals.

Whether an extremal arc is a minimizing or maximizing extremal arc it is necessary that along the extremal arc the condition of Legendre is satisfied. Along a

minimizing extremal arc the expression $F_1 = \frac{1}{\dot{x}_1^3} f_{pp} = \frac{1}{w_1^3} f_{pp} > 0$ should hold. Along a maximizing extremal arc it is necessary that $F_1 < 0$.

Partial differentiation of $f_p = \frac{\sin \xi}{c_e}$ with respect to p gives:

$$f_{pp} = \frac{\partial}{\partial p} f_p = \frac{\partial}{\partial p} \frac{\sin \xi}{c_e} = \frac{\partial}{\partial p} \frac{1}{w_1 \operatorname{cotan} \xi + w_2}$$

$$= - \sin^2 \xi \frac{\left(\operatorname{cotan} \xi \frac{\partial w_1}{\partial p} + \frac{\partial w_2}{\partial p} - \frac{w_1}{\sin^2 \xi} \frac{\partial \xi}{\partial p} \right)}{c_e^2}.$$

Now $$\frac{\partial w_1}{\partial p} = - c \sin \xi \frac{\partial \xi}{\partial p}, \qquad \frac{\partial w_2}{\partial p} = c \cos \xi \frac{\partial \xi}{\partial p}, \qquad \frac{\partial \xi}{\partial p} = \frac{w_1^2}{c \, . \, c_e},$$

so $$F_1 = \frac{1}{w_1^3} f_{pp} = \frac{w_1^3}{w_1^3 c \, c_e^3} = \frac{1}{c \, c_e^3}. \qquad \text{(III, 13)}$$

As the sign of F_1 is entirely determined by the sign of c_e the effective true velocity along a minimizing extremal arc must be positive and along a maximizing extremal arc the sign must be negative. According to III, 11 the sign of c_e is the same along the entire extremal. Therefore the extremal can be a minimizing extremal, if at one point on the extremal $c_e > 0$ and a maximizing extremal if at one point on the extremal $c_e < 0$. Since according to chapter I, 3 the sign of c_e is indicative of the navigational character of the field of flow the following results may be mentioned:

In a field of flow of limited manoeuvrability or in fields of flow with both regions of limited and unlimited manoeuvrability minimizing and maximizing extremals can exist. Since $c_e < 0$ only occurs in regions of limited manoeuvrability, maximizing extremals can only lie in regions of limited manoeuvrability.
In a field of flow of unlimited manoeuvrability ($c_e > 0$) maximizing extremals do not exist.

For anomalous line elements on limiting curves along which $c_e = 0$ the expression F_1 has no significance.

It is stated once more that these results hold for admissable trajectories along which everywhere $c_e < 0$ or $c_e > 0$. Trajectories along which the sign of c_e changes, that is, trajectories which for $c_e = 0$ contain anomalous line elements, are excluded.

The limiting curves may be regarded as extremals. This is trivial because in its own vicinity a limiting curve is the *only* trajectory, which exists between two of its points. The limiting curves cannot be varied for if a ship moving along a limiting curve abandons the curve at any point it can not get back to it but for a long way round.

3. The Jacobi condition. Fields of extremals. Weak and strong extremes. Absolute extremes

For an extremal arc e through the points P and Q to be a minimizing or a maximizing extremal arc it is generally necessary that, in addition to the Legendre condition being satisfied, P and Q are lying in between two *conjugate* points. In a few cases, however, Q may coincide with a conjugate point of P. The conjugate point of a point P on an extremal e is identical with the first tangent point of e with the envelope of the set of extremals trough P, often called *focal curve*. The condition to find this point is equivalent with the well-known Jacobi condition.

When the envelope of the set of extremals through P is known, an "improper" *field* of extremals with P as nodal point can also be defined. For this field is formed by extremal arcs with P as starting point and their first tangent points with the envelope as terminal points.

Since in aeronavigation the time of navigation depends on the direction of travel along the extremal one can also consider the set of extremal arcs through P with P as terminal point. On any extremal arc with P as terminal point a point $\underline{P}$ may be found for wich P is the conjugate point. The points $\underline{P}$ again lie on the envelope of this set of extremal arcs. Therefore a second field of extremal arcs through P may be considered, consisting of extremal arcs with P as terminal point and their first tangent points with the envelope as starting points.

In this manner *two* improper fields of extremals can be found through any given point P.

Since in the present variation problem both minimizing and maximizing extremals may occur, a distinction must also be made between sets of minimizing and sets of maximizing extremals. Both for the minimizing and maximizing extremals both improper fields described above can be defined. Therefore a total of *four* improper fields of minimizing and maximizing extremals respectively can be found with nodal point P. Two by two the fields are determined by the sign of c_e. For $c_e^* > 0$ *two fields of minimizing extremals are found, for* $c_e < 0$ *two fields of maximizing estremals.*

The case of four fields of minimizing and maximizing extremals with nodal point P only occurs in regions of limited manoeuvrability. The fields may partially overlap. It these four fields have a common section and if a point Q is chosen in that section there will be at least two minimizing and two maximizing extremals passing through P and Q, each with a definite sense of direction.

Fields of maximizing extremals always lie entirely within the region of limited manoeuvrability of a field of flow because according to III, 2 maximizing extremals cannot leave this region. Therefore, if an arbitrary point Q is given in the region of unlimited manoeuvrability, only minimizing extremals will be found between P and Q.

The minimizing or maximizing properties of an extremal are sensitive to the way in which the trajectories are varied. Therefore two types of extremes can be distinguished. An extremal furnishes a *weak extreme* for the line intregral, if there exists a neighbourhood N in x_1 x_2, p-space of the elements (x_1, x_2, p) on the extremal,

such that the value of the line integral along the extremal is either greater or smaller than the value given by every other admissible trajectory, whose elements lie in the neighbourhood N. An extremal furnishes a *strong extreme* for the line integral if there exists a neighbourhood F of the points (x_1, x_2) on the extremal such that the line integral along the extremal is either greater or smaller than the value given by every other admissible trajectory interior to F. Now consider an extremal arc e between two conjugate points P and Q. Suppose that e in the neighbourhood N of e can be embedded in a field of extremal arcs. Then the calculus of variation shows that these arcs yield a weak relative minimum if $F_1 = \frac{1}{cc_e^3} > 0$, or $c_e > 0$ at any point on the admissable trajectories within N and a weak relative maximum if $F_1 < 0$, or $c_e < 0$ at any point on the admissable trajectories within N. However this condition is automatically fulfilled, because by solving the navigation problem only those trajectories were admitted for which at any point $c_e > 0$, or $c_e < 0$.

It can be easily shown by means of the well-known E-function of Weierstras (c.f. part III, 8) that under the same conditions the extremal arcs also yield a strong relative minimum or maximum.

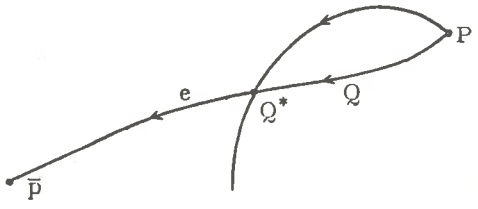

Fig. III, 2.

In practice the chief problem is to find not just a minimizing extremal between two points P and Q, which furnishes a relative minimum for the integral of the time of navigation, but rather the extremal, for which the value of the integral is an *absolute minimum* with respect to all trajectories through P and Q within the region B, in which the variation problem is defined.

Let an arbitrary minimizing extremal e be given with starting point P and conjugate point $\bar{P}$ (fig. III, 2). Every arc PQ of this extremal furnishes a relative minimum for the time of navigation provided Q lies between P and $\bar{P}$. If Q moves along the arc $P\bar{P}$, then, according to a theorem by Darboux, there is a point Q^* between P and $\bar{P}$ such that the arc PQ^* furnishes an absolute minimum for the time of navigation if Q lies between P and Q^*, but only a relative minimum if Q lies between Q^* and $\bar{P}$. The point Q^* is the point of intersection of the extremal arc e and a second extremal arc PQ *not in the neighbourhood of* e, but along which the time of navigation has the same value as along e. The locus of all points Q^* on the extremal arcs of an improper field of minimizing extremals with nodal point P is an important curve, which may be used to decide whether along a minimizing arc PQ the absolute minimum can be realised. In chapter III, 6 it will be shown how this curve can be constructed using the complete figure of Carathéodory.

The curve connecting the points Q^* in a field of extremals plays a similar role with respect to the absolute minimum as the envelope of the improper field with respect to the relative minimum.

4. Example

The extremals in a uniform rectilinear field of flow.

The field of flow is defined by the equations $u_1 = k$, $u_2 = 0$.

The navigation equation of Zermelo becomes: $\frac{d\xi}{dt} \equiv 0$ and the solution is $\xi = \xi_0 =$ constant. So the extremals in a uniform recti linear field of flow are simply single-heading trajectories. The trajectories are found by integrating the steering equation after substitution of $\xi = \xi_0$:

$$\dot{x}_1 = k + c \cos \xi_0,$$
$$\dot{x}_2 = c \sin \xi_0.$$

The solution is

$$x_1 = k (1 + \varepsilon \cos \xi_0)\, t$$
$$x_2 = k\varepsilon (\sin \xi_0)\, t,$$

where $\varepsilon = \frac{c}{k}$ is the velocity parameter.

Therefore the extremals are straight lines.

It follows from the navigation equation for c_e, which here reduces to $\frac{dc_e}{dt} \equiv 0$, that c_e remains constant along an extremal. The value of c_e is given by:

$$c_e = c + \frac{1}{c} \vec{u} \,.\, \vec{c} = c + k \cos \xi = k (\varepsilon + \cos \xi).$$

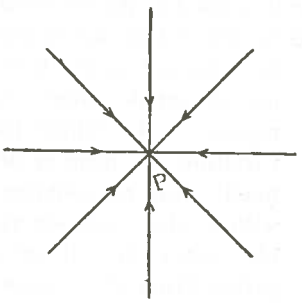

Fig. III, 3,a.

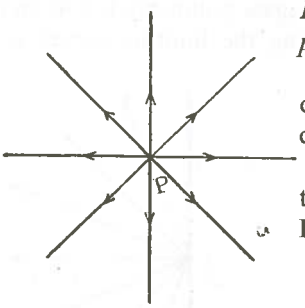

Fig. III, 3,b.

Improper fields with nodal point P.

The fields consist of sets of straight lines with P as common point.

Three cases may be distinguished:

I. Uniform recti linear fields of unlimited manoeuvrability ($\varepsilon > 1$). In this case there are two improper fields of minimizing extremals ($c_e > 0$). The sets of straight lines cover the entire interval ($0 - 2\pi$) (fig. III, 3*a*, *b*).

II. Uniform recti linear fields of limited manoeuvrability ($\varepsilon < 1$). The sets of straight lines cover a sector bounded by the limiting straight lines g_1 and h_1 which are defined by the condition $c_e = 0$ or $\cos \xi = -\varepsilon$.
Since c_e can be either positive or negative there exist according to part III, 3 two fields of minimizing and two fields of maximizing extremals (fig. III, 4*a*, *b*).
A point Q within the sector bounded by g_1 and h_1 can be reached from P both along a minimizing and along a maximizing extremal. Conversely P cannot be reached from Q (fig. III, 4*a*).

III. Uniform rectilinear fields in which the stream velocity is equal to the true velocity c ($\varepsilon = 1$).
The limiting angle is now equal to π. In these fields $c_e \geqslant 0$. Only minimizing extremals exist. There are also two improper fields of minimizing extremals (fig. III, 5*a*, *b*).

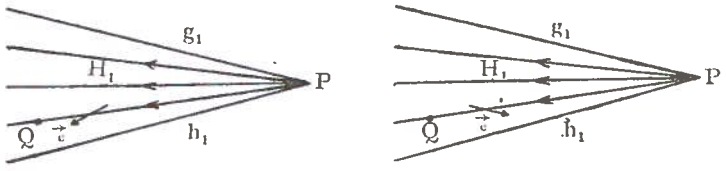

Fig. III, 4,a.

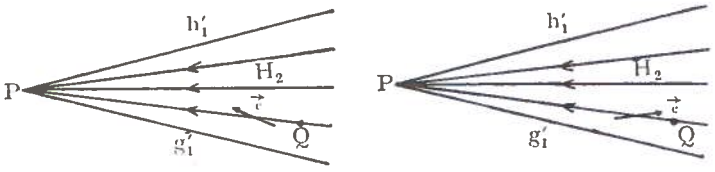

Fig. III, 4,b.

In all three cases no conjugate points are found on the extremals. For the extremals have no envelope, excluding the limiting curves g_1 and h_1, which themselves may be regarded as the limiting extremals. Since the region B, in which the variation problem is defined, must be contained within the manoeuvrable sector H_1, if navigation from P is considered, or in the sector H_2, if navigation to P is considered, it is entirely covered by the improper fields of extremals with P as nodal point. Therefore the minimizing and maximizing extremals furnish an *absolute* extreme for the time of navigation.

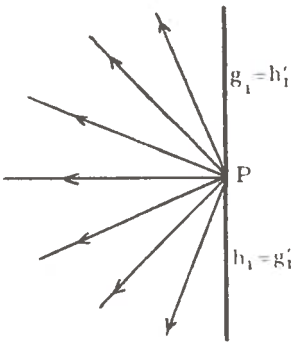

Fig. III, 5,a.

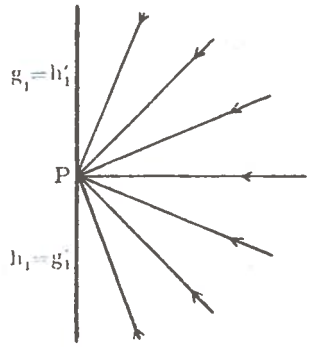

Fig. III, 5,b.

The boundary value problem can always be solved in this case since through any two points P and Q only one minimizing or maximizing extremal PQ or QP can be constructed, provided one of the points lies in the manoeuvrable sector of the other.

5. The theory of Hamilton-Jacobi, the theory of the indicatrix and the complete figure of Carathéodory

By means of the theory of Hamilton-Jacobi a second solution of the variation problem can be found, which presents a very clear picture and which in special problems admits a simple interpretation. This theory also contains the elements required for a quick graphical construction method and clarifies the connection which exists between the present variation problem and the principle of Huygens in the theory of light. Using the results of this theory the navigation equation of Zermelo can be derived in an elementary manner.

Hilberts invariant integral.

Consider a field of extremals and an arbitrary rectifiable curve γ within the field through two points P and Q. Then the line integral

$$J = \int_\gamma \{f(x_1, x_2, p) - pf_p(x_1, x_2, p)\}\, dx_1 + f_p(x_1, x_2, p)\, dx_2,$$

where p refers to a line element of a field extremal at a point on γ, is independent of the path of integration and only depends on the position of the terminal points P and Q. This is Hilberts invariant integral, which, in case γ coincides with a field extremal e, reduces to the ordinary fundamental integral $\int_e f(x_1, x_2, p)\, dx_1$.

If P is kept stationary and Q is allowed to vary, the value of Hilberts invariant integral J is a function of the coordinates of Q only and one may write:

$$J = W(x_1, x_2) + \text{a constant.}$$

The value of the integral J along an arbitrary curve γ is determined by the values of W at P and Q respectively:

$$J_{PQ} = W_Q - W_P.$$

The integral J may also be written:

$$J = \int_\gamma \frac{\partial W}{\partial x_1}\, dx_1 + \frac{\partial W}{\partial x_2}\, dx_2,$$

where

$$\frac{\partial W}{\partial x_1} = f - pf_p,$$

$$\frac{\partial W}{\partial x_2} = f_p.$$

In the present problem W is identical with the time of navigation and therefore will be called *time function*.

According to III, 5 f_p and $f - pf_p$ may be expressed in ξ and c_e:

$$f_p = \frac{\sin\xi}{c_e},\quad f - pf_p = \frac{1}{w_1} - \frac{w_2}{w_1}\frac{\sin\xi}{c_e} = \frac{w_1\cos\xi + w_2\sin\xi - w_2\sin\xi}{w_1 c_e} = \frac{\cos\xi}{c_e}.$$

so

$$\frac{\partial W}{\partial x_1} = \frac{\cos\xi}{c_e} \text{ and } \frac{\partial W}{\partial x_2} = \frac{\sin\xi}{c_e}. \qquad \text{(III, 14)}$$

From these relations two important properties can be derived, the gradient property and the property of transversality.

I. *The gradient property.*

Eliminating the heading ξ from the relations III, 14 one finds:

$$c_e^2 \left\{ \left(\frac{\partial W}{\partial x_1} \right)^2 + \left(\frac{\partial W}{\partial x_2} \right)^2 \right\} = 1,$$

$$\text{or} \quad \boxed{(\text{grad } W)^2 = \frac{1}{c_e^2}.} \qquad \text{(III, 15)}$$

The relation states that: *the gradient of W is equal in magnitude to the reciprocal absolute value of the effective true velocity* c_e.

It follows that, if a set of curves $W =$ constant is drawn at unit intervals, the distance between the curves is proportional to c_e.

II. *The property of transversality.*

Eliminating the effective true velocity c_e from the relations III, 14 one finds:

$$\cos \xi \frac{\partial W}{\partial x_2} - \sin \xi \frac{\partial W}{\partial x_1} = 0,$$

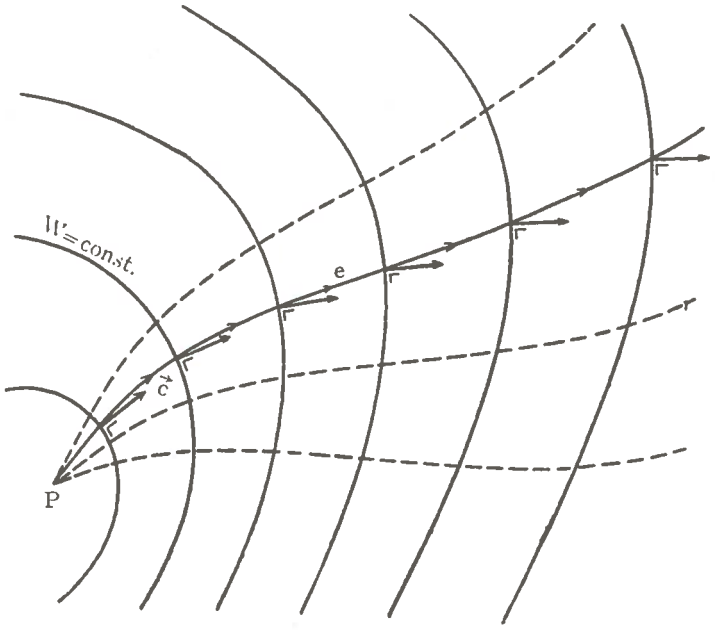

Fig. III, 6.

or in vector form: $\boxed{\vec{c} \times \text{grad } W = 0.}$ (III, 16)

In words: *The vector of the true velocity $\vec{c}$ associated with a line element on a field extremal e is perpendicular to the curve W = constant through its starting point* (fig. III, 6).

If the field formed by the true velocity vectors $\vec{c}$ is regarded as a pseudo field of flow, relation III, 16 may be formulated as follows:

The stream-lines of the pseudo field of flow $\vec{c}$ associated with a field of extremals are the orthogonal trajectories of the set of curves W = constant.

A close connection exists between the field of extremals and the curves W = constant. This connection will now be examined by means of the concept of *transversality*.

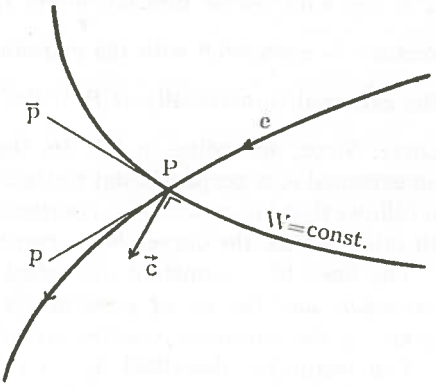

Fig. III, 7.

Let a point P (x_1^0, x_2^0) be given on an arbitrary extremal e and an arbitrary curve γ passing through this point (fig. III, 7). The curve γ is now said to intersect the extremal transversally if the transversality condition:

$$f(x_1^0, x_2^0, p) + (\bar{p} - p) f_p(x_1^0, x_2^0, p) = 0,$$

where p refers to a line element on the extremal and $\bar{p}$ to a line element on the curve γ, is satisfied at P.

In the present problem

$$f = \frac{1}{w_1}, \quad p = \frac{w_2}{w_1}, \quad \bar{p} = \frac{\bar{w}_2}{\bar{w}_1} \quad \text{and} \quad f_p = \frac{\sin \xi}{c_e},$$

where $\bar{w}_1$ and $\bar{w}_2$ are the components of the sum vector $\vec{\bar{w}}$ of the stream vector and the true velocity vector, associated with a manoeuvre along γ. So the condition here becomes:

$$\frac{1}{w_1} + \left(\frac{\bar{w}_2}{\bar{w}_1} - \frac{w_2}{w_1}\right) \frac{\sin \xi}{c_e} = 0,$$

or

$$\frac{\bar{w}_1 (w_1 \cos \xi + w_2 \sin \xi) + w_1 \bar{w}_2 \sin \xi - w_2 \bar{w}_1 \sin \xi}{w_1 \cdot \bar{w}_1 \cdot c_e} = 0,$$

or

$$\frac{w_1 (\bar{w}_1 \cos \xi + \bar{w}_2 \sin \xi)}{w_1 \bar{w}_1 c_e} = 0.$$

So the transversality condition finally reduces to:

$$\overline{w}_1 \cos \xi + \overline{w}_2 \sin \xi = 0,$$

or in vector form:

$$\vec{\overline{w}} \,.\, \vec{c} = 0.$$

$\vec{\overline{w}}$ is the sum vector directed along the tangent of the curve γ. The true-velocity vector $\vec{c}$ is associated with the extremal through P. The curve γ therefore intersects the extremal transversally at P, if the vector $\vec{c}$ at that point is perpendicular to the curve. Since, according to III, 16, the vector $\vec{c}$, associated with a line element on an extremal e, is perpendicular to the curve $W =$ constant through its starting point, it follows that *the curves $W =$ constant intersect the extremals of the field transversally*. In other words, the curves $W =$ constant are the *transversals* of the field extremals.

The lines $W =$ constant are called *geodesically equidistant* lines. *The set of field extremals and the set of geodesically equidistant lines together form the complete figure of the variation problem according to* Carathéodory (7).

The methodes, described by Galton (8), Giblett (4), Bessemoulin and Pône (9), can be regarded as graphical integration methods for the construction of this complete figure (see part V).

The description of the problem now corresponds completely to the description of the principle of Huygens.

In non-homogeneous isotropic media for instance, which are characterized by a refractive index n, which only depends on the plane coordinates x_1 and x_2 the path of a ray of light from a point P to a point Q is determined by the curve which furnishes a minimum for the "optical length": $S = \int_P^Q n \,.\, ds$ or $\int_P^Q \frac{ds}{v}$ if v is the ratio of the velocity of light in the medium to the velocity of light in vacuum.

Here also the solution of the variation problem can be interpreted in two ways (10):

1. Using Lagrange's differential equations one obtains the equation of motion for a ray of light:

$$n \frac{d}{dt}(\vec{nt}) = \text{grad } n, \text{ where } \vec{t} \text{ is the tangential unit vector.}$$

2. Using the theory of Hamilton-Jacobi one finds:
   a. the gradient property:

$$(\text{grad } S)^2 = n^2.$$

   b. the orthogonal property:
   The path of a ray of light intersects the set of lines $S =$ constant perpendicularly. The lines $S =$ constant are *wave fronts*.

Since the above summary applies to a two-dimensional problem the analogy with the variation problem in aeronavigation is obvious. With the first interpretation corresponds the navigation equation of Zermelo together with the steering equation, while the properties deduced by means of the theory of Hamilton-Jacobi are equivalent to the gradient property and the property of transversality. The reciprocal value of the effective true velocity is analogous to the refractive index and the geodesically equidistant lines correspond with the wave fronts. Because the optical length S is equivalent to the time of navigation W, the geodesically equidistant lines will therefore be called *time fronts. The complete figure of time fronts and extremals corresponds with the figure of rays of light and wave fronts associated with the principle of Huygens.*

For example the figure of wave fronts and rays of light emitted by a point source corresponds with the complete figure of time fronts and extremals for an improper field of extremals with a nodal point. Since in aeronavigation P may be a nodal point of four improper fields of extremals, four complete figures may be constructed about P.

6. The complete figures and the boundary problem

By means of the complete figure of an improper field of extremals the problem of constructing an extremal though two given points P and Q can be solved in an elegant manner.

Consider an extremal e through P and Q, which for the sake of convenience will be assumed to be a minimizing extremal with P as starting point and Q as terminal point (fig. III, 8).

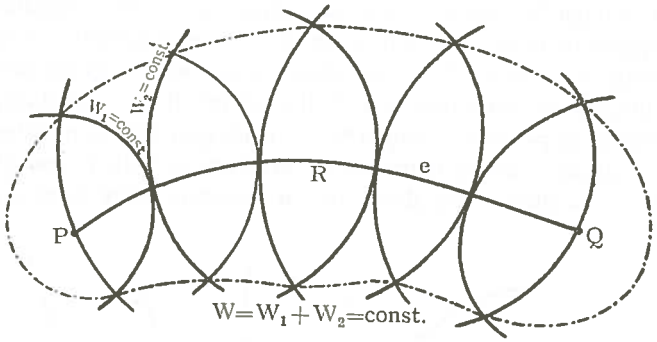

Fig. III, 8.

The minimizing extremal belongs to the improper field of minimizing extremals with P as starting point, but also to the improper field of minimizing extremals with Q as terminal point. With these fields are associated two complete figures, the time fronts of which are defined by the time functions W_1 and W_2. These time functions are normalized in such a manner that W_1 and W_2 are equal to zero at P and Q respectively and positive elsewhere. The value at Q of the time function W_1 associated with the complete figure for P is equal to the time of navigation along the minimizing extremal e. Similarly the value at P of the time function W_2 associated with the complete figure for Q is equal to the time of navigation along the extremal e, so:

$$T = W_1^Q = W_2^P.$$

But also the sum of the values of the time functions W_1 and W_2 at any point R on the extremal arc e must be equal to the time of navigation T, so along the entire arc e the relation:

$$W_1^R + W_2^R = W_1^Q = W_2^P = T \qquad \text{(III, 17)}$$

must hold.

Conversely it follows that the minimizing extremal is the locus of the points of intersection of time fronts $W_1 =$ constant and $W_2 =$ constant, for which the sum of the values of W_1 and W_2 is equal to the value of W_1 at Q and of W_2 at P.

Because of the transversality of time fronts and extremals, the transversal directions in both complete figures through any point on the minimizing extremal must coincide. This means that at any point on the minimizing extremal the associated time fronts $W_1 =$ constant and $W_2 =$ constant must be tangent to each other. These properties also hold for maximizing extremals and may be summarized in the following theorem:

The extremal through two given points P and Q is the locus of the tangent points of the time fronts belonging to the complete figures associated with P and Q, for which the sum of the values of the time functions is constant and equal to the sum of the values at P and *Q*.

In figure III, 8 curves may be drawn through points of intersection of time fronts for which $W_c = W_1 + W_2 =$ constant, which are important in practice. The time of navigation along curves composed of two extremal arcs with a corner or composite point on such a curve remains constant if the composite point moves along this curve ($W_c =$ constant). The time of navigation T is then equal to W_c. Similarly as described in I, 6 the curves $W_c =$ constant, which form the loci of composite points of *composite extremal arcs PQ* along which the time of navigation is constant, can be regarded as *focal curves* with P and Q as foci. Since all curves $W_c =$ constant have these foci in common, they form a confocal set.

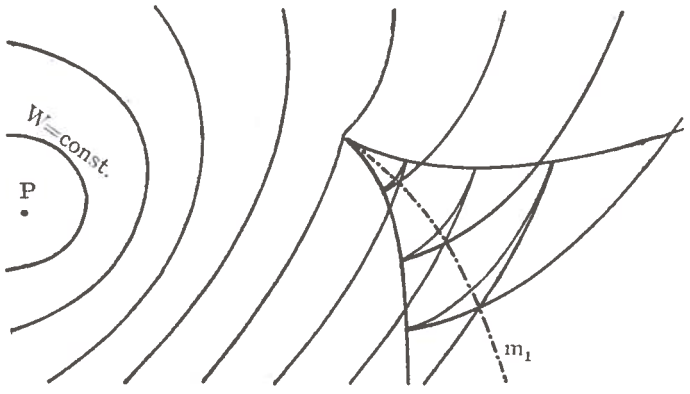

Fig. III, 9.

It is obvious that fig. III, 8 is to be considered as an idealized picture of fig. I, 13.

In III, 3 the occurrence was discussed of a point Q^* on the extremal arc PQ, at which the extremal arc ceases to furnish an absolute minimum for the time of navigation. If Q lies beyond Q^* the extremal arc PQ only guarantees a relative minimum with respect to adjacent trajectories. According to a theorem of D a r b o u x Q^* is the point of intersection of two extremals, not in each others vicinity, along which the time of navigation is the same. D a r b o u x also showed that this point coincides with a *double point* of a time front. Therefore the curve connecting the points Q^*, which in an improper field of extremals plays a similar role with respect to the absolute minimum as the envelope of the improper field of extremals with respect to the relative minimum, consists of the double points of the set of time fronts, which forms part of the complete figure associated with the improper field of extremals.

In fig. III, 9 a set of time fronts such as frequently occur in practice has been drawn together with the "double line" m_1. This figure is of great importance in practice.

7. Hamilton's partial differential equation

The gradient property and the transversality property are characterized by two equations which were derived from the components of grad W by elimination of ξ and c_e respectively. Since the effective true velocity c_e also contains the factor ξ the components of grad W may be regarded as functions of ξ (cf. III, 14). Elimination of ξ then leads to a first-order partial differential equation, which is called H a m i l t o n 's partial differential equation, and which in aeronavigation may be regarded as the second solution of the variation problem.

The elimination of ξ is carried out in the following manner:
From the gradient property it follows that:

$$\sqrt{\left(\frac{\partial W}{\partial x_1}\right)^2 + \left(\frac{\partial W}{\partial x_2}\right)^2} = \frac{1}{c_e} = \frac{1}{c + u_1 \cos\xi + u_2 \sin\xi}.$$

According to the property of transversality the following relation holds:

$$\cos\xi \frac{\partial W}{\partial x_2} - \sin\xi \frac{\partial W}{\partial x_1} = 0.$$

So
$$\sqrt{\left(\frac{\partial W}{\partial x_1}\right)^2 + \left(\frac{\partial W}{\partial x_2}\right)^2} = \frac{\dfrac{\partial W}{\partial x_2}}{c\dfrac{\partial W}{\partial x_2} + \left(u_1 \dfrac{\partial W}{\partial x_1} + u_2 \dfrac{\partial W}{\partial x_2}\right)\sin\xi}.$$

Now according to III, 14 and 15

$$\sin \xi = \frac{\dfrac{\partial W}{\partial x_2}}{\sqrt{\left(\dfrac{\partial W}{\partial x_1}\right)^2 + \left(\dfrac{\partial W}{\partial x_2}\right)^2}}.$$

Substituting this in the above equation one obtains:

$$1 = \frac{1}{c\sqrt{\left(\dfrac{\partial W}{\partial x_1}\right)^2 + \left(\dfrac{\partial W}{\partial x_2}\right)^2} + u_1 \dfrac{\partial W}{\partial x_1} + u_2 \dfrac{\partial W}{\partial x_2}},$$

$$\text{or} \quad \boxed{\left(c^2 - u_1^2\right)\left(\frac{\partial W}{\partial x_1}\right)^2 - 2u_1u_2 \frac{\partial W}{\partial x_1}\frac{\partial W}{\partial x_2} + \left(c^2 - u_2^2\right)\left(\frac{\partial W}{\partial x_2}\right)^2 + 2u_1 \frac{\partial W}{\partial x_1} + 2u_2 \frac{\partial W}{\partial x_2} - 1 = 0.} \qquad \text{(III, 18)}$$

This is Hamilton's partial differential equation for the variation problem of aeronavigation.

In vector form: $$c\,|\,\text{grad}\ W\,| = 1 - \vec{u}\,.\,\text{grad}\ W. \qquad \text{(III, 19)}$$

The general solution of the variation problem as given by the Euler-Lagrange differential equations and, in particular, by the navigation equation of Zermelo together with the steering equation can now also be derived by means of Hamilton's partial differential equation.

For if $W(x_1\ x_2, \alpha)$ is an integral of Hamilton's partial differential equation and if α is not an additive constant, the relation $\dfrac{\partial W}{\partial \alpha} = \beta =$ constant furnishes a doubly infinite set of extremals for the variation problem.

If in $W(x_1, x_2, \alpha)$ α is assumed constant, then $W(x_1, x_2, \alpha)$ represents the set of transversals of the extremals $W_\alpha(x_1, x_2, \alpha) = \beta$. For a given value of α, $W(x_1, x_2, \alpha)$ and $W_\alpha(x_1, x_2, \alpha)$ determine a complete figure.

The *complete* integral of equation III, 18 contains two constants, one of which is additive, because the equation does not contain W itself. Therefore the solution can be written in the form $W = W(x_1, x_2, a) + b$ or $F = W - W(x_1, x_2, a) - b = 0$. In the $(W\,;\,x_1\,;\,x_2)$ space this solution represents a doubly infinite set of integral surfaces. The envelopes of every singly infinite subset of this doubly infinite set form a general solution of the differential equation. According to a theorem due to Kneser (11) the extremals in the $(x_1;\ x_2)$-plane are the projections of the characteristics, which are the limiting positions of the curves of intersection of adjacent integral surfaces. All characteristics passing through one point form an integral surface called *integral conoid. A complete figure for a point P in the $(x_1;\ x_2)$-plane then consists of the projections of the above characteristics and of the curves of intersection of surfaces $W =$ constant and the integral conoid.* Since F contains

an additive constant the integral conoids with their tops on the normal in a point in the $(x_1; x_2)$-plane are equal and similar as well as homologous. A displacement of the conoid perpendicular to the $(x_1; x_2)$-plane makes no difference except that the time function W on the time fronts will be differently normalized. The projecting tangent planes of an integral conoid are also integral surfaces because they form the envelope of a set of homologous, equal and similar integral conoids centred on a normal. The true contour, the tangent curve of this envelope and the conoid, is again a characteristic and therefore the projection of this characteristic, which is the envelope of the set of time fronts in the $(x_1; x_2)$-plane, is the limit of the extremals.

The lines of regression of integral surfaces are important in view of the Jacobi condition. For instance the characteristics on an integral conoid with top P in the $(x_1; x_2)$-plane envelop a curve, a line of regression, the projection of which coincides with the envelope of the extremals through a point P, i.e., the locus of the points $\overline{P}$ conjugate to P.

Consider an integral conoid in the $(W; x_1; x_2)$-space with its top at a point P in a field of flow in the $(x_1; x_2)$-plane $W = 0$. Consider next a second point Q in the field of flow and let the normal at Q on the $(x_1; x_2)$-plane intersect the integral conoid at a point Q'. Through Q' passes the time front $W = W^Q$, where W^Q is equal to the distance QQ'. Consider now at Q' the integral conoid with top Q'. One of the characteristics on this conoid is the characteristic through P and Q' of the conoid with top P. If at every point on the characteristic a tangent plane to the conoid with top P is constructed these tangent planes and the characteristic itself form a so-called *characteristic strip*. Since every integral conoid is composed of characteristic strips it follows that also the integral conoid with top Q' contains the characteristic strip through P and Q'. In other words, the integral conoids with tops P and Q' are tangent to each other along the characteristic through P and Q'. If now the characteristics of both conoids as well as the curves of intersection of the conoids with planes $W =$ constant are projected onto the $(x_1; x_2)$-plane the projection figure is the complete figure for the boundary value problem, described in chapter III, 6. This method again shows that *the extremal through P and Q is the locus of tangent points of time fronts associated with the complete figures for P and Q separately.*

Through any point of intersection Q' on the normal at Q on the $(x_1; x_2)$-plane and the integral conoid with top P passes a characteristic PQ'. The projections of these characteristics are extremals through P and Q, each of which guarantees a relative extreme for the time of navigation. Therefore the number of extremals through two points P and Q is equal to the number of points of intersection of the normal at Q on the $(x_1; x_2)$-plane and the integral conoid with top P. The extremal furnishing an absolute extreme for the time of navigation corresponds to the characteristic through P and the *first* point of intersection Q' on the normal through Q.

If two points of intersection Q' coincide, the normal through Q intersects a *double curve* on the integral conoid. In that case Q lies on the locus of the double points of the set of time fronts associated with P. This locus is the

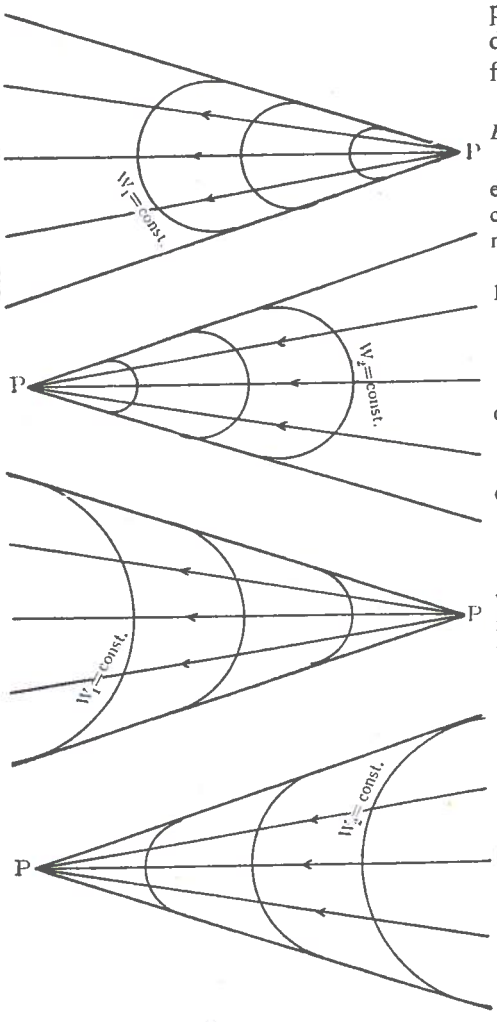

Fig. III, 10.

projection on the $(x_1; x_2)$-plane of the double curve on the integral conoid (see fig. III, 9).

Examples.

1) In the trivial case in which no field of flow exists the problem corresponds with the principle of H u y g e n s in homogeneous isotropic media.

Substitution of $u_1 = 0$, $u_2 = 0$ reduces III, 18 to:

$$\left(\frac{\partial W}{\partial x_1}\right)^2 + \left(\frac{\partial W}{\partial x_2}\right)^2 = \frac{1}{c^2},$$

or: $$(\text{grad } W)^2 = \frac{1}{c^2}.$$

A solution of this equation can be written down at once:

$$W(x_1, x_2\, \alpha) = \frac{1}{c}(x_1 \sin \alpha - x_2 \cos \alpha).$$

where α is a non-additive constant. A doubly infinite set of extremals is now given by the relation $W_\alpha = \beta$ = constant, or:

$$\frac{1}{c}(x_1 \cos \alpha + x_2 \sin \alpha) = \beta.$$

The extremals therefore are straight lines.

The set of transversals: $\frac{1}{c}(x_1 \sin \alpha - x_2 \cos \alpha)$ = constant is now orthogonal with the set of extremals $\frac{1}{c}(x_1 \cos \alpha + x_2 \sin \alpha)$ = constant. The gradient property and the orthogonal property associated with the principle of H u y g e n s and described in chapter III, 5 apparently derive from a specialization of the variation problem in aeronavigation.

In a $(W; x_1; x_2)$-space a set of integral surfaces is given by:

$$W = \frac{1}{c}(x_1 \sin \alpha - x_2 \cos \alpha).$$

On these plane surfaces, characteristics are found by intersecting the planes with the planes

$$\frac{\partial W}{\partial \alpha} = 0 \text{ or } \frac{1}{c}(x_1 \cos \alpha + x_2 \sin \alpha) = 0.$$

Since for any given value of α the plane $\frac{\partial W}{\partial \alpha} = 0$ is perpendicular both to the integral plane $W = \frac{1}{c}(x_1 \sin \alpha - x_2 \cos \alpha)$ and to the $(x_1; x_2)$-plane, the characteristics are straight lines which

make an angle $\varphi = \text{arc tan } \frac{1}{c}$ with the $(x_1; x_2)$-plane. The integral conoid is found after elimination of α from both equations. The resulting equation for the integral conoid is: $W = \frac{1}{c}\sqrt{x_1^2 + x_2^2}$.

The integral conoid therefore is a cone with the W-axis as axis. The complete figure for the origin consists of the projections of the characteristics (conic generators) and the circular cross-sections of the cone and the planes $W =$ constant.

2) In a uniform recti-linear field of flow $u_1 = k$, $u_2 = 0$ H a m i l t o n 's partial differential equation reduces to:

$$c^2 \left\{ \left(\frac{\partial W}{\partial x_1}\right)^2 + \left(\frac{\partial W}{\partial x_2}\right)^2 \right\} = \left(k \frac{\partial W}{\partial x_1} - 1\right)^2.$$

It is not so simple to find at once an integral $W(x_1, x_2, \alpha)$ of this equation. However, from the treatment in part III, 4 it follows that the time fronts, associated with the improper fields of extremals are circles given by the equation:

$$(x_1 - Wk)^2 + x_2^2 = W^2 c^2.$$

After solving for W and calculating $\frac{\partial W}{\partial x_1}$ and $\frac{\partial W}{\partial x_2}$ the results can be substituted in H a m i l t o n' s partial differential equation and shown to satisfy this equation.

In fig. III, 10 the complete figures have been drawn for the four possible improper fields of extremals with nodal point P in the case of a uniform recti linear field of flow with limited manoeuvrability.

8. Comparison of times of navigation

It is possible to calculate the difference in time of navigation between a manoeuvre along an extremal and a manoeuvre along an admissable trajectory by means of the well-known *E-function of W e i e r s t r a s s*. For if the extremal e through

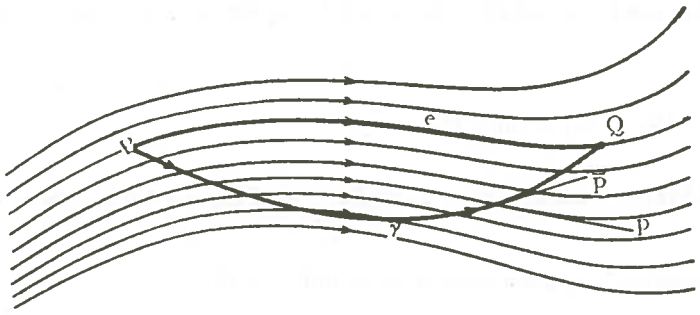

Fig. III, 11.

the points P and Q can be embedded in a field of extremals and if the trajectory, for which the time of navigation is to be compared with the time of navigation along the extremal, lies entirely within the field (fig. III, 11), the difference in time $\triangle W$ is given by:

$$\triangle W = \int_P^Q{}_{\gamma} f(x_1, x_2, \bar{p})\, dx_1 - \int_P^Q{}_{e} f(x_1, x_2, p)\, dx_1,$$

where x_1, x_2 $\bar{p}$ refers to a line element on γ and x_1, x_2, p to a line element on e. Applying Hilberts invariant integral, one may write the second term as follows:

$$\int_P^Q{}_{e} f(x_1, x_2, p)\, dx_1 = \int_P^Q{}_{\gamma} \{f(x_1, x_2, p) + (\bar{p} - p) f_p(x_1, x_2, p)\}\, dx_1.$$

So: $$\triangle W = \int_P^Q{}_{\gamma} E\, dt = \int_P^Q{}_{\gamma} \{f(x_1, x_2, \bar{p}) - f(x_1, x_2, p) - (\bar{p} - p) f_p(x_1, x_2, p)\}\, dx_1,$$

where $E = \dot{x}_1 \{f(x_1, x_2, \bar{p}) - f(x_1, x_2, p) - (\bar{p} - p) f_p(x_1, x_2, p)\}$ is by definition the excess function of Weierstrass.

According to III, 2 and III, 5 the terms become

$$f(x_1, x_2, p) = \frac{1}{w_1}, \quad f(x_1, x_2, \bar{p}) = \frac{1}{\bar{w}_2},$$

$$p = \frac{w_2}{w_1}, \quad \bar{p} = \frac{\bar{w}_2}{\bar{w}_1}, \quad f_p(x_1, x_2, p) = \frac{\sin \xi}{c_e},$$

where w_i, ξ and c_e refer to the extremal and $\bar{w}_i$ to the trajectory γ.

So: $$E = \bar{w}_1 \left\{ \frac{1}{\bar{w}_1} - \frac{1}{w_1} - \left(\frac{\bar{w}_2}{\bar{w}_1} - \frac{w_2}{w_1} \right) \frac{\sin \xi}{c_e} \right\}.$$

Substituting for $c_e = w_1 \cos \xi + w_2 \sin \xi$ one gets

$$E = \frac{w_1 (w_1 \cos \xi + w_2 \sin \xi) - \bar{w}_1 (w_1 \cos \xi + w_2 \sin \xi) - \bar{w}_2 w_1 \sin \xi + w_2 \bar{w}_1 \sin \xi}{w_1 c_e},$$

or:

$$E = \frac{\cos \xi (w_1 - \bar{w}_1) + \sin \xi (w_2 - \bar{w}_2)}{c_e} =$$

$$= \frac{\cos \xi (u_1 + c \cos \xi - u_1 - c \cos \xi') + \sin \xi (u_2 + c \sin \xi - u_2 - c \sin \xi')}{c_e},$$

where the heading ξ is associated with p and ξ' with $\bar{p}$.

So: $$E = \frac{c \{1 - \cos (\xi' - \xi)\}}{c_e}. \qquad \text{(III, 20)}$$

Finally the time difference becomes

$$\triangle W = \int_P^Q{}_{\gamma} \frac{c \{1 - \cos (\xi' - \xi)\}}{c_e}\, dt. \qquad \text{(III, 21)}$$

This formula can be used in practice, where the time difference is an important factor. For instance in aviation the time difference gives an idea of the economic efficiency of flying along the minimizing extremal usually called "minimum flight path". By means of the excess function, it can also be decided whether an extremal yields a relative strong maximum or relative strong minimum. Since the sign of E is entirely determined by the sign of c_e, one finds the same results when applying the condition of Legendre (cf. part III, 3).

9. The indicatrix

Carathéodory introduced a curve in the calculus of variation, which shows much resemblance to the indicatrix of Dupin in differential geometry and by means of which it is possible to derive many properties geometrically (12). This curve, also called *indicatrix*, is defined by the equations:

$$X = \frac{\dot{x}_1}{F}, \qquad Y = \frac{\dot{x}_2}{F},$$

where X and Y are coordinates in a rectangular coordinate system PXY at an arbitrary point P of the region B, in which the variation problem has been defined, and F is the basic function of the variation problem $\delta \int F(x_1, x_2, \dot{x}_1, \dot{x}_2)\, dt = 0$.

However since $F \equiv \dot{x}_1 f(x_1, x_2, p)$, if $\dot{x}_1 > 0$, the equation for the indicatrix becomes:

$$X^2 + Y^2 = \frac{1}{f^2} + \frac{p^2}{f^2} = \frac{1 + p^2}{f^2} \qquad \text{(III, 22)}$$

where $$p = \frac{Y}{X},$$

or $$Xf\left(x_1, x_2, \frac{Y}{X}\right) = 1. \qquad \text{(III, 23)}$$

Since it is unnecessary in the present problem to write the result explicitly in X and Y, formula III, 22 will here be used.

In the present problem $f = \frac{1}{w_1}$ and $p = \frac{w_2}{w_1}$. So the indicatrix for aeronavigation becomes:

$$X^2 + Y^2 = {w_1}^2 + {w_2}^2,$$

or in vector notation:

$$\boxed{\vec{r} = \vec{w}} \quad \text{(fig. I, 2}a\text{, }b\text{, }c\text{).}$$

It follows that the indicatrix for the variation problem in aeronavigation is a circle

with radius c centred on the terminal point of the vector $\vec{u}$. *The starting point of* $\vec{u}$ *is the base point for the indicatrix.*

Therefore the entire indicatrix is *convex*.

According as the velocity parameter $\varepsilon = \frac{c}{u}$ is smaller or greater than one or equal to one the base point lies outside, inside or on the circle. This property has been made use of already in part I, 3.

It is known that the concept of tranversality and the *E*-function of Weierstrass can be derived in a simple geometrical manner from this figure.

Besides the set of time fronts can be constructed by means of the indicatrix, which comes to the same thing as the construction methods of Galton (8) and Giblett (4). If the construction of the time fronts is regarded as a contact transformation, then this construction can be realized by means of "reduced" indicatrices. This method will not be further gone into. However, the indicatrix is encountered in many other problems as well, some of which will be discussed.

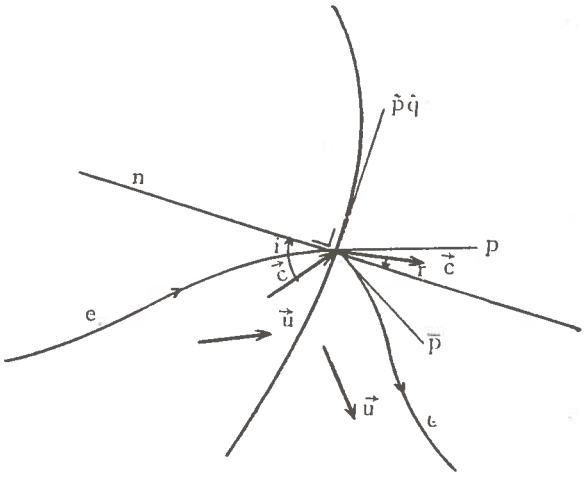

Fig. III, 12.

10. The law of refraction due to Von Mises

If the variation problem is continuous, i.e. if the fundamental function $f(x_1, x_2, p)$ is continuous, discontinuous solutions consisting of broken extremals made up of a finite or enumerable infinite number of extremal arcs, can only exist when the indicatrix has double tangents. Since however in the present problem the indicatrix is convex *no* discontinuous solutions can be found if the fundamental function $f(x_1, x_2, p)$ is continuous. If on the contrary the fundamental function is discontinuous then discontinuous solutions do occur.

The problem then bears some resemblance to the law of refraction due to Snellius in the theory of light.

If in the field of flow a line exists along which the stream vector $\vec{u}$ has a discontinuity, the variation problem becomes a discontinuous variation problem. On the "frontal" line the extremals will then have a corner. In the region of the field of flow in which f is continuous the extremals are integral curves of Zermelo's navigation equation. At the corner the following condition known as the corner condition must be satisfied (see fig. III, 12):

$$(f - p f_p)\,\tilde{p} + f_p\,\tilde{q} = (\bar{f} - \bar{p}\,\bar{f}_p)\,\tilde{p} + \bar{f}_p\,\tilde{q}$$

Here f and $\bar{f}$ are the fundamental functions backward and forward of the frontal line respectively, p is the backward and $\bar{p}$ the forward direction of the extremal arc at the corner. $\tilde{p}$ and $\tilde{q}$ are the direction cosines of a line element along the frontal line.

The various terms have the following values:

$$f - p f_p = \frac{\cos \xi}{c_e} \qquad f_p = \frac{\sin \xi}{c_e}$$

$$\bar{f} - \bar{p}\bar{f}_p = \frac{\cos \xi'}{c_e'} \qquad \bar{f}_p = \frac{\sin \xi'}{c_e'}.$$

Substitution of these terms in the corner condition leads to the relation:

$$\frac{\cos \xi\,\tilde{p} + \sin \xi\,\tilde{q}}{c_e} = \frac{\cos \xi'\,\tilde{p} + \sin \xi'\tilde{q}}{c_e'}.$$

The numerator on the left-hand side is the scalar product of the unit vector along the frontal line and the unit vector in the backward direction of $\vec{c}$. The numerator on the right hand side is the scalar product of the unit vector along the frontal line and the unit vector in the forward direction of $\vec{c}$.

These scalar products are equal to the sines of the angles between the true velocity vectors $\vec{c}$ on either side of the frontal line respectively and the normal to the frontal line. If these angles are i and r respectively the corner condition can be written:

$$\boxed{\frac{\sin i}{\sin r} = \frac{c_e}{c_e'}.} \qquad \text{(III, 24)}$$

This law is known as the law of Von Mises (13). Von Mises derived this law in a complicated manner by means of a geometrical treatment. This law of refraction is entirely analogous to the law of refraction due to Snellius. The law of refraction may be formulated as follows:

At a line of discontinuity, the ratio of the sine of the angle of refraction on an extremal, (i.e. the angle between the vector of the true velocity and the normal to the frontal line) and the effective true velocity is constant.

For the sake of completeness it must be noticed that Von Mises also succeeded in deriving the navigation equation of Zermelo by means of a transition to the limit of the law of refraction for a continuous field of flow, using the condition $d\left(\frac{\sin i}{c_e}\right) = 0$ as a starting point.

If an improper field of extremals is given with nodal point P, the extremals which

intersect a frontal line, may be continued on the other side of the frontal line. In this manner a complementary field of extremals is obtained behind the frontal line. The original field and the complementary field together form a field of broken extremals.

11. Reflection

It will be obvious that in aeronavigation also a law of reflection must exist analogous to the well-known law of reflection in the theory of light. The problem may be formulated as follows:

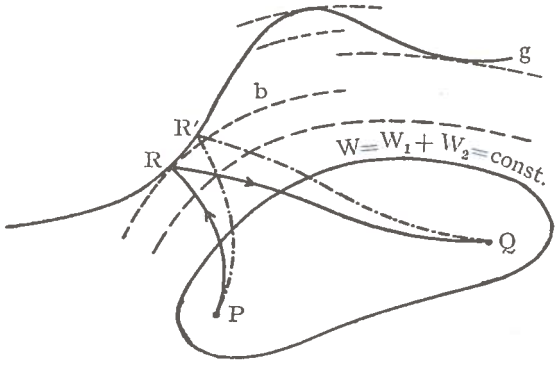

Fig. III, 13.

When for operational or other reasons a ship must call at an arbitrary point on a boundary g, it is desirable to find the (broken) extremal along which the ship can be navigated in the shortest possible time from a given point P to another point Q (fig. III, 13). Coincidence of P and Q is not excluded.

In case the composite curve PRQ, R on g, satisfies the above requirements, then the arc PR is an extremal for the fundamental integral. Similarly the arc RQ is an extremal for the fundamental integral. Finally at the corner R a condition set up by Weierstrass must be satisfied. This condition requires that at R the values of the excess functions $E(x_1, x_2, p, \bar{p})$ and $E(x_1, x_2, \bar{p}, \bar{p})$ on the arcs PR and RQ respectively are equal. Here p, $\bar{p}$ and $\bar{p}$ refer to line elements along the extremal arcs PR and RQ and along the boundary g respectively.

This condition can be given a simple geometrical interpretation by means of the indicatrix.

Let i be the indicatrix with base point R (fig. III, 14). Draw the tangents at R to the extremal arc PR and to the boundary line g. These intersect i at T and R_1 respectively. Let the tangent at T to i be t and the base points of the normals from R and R_1 to t, N and N_1. Then according to a known property of the indicatrix $E(x_1, x_2, p, \bar{p})$ is equal to $\frac{RN}{R_1N_1}$.

Continue RR_1 to the point of intersection S with t and draw through S the second tangent t_1 to i. Let the tangent point be T_1. The base points of the normals from R and R_1 to t_1 are M and M_1. Since $\frac{RM}{R_1M_1} = \frac{RN}{R_1N_1}$ it follows that the condition of Weierstrass for "reflection", $E(x_1\, x_2, p, \bar{p}) = E(x_1, x_2, \bar{p}, \bar{p})$, is satisfied

if the line RT_1 is tangent to the extremal arc RQ at R. If Q coincides with P, the extremal arcs PR and RQ are not in general coincident.

The point R can be found by means of the set of focal curves b in the complete figure for the points P and Q (see part III, 6 and fig. III, 13).

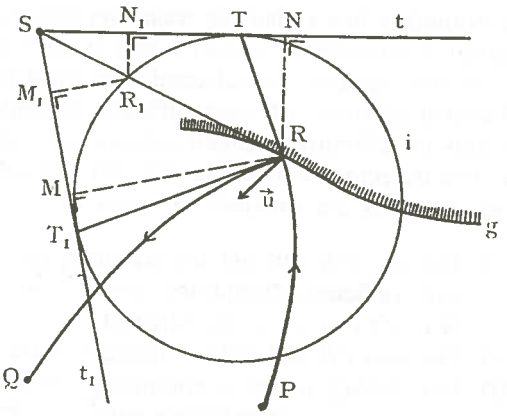

Fig. III, 14.

Consider a focal curve b tangent to the boundary line g at a point R. The time of navigation along the composite extremal PRQ is now either longer or shorter than the time of navigation along any composite extremal $P\,R'\,Q$, if R' is a point on g in the neighbourhood of R. The time of navigation will be shorter along $P\,R\,Q$ than along $P\,R'\,Q$, if in a neighbourhood of R the tangent arc of b lies within the region B, but longer, if the tangent arc of b lies outside the region B.

If g has several tangent points in common with the confocal set of focal curves, then an absolute extreme for the time of navigation with respect to all composite extremals with composite point on g will be furnished by the extremal "reflected" at the tangent point, where the sum value $W = W_1 + W_2$ is smallest or largest. In the special case, in which Q coincides with P, the "reflected" extremal PRP can be found in the same manner.

12. The variation problem in fields of flow with forbidden regions

Generally the variation problem will be defined in a region B covering the entire plane. However, for special reasons one may obliged to limit this region and to consider some parts of the field of flow unsuitable for navigation.

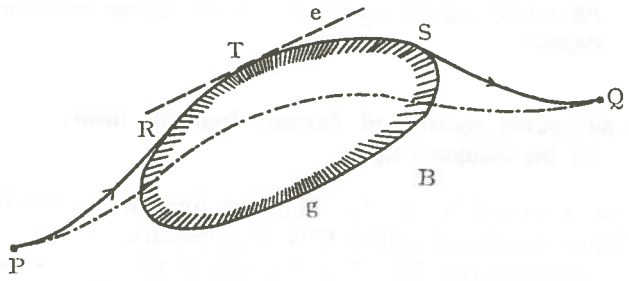

Fig. III, 15.

In air traffic it is conceivable that because of mountain ridges, bad weather zones, forbidden flight regions etc. a diversion must be made and that navigation will be restricted to a region B bounded by several boundary lines g. In such a case the points P and Q may happen to be situated so unfavourably with respect to

a boundary line g that the trajectory through P and Q along which the time of navigation is a minimum, contains part of this boundary line (fig. III, 15). If the problem is positive regular, several conditions must be satisfied for such a trajectory to exist. These conditions are also sufficient conditions for the existence of the extremal. Fields of unlimited manoeuvrability will only be considered.

The trajectory $PRSQ$ (fig. III, 15) is a solution for the problem, if the following requirements are satisfied (B l i s s):

I. The arcs PR and SQ are extremals for the variation problem and all necessary and sufficient conditions for a strong extreme (J a c o b i, L e g e n d r e, W e i e r s t r a s s) are satisfied.

II. The arcs PR and SQ are tangent to the boundary line g.

III. For $PRSQ$ to be a minimizing trajectory the curvature of the extremal e, tangent to g at an arbitrary point T of RS must be such, that in a neighbourhood of T the extremal lies entirely within the region B, irrespective of the way in which the convex or concave side of the boundary line faces the region B.

If these three conditions are satisfied a minimizing trajectory $PRSQ$ exists.

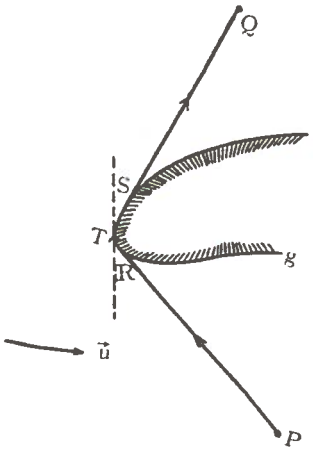

Fig. III, 16.

Example.

Let a uniform rectilinear field of flow with unlimited manoeuvrability be given within a region B bounded by a boundary line g (fig. III, 16). Now construct the minimizing extremal through two points P and Q, if the straight line PQ intersects the boundary line g.

Since the extremals in this field of flow are straight lines, the required minimizing trajectory will be composed of straight lines and arcs of the boundary line g. Draw a tangent from P to g and similarly a tangent from Q to g. Let the tangent points be R and S. At any point T on the arc RS the minimizing extremal tangent to g lies entirely within B in a neighbourhood of T, so that condition III is satisfied. Since the conditions I and II are also satisfied the composite curve consisting of the tangents PR and SQ and the arc RS on g is the required minimizing trajectory.

13. Derivation of the navigation equation of Zermelo from the theory of the complete figure

The navigation equation of Z e r m e l o in the simplified form III, 9 can be derived from the complete figure associated with a field of extremals.

Consider a time front $W =$ constant (fig. III, 17) and a section $PP' = \triangle x_2$ on this time front (the x_1-axis of the coordinate system coincides with the normal at P to $W =$ constant). Then draw the normals PP_1 and $P'P_1'$ to the time front W, such that $PP_1 = c_e \triangle t = (c + u_1) \triangle t$ and $P'P_1' = (c_e + \triangle c_e) \triangle t =$

$$(c + u_1 + \triangle u_1) \triangle t.$$

P_1P_1' is then a section of the time front $W + \triangle W =$ constant. The heading on this time front is determined by the direction of the normal to the front.

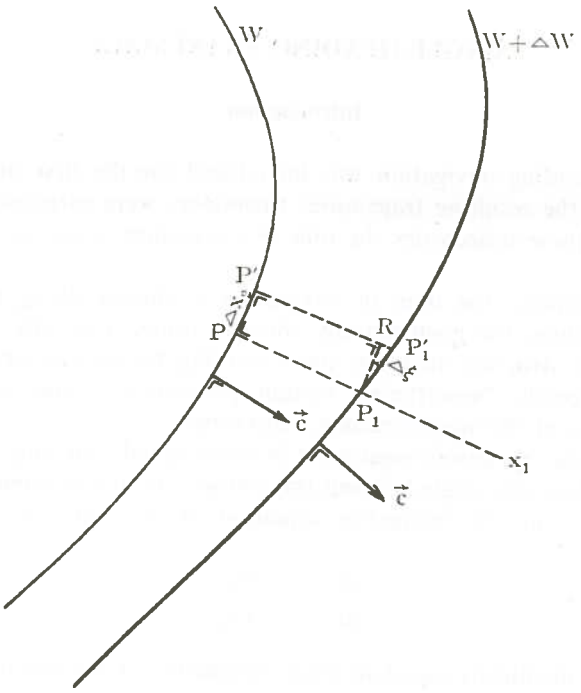

Fig. III, 17.

Consider triangle $P_1P_1'\,R$, where $P_1R = PP'$. The angle $P_1'P_1R = \arctan \dfrac{\triangle u_1 \cdot \triangle t}{\triangle x_2}$ or, if $\triangle t$ is small:

$$\triangle \xi = -\frac{\triangle u_1 \cdot \triangle t}{\triangle x_2}$$

or

$$\frac{\triangle \xi}{\triangle t} = -\frac{\triangle u_1}{\triangle x_2}.$$

If finally the limit is taken for $\triangle t \to 0$, one finds the relation

$$\frac{d\xi}{dt} = -\frac{\partial u_1}{\partial x_2}$$

which is the simplified form of the navigation equation of Z e r m e l o (see III, 9).

PART IV

SINGLE-HEADING EXTREMALS

Introduction

When single-heading navigation was introduced for the first time it was taken for granted that the resulting trajectories themselves were extremals and that consequently along these trajectories the time of navigation would assume an extreme value.

Although in general the time of navigation is shorter along a single-heading trajectory than along the geometrically shortest route, it is only in fields of flow with a particular structure that the single-heading trajectories are minimizing or maximizing extremals. Nevertheless certain properties of the extremals can be derived by means of the single-heading trajectories.

In several articles on aeronavigation it is often stated that only in uniform recti linear fields of flow the single-heading trajectories are at the same time extremals. This is inferred from the navigation equation of Zermelo in its simplified form (III, 9):

$$\frac{d\xi}{dt} = -\frac{\partial u_1}{\partial x_2}.$$

If here $\frac{\partial u_1}{\partial x_2}$ is identically equal to zero irrespective of the heading ξ the field of flow is uniform and rectilinear and the equation reduces to:

$$\frac{d\xi}{dt} = 0,$$

which means that ξ is constant along an extremal. The single-heading trajectories in a uniform rectilinear field of flow are straight lines and these straight lines are at the same time extremals.

This description is incomplete. For a proper investigation it will be necessary to take the *original* navigation equation of Zermelo as a starting point.

But in order to investigate the structure of the fields of flow, in which all or selected single-heading trajectories are at the same time extremals, one may also use Hamilton's partial differential equation. Both equations must lead to the same results. From various considerations, however, it appears that Zermelo's equation is easier to handle than Hamilton's partial differential equation, unless a particular part of the theory is investigated, which is more closely related to the theory of Hamilton-Jacobi.

The single-heading trajectories, which at the same time are also extremals, will be called *single-heading extremals.*

1. Fields of flow, in which all extremals are single-heading extremals

In the investigation of this part the result will be derived both by means of the navigation equation of Zermelo and by means of Hamilton's partial differential equation.

The navigation equation of Zermelo is III, 8:

$$\frac{d\xi}{dt} = \frac{\partial u_2}{\partial x_1} \sin^2 \xi + \left(\frac{\partial u_1}{\partial x_1} - \frac{\partial u_2}{\partial x_2}\right) \sin \xi \cos \xi - \frac{\partial u_1}{\partial x_2} \cos^2 \xi.$$

The single-heading trajectories are characterized by the equation:

$$\frac{d\xi}{dt} \equiv 0.$$

If all single-heading trajectories are to be also extremals, the coefficients on the right hand side of the navigation equation must be identically equal to zero or:

$$\frac{\partial u_2}{\partial x_1} \equiv \frac{\partial u_1}{\partial x_2} \equiv 0, \qquad \frac{\partial u_1}{\partial x_1} - \frac{\partial u_2}{\partial x_2} \equiv 0.$$

From the first relation it follows that u_2 is independent of x_1 and u_1 independent of x_2, so one may write:

$$u_1 = F(x_1), \; u_2 = G(x_2)$$

where F and G are arbitrary functions with first partial derivatives.

The second relation requires that:

$$\frac{\partial F(x_1)}{\partial x_1} = \frac{\partial G(x_2)}{\partial x_2}.$$

This is only possible, if both sides are equal to a constant k.

$$\frac{\partial F(x_1)}{\partial x_1} = k, \qquad \frac{\partial G(x_2)}{\partial x_2} = k.$$

The solution of these equations is:

$$F(x_1) = kx_1 + l, \; G(x_2) = kx_2 + m,$$

where l and m are constants.

Therefore the equations for the field of flow, in which all single-heading trajectories are extremals, are:

$$u_1 = kx_1 + l,$$
$$u_2 = kx_2 + m.$$

This field of flow is composed of a convergent or divergent field $u_1 = kx_1$, $u_2 = kx_2$ (k negative or positive) and a uniform rectilinear field $u_1 = l$, $u_2 = m$.

The resultant field is identical with the component convergent or divergent field and is merely displaced with respect to the former.

The above results may be summed up in the following theorem:

All extremals are single-heading extremals in convergent or divergent fields of flow $\dot{\alpha} = 0$, $\dot{r} = kr$ *and in uniform rectilinear fields of flow.*

In fig. IV, 1, *a*, *b*, *c* the three possible fields of flow have been drawn.

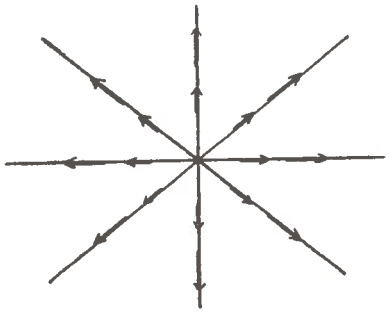

Fig. IV, 1,a.

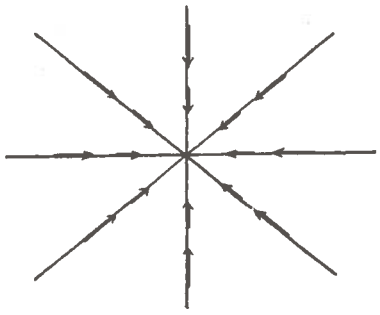

Fig. IV, 1,b.

The above theorem will next be proved by means of Hamilton's partial differential equation. Since along an extremal the vector $\vec{c}$ is perpendicular to a time front $W =$ constant, the transversal line elements along an extremal in a field of flow, in which all extremals are single-heading trajectories, will be parallel to each other. Considering in particular a set of single-heading trajectories with the same constant heading one finds that the associated set of time fronts $W =$ const. consists of parallel straight lines (fig. IV, 2). Since all single-heading trajectories are extremals irrespective of the heading, every straight line in the field of flow must belong to a set of time fronts $W =$ constant. So W must be of the form $W\{x_1 \cos\alpha + x_2 \sin\alpha + \beta(\alpha)\}$, where β is a constant, determined by the angle α between the straight line and the x_1-axis.

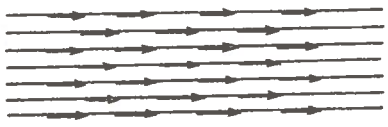

Fig. IV, 1,c.

Differentiate partially with respect to x_1 and x_2:

$$\frac{\partial W}{\partial x_1} = \cos\alpha \,.\, W',$$

$$\frac{\partial W}{\partial x_2} = \sin\alpha \,.\, W'.$$

W' is the derivative with respect to the argument $x_1 \cos\alpha + x_2 \sin\alpha + \beta(\alpha)$. Substituting these partial derivatives in Hamilton's partial differential equation III, 19 one obtains:

$$cW' = 1 - (u_1 \cos\alpha + u_2 \sin\alpha)\, W',$$

or

$$W'(c + u_1 \cos\alpha + u_2 \sin\alpha) = 1.$$

In this equation such functions must be substituted for the unknown quantities W', u_1, u_2 and β, as to satisfy the equation identically for all values of α. In addition u_1 and u_2 must be functions of x_1 and x_2 only.

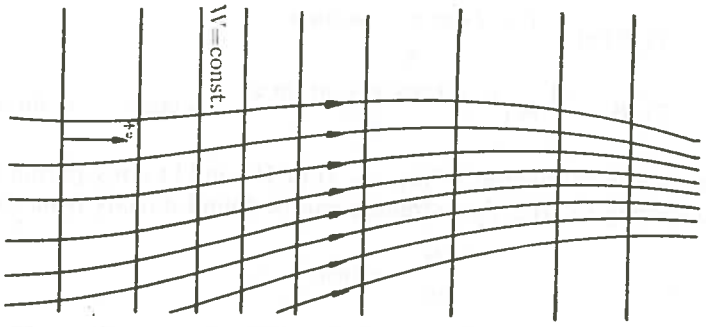

Fig. IV, 2.

Differentiate again partially with respect to x_1 and x_2:

$$\frac{\partial u_1}{\partial x_1}\cos\alpha + \frac{\partial u_2}{\partial x_1}\sin\alpha = -\frac{1}{W'^2}\cdot W''\cdot\cos\alpha,$$

$$\frac{\partial u_1}{\partial x_2}\cos\alpha + \frac{\partial u_2}{\partial x_2}\sin\alpha = -\frac{1}{W'^2}\cdot W''\cdot\sin\alpha.$$

The subtraction of the second equation divided by sin α from the first equation divided by cos α gives:

$$\frac{\partial u_1}{\partial x_1} + \frac{\partial u_2}{\partial x_1}\tan\alpha - \frac{\partial u_1}{\partial x_2}\operatorname{cotan}\alpha - \frac{\partial u_2}{\partial x_2} = 0.$$

In order to satisfy this equation identically for all values of α the following relations must hold:

$$\frac{\partial u_1}{\partial x_1} - \frac{\partial u_2}{\partial x_2} \equiv 0, \quad \frac{\partial u_2}{\partial x_1} \equiv \frac{\partial u_1}{\partial x_2} \equiv 0.$$

These are the same relations as those derived above from the navigation equation of Zermelo.

The equations for the field of flow are:

$$u_1 = kx_1 + l, \; u_2 = kx_2 + m$$

with l and m arbitrary constants.

Substitution of these equations in Hamilton's partial differential equation leads to:

$$W' = \frac{1}{k\left(\frac{c + l\cos\alpha + m\sin\alpha}{k} + x_1\cos\alpha + x_2\sin\alpha\right)}.$$

Since W' is a function of the argument $x_1\cos\alpha + x_2\sin\alpha + \beta(\alpha)$, it follows that:

1) $\beta(\alpha) = \frac{c + l\cos\alpha + m\sin\alpha}{k}$.

2) $W = \frac{1}{k} ln\left(\frac{c + l\cos\alpha + m\sin\alpha}{k} + x_1\cos\alpha + x_2\sin\alpha\right)$.

This expression is an integral $W(x_1, x_2, \alpha)$ of Hamilton's partial differential equation. According to III,5 the extremals can be found directly from the relation:

$$\frac{\partial W}{\partial\alpha} = \text{const.} = \gamma.$$

The differentiation yields a linear relation between x_1 and x_2. *The extremals therefore are straight lines.*

The argumentation based on Hamilton's partial differential equation is more complete than that based on Zermelo's navigation equation in so far, that it enables one to find the sets of time fronts W = constant associated with the single-heading extremals with the same constant heading.

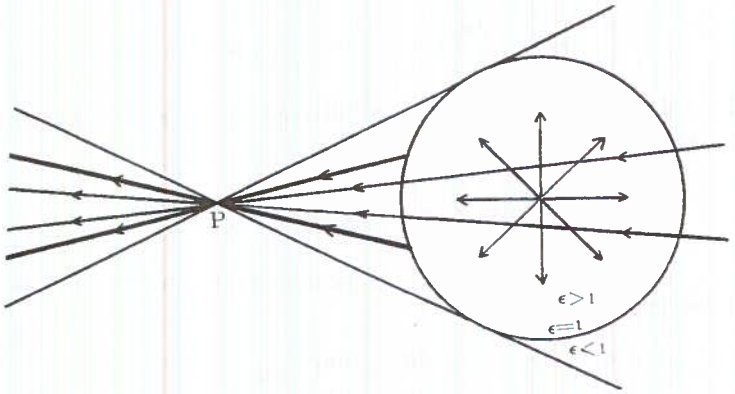

Fig. IV, 3.

For a discussion of the extremals in a uniform rectilinear field of flow the reader is referred back to part III, 4.

In a convergent or divergent field of flow $\dot{r} = kr$, $\dot{\alpha} = 0$, the limiting isotach is a circle with radius $r = \frac{c}{|k|}$. It can be shown that all minimizing and maximizing

extremals through a point P, which are straight lines or line segments, are contained within the sector bounded by the tangents from P to the limiting isotach (fig. IV, 3). P is again the nodal point of four improper fields of extremals, whereas a point P within the circle $r = \frac{c}{|k|}$ is the nodal point of two improper fields only.

Since all maximizing extremals lie entirely in the region of limited manoeuvrability the corresponding line segments will end at the limiting isotach. The four different improper fields of extremals, two of which with P as starting point, and the other two with P as terminal point, are taken together in one figure (fig. IV, 3)

The heavy lines are maximizing, the thin lines minimizing extremals.

All extremals furnish an absolute extreme value for the time of navigation.

2. The field of extremals and the set of single-heading trajectories through one point

Consider an improper field of extremals with an arbitrary point P as nodal point and the (singly infinite) set of single-heading trajectories originating from this point. The latter covers a region, which partially overlaps the field of extremals.

An extremal and a single-heading trajectory will be tangent to each other at P, if they have the same initial heading. However, some directions may be found at P, for wich the tangent point transforms into a point of osculation.

Since the heading of a single-heading trajectory is constant by definition, this can only happen, if the heading of the tangent extremal does not change in the vicinity of P.

From the navigation equation III, 8 written in the form III, 10:

$$\frac{d \tan \xi}{dt} = \frac{\partial u_2}{\partial x_1} \tan^2 \xi + \left(\frac{\partial u_1}{\partial x_1} - \frac{\partial u_2}{\partial x_2} \right) \tan \xi - \frac{\partial u_1}{\partial x_2},$$

it follows that for an extremal having a three-pointic contact with a single-heading trajectory at P, $\frac{d \tan \xi}{dt}$ must be equal to zero at P. Since the coefficients on the right-hand side of the above equation have definite values at P, this right hand side represents an ordinary quadratic in $\tan \xi$, which vanishes, if $\tan \xi$ is equal to either of the roots of the quadratic. With these two values of $\tan \xi$ correspond four values of $\xi : \xi_1, \xi_1 + \pi, \xi_2$ and $\xi_2 + \pi$, which may be complex. Therefore an extremal through P with one of these "*optimum headings*" as initial heading will have a three-pointic contact at P with a single-heading trajectory with the same heading. The corresponding true velocity vector $\vec{c}$ must be directed along one of the four line elements defined by the values $\xi_1, \xi_1 + \pi, \xi_2$ and $\xi_2 + \pi$.

Since at every point of the field of flow two values are found for $\tan \xi$, two sets of curves can be constructed, for which at every point $p = \frac{dx_2}{dx_1} = \tan \xi$.

These curves will be called *zero-shear lines.*

The investigation of the fields of flow with single-heading extremals will be considerably simplified by using these auxiliary lines.

At each point P on the zero-shear lines two line elements can be found of the corresponding extremals, which have a three-pointic contact with a single-heading trajectory. Therefore four curves can be constructed, one for each optimum heading $\xi_1, \xi_1 + \pi, \xi_2, \xi_2 + \pi$, which at every point contain such a line element. These curves are called *osculation lines.*

3. Zero-shear lines

At every point of the field of flow the line elements of the zero-shear lines are determined by the relation:

$$\frac{dx_2}{dx_1} = \tan \xi,$$

where ξ is an optimum heading.

Therefore the differential equation for the zero-shear lines is:

$$\frac{\partial u_2}{\partial x_1}\left(\frac{dx_2}{dx_1}\right)^2 + \left(\frac{\partial u_1}{\partial x_1} - \frac{\partial u_2}{\partial x_2}\right)\frac{dx_2}{dx_1} - \frac{\partial u_1}{\partial x_2} = 0. \qquad \text{(IV, 1)}$$

At any point on a zero-shear line the relation IV, 1 holds for the extremals which are tangent to the corresponding osculation lines through that point. Since according to III, 9, $\frac{d \tan \xi}{dt}$ at every point on an extremal is equal to the shear of the component of flow along the direction of $\vec{c}$, which here vanishes, a zero-shear line can also be defined as follows:

A zero-shear line is a curve in the field of flow, such that at every point on the curve the shear of the component of flow along the tangent is equal to zero (fig. IV, 4).

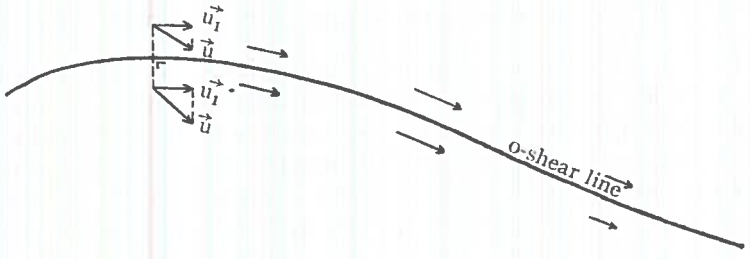

Fig. IV, 4.

The zero-shear lines will not always be real. At any point of the field of flow it depends on the sign of the discriminant $\triangle$ of the quadratic IV,1 whether the optimum headings are real or imaginary.

The discriminant is:

$$\triangle = \left(\frac{\partial u_1}{\partial x_1} - \frac{\partial u_2}{\partial x_2}\right)^2 + 4\,\frac{\partial u_1}{\partial x_2} \cdot \frac{\partial u_2}{\partial x_1}. \qquad \text{(IV, 2)}$$

Depending on the sign of $\triangle$ the following properties can be derived: In a field of flow or in a region of a field of flow, where $\triangle > 0$, the optimum headings are real.

In a field of flow or in a region of a field of flow, where $\triangle < 0$, the optimum headings are imaginary.

In a field of flow, where $\triangle \equiv 0$, or on the curve in a field of flow, which divides the field of flow into regions, where $\triangle > 0$ and regions, where $\triangle < 0$, the optimum headings are real and coincide two by two.

Therefore in an arbitrary field of flow the zero-shear lines will lie entirely in the region, where $\triangle \geqslant 0$.

In a field of flow, in which a velocity-potential is defined, the zero-shear lines intersect each other perpendicularly.

This can be shown as follows.

A field of flow has a velocity-potential φ, if the field is irrotational, i.e. if $\frac{\partial u_2}{\partial x_1} = \frac{\partial u_1}{\partial x_2}$. The components u_1 and u_2 of the stream vector are the partial derivatives of the velocity-potential with respect to x_1 and x_2 respectively, (see I, 2):

$$u_1 = \frac{\partial \varphi}{\partial x_1}, \quad u_2 = \frac{\partial \varphi}{\partial x_2}.$$

The zero-shear lines are determined by the differential equation:

$$\frac{\partial^2 \varphi}{\partial x_1\, \partial x_2}\left(\frac{dx_2}{dx_1}\right)^2 + \left(\frac{\partial^2 \varphi}{\partial {x_1}^2} + \frac{\partial^2 \varphi}{\partial {x_2}^2}\right)\frac{dx_2}{dx_1} - \frac{\partial^2 \varphi}{\partial x_1\, \partial x_2} = 0.$$

It follows that at every point the product of the roots of this equation is equal to -1. Therefore the zero-shear lines must be perpendicular to each other.

In some fields of flow one may find that at a point, along a curve, or everywhere in the field, $\frac{d \tan \xi}{dt} \equiv 0$ for any value of ξ. This will be the case, when the coefficients $\frac{\partial u_1}{\partial x_2}$, $\frac{\partial u_2}{\partial x_1}$ and $\frac{\partial u_1}{\partial x_1} - \frac{\partial u_2}{\partial x_2}$ are simultaneously or identically equal to zero.

Since $\triangle = \left(\frac{\partial u_1}{\partial x_1} - \frac{\partial u_2}{\partial x_2}\right)^2 + 4\frac{\partial u_1}{\partial x_2} \cdot \frac{\partial u_2}{\partial x_1}$, $\triangle$ vanishes simultaneously with these coefficients. The points, where $\frac{d \tan \xi}{dt} \equiv 0$, lie either on the curve $\triangle = 0$ in fields, where the sign of $\triangle$ is not permanent, or in fields of flow, where $\triangle \equiv 0$.

The coefficients are identically equal to zero in convergent (divergent) fields of flow $\dot{\alpha} = 0$, $\dot{r} = kr$ and in uniform rectilinear fields. In these fields the zero-shear lines are trivial.

4. Fields of flow, in which single-heading extremals exist

If one or both sets of zero-shear lines consist of parallel straight lines, then the single-heading trajectories with a corresponding optimum heading ξ_0 which is constant, are extremals. For both $\frac{d \tan \xi}{dt} \equiv 0$ and $\frac{\partial u_1}{\partial x_2} \equiv 0$ if the x_1-axis is taken along a straight optimum-heading line and so the navigation equation of Zermelo is satisfied:

$$\frac{d \tan \xi}{dt} = -\frac{\partial u_1}{\partial x_2} \equiv 0.$$

A single-heading trajectory with the optimum heading ξ_0 is then a *single-heading extremal.* The single-heading extremals are identical with the osculation lines, which correspond to these zero-shear lines. Moreover according to the property of transversality, part III 5, formula III, 16, the true velocity vector $\vec{c}$ along an extremal is perpendicular to a transversal, so all straight lines, which intersect the set of parallel straight zero-shear lines perpendicularly are transversals or time fronts of the set of single-heading extremals.

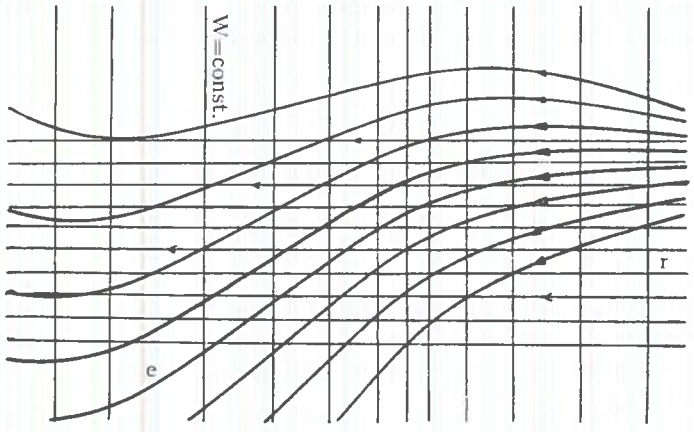

Fig. IV, 5.

A complete figure then consists of one of the sets of osculation lines, and the set of lines perpendicular to the rectilinear zero-shear lines. In fig. IV, 5 the lines W = constant are time fronts, the lines r are straight zero-shear lines and the curves e are the corresponding osculation lines or single-heading extremals.

With a given constant optimum heading ξ_0 and the associated constant optimum heading $\xi_0 + \pi$ correspond two complete figures with mutually parallel sets of time fronts W = constant. Since at the most two sets of straight zero-shear lines are possible there can be no more than *four complete figures* of single-heading extremals. Therefore at the most four single-heading extremals can pass through any point.

Depending on the existence of one or two sets of parallel rectilinear zero-shear lines the following result can be found:

A. *If one of the sets of zero-shear lines consists of parallel straight lines, two single-heading extremals determined by the optimum headings* ξ_0 *and* $\xi_0 + \pi$ *will pass through any point P in the field of flow.*

B. *If both sets of zero-shear lines consist of parallel straight lines, four single-heading extremals determined by the optimum headings* ξ_1, $\xi_1 + \pi$, ξ_2 and $\xi_2 + \pi$ *will pass through any point P in the field of flow.*

C. *If both sets of zero-shear lines consist of parallel straight lines, both sets coinciding, the four single-heading extremals passing through any point P in the field of flow will also coincide two by two.*

The structure of the field of flow, in which any of these three cases occur, can be analysed by calculating the roots of the quadratic IV, 1 and by putting these equal to a constant.

Although this subject matter can be fully worked out, here only the special case of a field of flow with a stream-function ψ will be considered in view of the application to aerology.

5. The theory of single-heading extremals in fields of flow with a stream-function

According to I, 1 such a field of flow is defined by a stream-function $\psi\ (x_1, x_2)$.

$$u_1 = \frac{\partial \psi}{\partial x_2}, \quad u_2 = -\frac{\partial \psi}{\partial x_1}.$$

The stream-lines are the lines $\psi =$ constant and the intensity of the flow at any point is determined by the magnitude of grad ψ. If the velocity components u_1 and u_2 are given as functions of x_1 and x_2, the stream-functions can be determined by integrating the above partial differential equations. It is, however, more convenient to define a stream-function ψ first and to derive the velocity components u_1 and u_2 afterwards by partial differentiation of ψ.

The stream-function ψ can be represented by a surface in the (x_1, x_2, ψ)-space. The streamlines $\psi =$ constant are then the projections of the curves of intersection of planes parallel to the (x_1, x_2)-plane and the ψ-surface.

In order to determine the structure of the fields of flow with a stream-function, in which single-heading extremals occur, one may study this structure from a differential-geometrical point of view, by means of the ψ-surface in (x_1, x_2, ψ)-space. This method in particular enables one to obtain a good survey of the various possibilities.

By means of a three-dimensional representation in (x_1, x_2, ψ)-space "ψ-surface models" can be constructed of the required fields of flow. These models are of

particular value for the application of the theory in practice. When the actual field of flow is given, an attempt may be made to recognize in the ψ-surface associated with this field, one of the ψ-surface models, in which single-heading extremals exist. If such a similarity is obvious the theoretical considerations based on these models will apply to the actual field of flow.

The analysis will be based on the definition of zero-shear lines.

Consider again the differential equation IV, 1 for the zero-shear lines. After substitution of the expressions.

$$u_1 = \frac{\partial \psi}{\partial x_2},$$

$$u_2 = -\frac{\partial \psi}{\partial x_1},$$

this equation transforms to:

$$\frac{\partial^2 \psi}{\partial x_1^2}\left(\frac{dx_2}{dx_1}\right)^2 - 2\frac{\partial^2 \psi}{\partial x_1 \partial x_2}\frac{dx_2}{dx_1} + \frac{\partial^2 \psi}{\partial x_2^2} = 0. \qquad \text{(III, 3)}$$

Whether the zero-shear lines are real or imaginary depends on the discriminant $\triangle$, which, but for a factor 4, is equal to:

$$\triangle = \left(\frac{\partial^2 \psi}{\partial x_1 \partial x_2}\right)^2 - \frac{\partial^2 \psi}{\partial x_1^2} \cdot \frac{\partial^2 \psi}{\partial x_2^2}.$$

At every point on the ψ-surface the sign of $\triangle$ determines whether the point is an *elliptic*, a *hyperbolic* or a *parabolic* point.

The region of the field of flow, where $\triangle > 0$ corresponds with a region of hyperbolic points on the ψ-surface. In this region the zero-shear lines are real.

The region of the field of flow, where $\triangle < 0$ corresponds with a region of elliptic points on the ψ-surface. In this region the zero-shear lines are imaginary.

The boundary line between the regions of the field of flow, in which $\triangle$ has a different sign, corresponds with a line of parabolic points or a "spinodal" line on the ψ-surface. Therefore the projection of the "spinodal" line on the (x_1, x_2)-plane forms the boundary of the region of the field of flow, where the zero-shear lines are real.

Among the ψ-surface models there are some, which contain only hyperbolic points. At all points on these surfaces the *total curvature or Gaussian curvature* is *negative.* The total curvature is defined by $-\triangle = \frac{1}{\varrho_0 \varrho_{\frac{\pi}{2}}}$. ϱ_0 and $\varrho_{\frac{\pi}{2}}$ are the principal radii of curvature.

In the corresponding field of flow the zero-shear lines are real everywhere. ψ-surface models, which contain only elliptic points, i.e. surfaces, whose *total curvature* is positive everywhere, have only imaginary zero-shear lines in the corresponding field of flow. Finally surfaces, on which $\triangle \equiv 0$ correspond with fields of flow, with only real and straight zero-shear lines, which two by two coincide.

Also in non-divergent fields of flow it is possible that at certain points, along certain curves, or everywhere in the field $\frac{d \tan \xi}{dt} \equiv 0$, for all values of ξ. At such points the equalities: $\frac{\partial^2 \psi}{\partial x_1^2} = \frac{\partial^2 \psi}{\partial x_2^2} = \frac{\partial^2 \psi}{\partial x_1 \partial x_2} = 0$ must hold.

These exceptional cases arise:

1) At certain points on the projection of the spinodal line $\triangle = 0$.
2) On certain curves in fields of flow, whose corresponding ψ-surface is a developable surface, $\triangle \equiv 0$.
3) In uniform rectilinear fields. Here the corresponding ψ-surface is a plane.

Apparently the second case may occur in fields of flow, in which four single-heading extremals which two by two coincide, pass through every point. In these fields curves exist, along which the condition $\frac{d \tan \xi}{dt} \equiv 0$ is satisfied for every ξ. These curves are themselves extremals of the field.

In addition to the zero-shear lines now consider the *asymptotic* lines of the ψ-surface. The differential equation for the projections of the asymptotic lines on the (x_1, x_2)-plane is:

$$\frac{\partial^2 \psi}{\partial x_2^2}\left(\frac{dx_2}{dx_1}\right)^2 + 2\frac{\partial^2 \psi}{\partial x_1 \partial x_2} \cdot \frac{dx_2}{dx_1} + \frac{\partial^2 \psi}{\partial x_1^2} = 0. \qquad \text{(IV, 4)}$$

When one compares this equation with the differential equation for the zero-shear lines:

$$\frac{\partial^2 \psi}{\partial x_1^2}\left(\frac{dx_2}{dx_1}\right)^2 - 2\frac{\partial^2 \psi}{\partial x_1 \partial x_2} \cdot \frac{dx_2}{dx_1} + \frac{\partial^2 \psi}{\partial x_2^2} = 0,$$

it will be seen at once that both sets of curves are perpendicular to each other, since the roots of both equations are reciprocal and opposite. Two by two the products of the roots are equal to —1.

There are two sets of asymptotic lines on the ψ-surface. Whether these are real or imaginary depends again on the sign of $\triangle$. The following theorem may now be formulated:

The zero-shear lines are the orthogonal trajectories of the projections of the asymptotic lines.

There are two orthogonal sets, which are real or imaginary according to the sign of $\triangle = \left(\frac{\partial^2 \psi}{\partial x_1 \partial x_2}\right)^2 - \frac{\partial^2 \psi}{\partial x_1^2} \cdot \frac{\partial^2 \psi}{\partial x_2^2}$ being positive or negative.

The boundary of the real zero-shear lines and the projections of the real asymptotic lines is the projection on the (x_1, x_2)-plane of the spinodal line on the ψ-surface.

By means of the orthogonality of the sets of curves the ψ-surface models of the required fields of flow with single-heading extremals can now be found. For if in the field of flow a set of single-heading extremals exits, one of the sets of zero-shear lines must consist of parallel straight lines. With this set corresponds a set of pro-

jections of asymptotic lines, which consists of parallel straight lines perpendicular to the parallel zero-shear lines. *The projections of asymptotic lines are the time fronts of the complete figure associated with the set of single-heading extremals.*

On the ψ-surface accordingly a set of asymptotic lines must exist, which can be projected as a set of parallel straight lines on the (x_1, x_2)-plane. The nature of the ψ-surface is entirely determined by this condition.

Again three cases are possible:

Case A. *One of the sets of zero-shear lines consists of parallel straight lines. Similarly one of the sets of projections of asymptotic lines consists of parallel straight lines. In the field of flow two single-heading extremals pass through every point.*

Case B. *Both sets of zero-shear lines consist of parallel straight lines. Similarly both sets of projections of asymptotic lines consist of parallel straight lines. In the field of flow four single-heading extremals pass through every point.*

Case C. *If both the sets of zero-shear lines and the sets of projections of asymptotic lines consist of straight lines and coincide, four single-heading extremals, which two by two coincide, pass through every point.*

Case A.

Fields of flow with a stream-function, in which two single-heading extremals pass through every point.

One of the sets of asymptotic lines on the ψ-surface consists of straight lines, which are projected as parallel straight lines on the (x_1, x_2)-plane. The ψ-surface is then a *ruled surface whose generators lie in parallel projecting vertical planes.* For one of the sets of asymptotic lines on a ruled surface consists of the generators of the ruled surface.

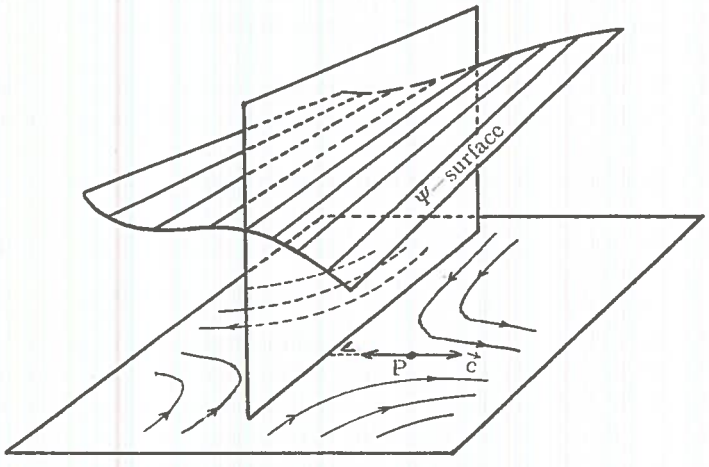

Fig. IV, 6.

Now a ruled surface consists of all straight lines, which intersect three given directrices. If one of these directrices lies at infinity in a projecting plane the generators are all parallel to this plane and the ruled surface belongs to the class A. *So all ruled surfaces with two directrices and a projecting directive plane satisfy the conditions of case A* The straight lines are projected as parallel straight lines and the true velocity vector for the single-heading extremals is at right angles to the projecting directive plane (fig. IV, 6).

Case B.

Fields of flow with a stream-function, in which four single-heading extremals pass through every point.

Both sets of asymptotic lines on the ψ-surface now consist of straight lines, which are projected as parallel straight lines on the (x_1, x_2)-plane. The only ψ-surfaces, which have this property, are the *elliptic and hyperbolic paraboloids.* In general there are two sets of straight lines on a quadric, which are either real or imaginary. In the present case however both sets of generators have a directive plane, so the quadric must be either an elliptic or a hyperbolic paraboloid. The directive planes of the elliptic paraboloid are imaginary, so the asymptotic lines, their projections and the optimum heading lines are also imaginary. In the corresponding field of flow four imaginary single-heading extremals pass through every point. The directive planes of the hyperbolic paraboloid however are real, so the asymptotic lines etc. are also real. In the corresponding field of flow four *real* single-heading extremals pass through every point.

The position of the ψ-surface concerned must be such that the directive planes are perpendicular to the (x_1, x_2)-plane. Therefore the axis of the elliptic or hyperbolic paraboloids must be perpendicular to the (x_1, x_2)-plane.

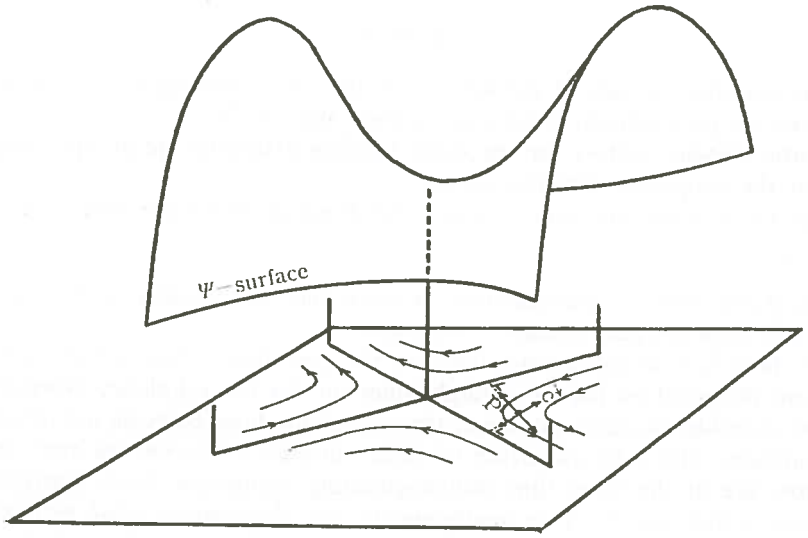

Fig. IV, 7.

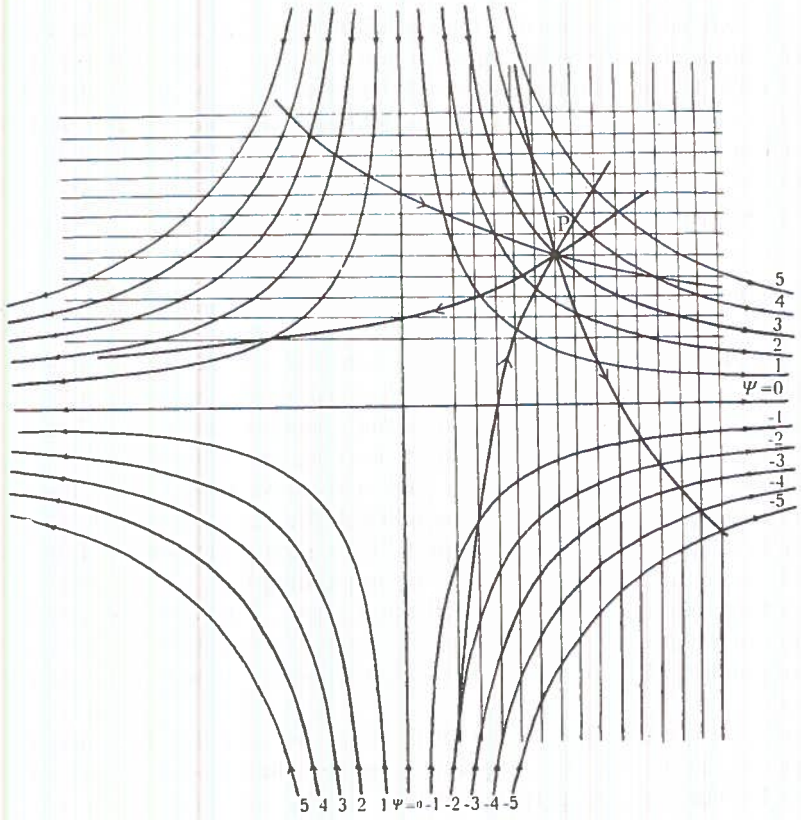

Fig. IV, 8.

So the conditions of case B are satisfied by the elliptic and hyperbolic paraboloids, whose axis are perpendicular to the (x_1, x_2)*-plane* (fig. IV, 7).

The true velocity vectors for the single-heading extremals are at right angles to either of the projecting directive planes.

Figure IV, 8 shows the case in which the directive planes are perpendicular.

Case C.

Fields of flow with a stream-function, in which four single-heading extremals, which two by two coincide, pass through every point.

Again both sets of asymptotic lines on the ψ-surface consist of straight lines, which are projected as parallel straight lines on the (x_1 x_2)-plane; however both sets now coincide. Surfaces on which the asymptotic lines coincide are *developable* ruled surfaces. The total curvature of these surfaces is everywhere zero and the generators are at the same time double-counting asymptotic lines. Therefore the ψ-surfaces, which satisfy these requirements, are *developable ruled surfaces with a directive plane.* It may be shown however that such developable ruled surfaces

are *cylindrical surfaces*. Not all cylindrical surfaces can be used for case *C*, but only those, whose intersection with the projecting directive plane consists of one straight line only (fig. IV, 9 and IV, 10).

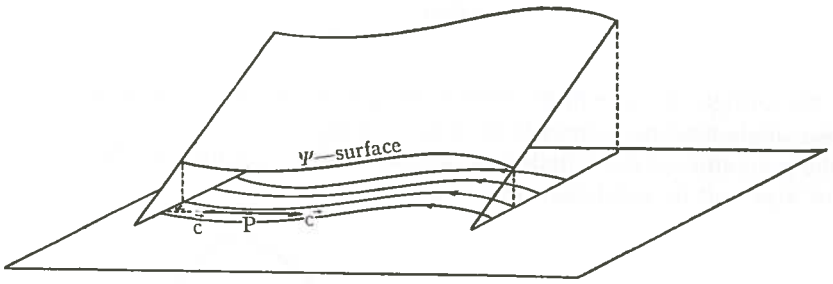

Fig. IV, 9.

On the generators, which connect the points of inflection on the lines $\psi = \text{const.}$, the relations $\frac{\partial^2\psi}{\partial x_1^2} = \frac{\partial^2\psi}{\partial x_2^2} = \frac{\partial^2\psi}{\partial x_1\,\partial x_2} = 0$ hold at every point for every ξ.

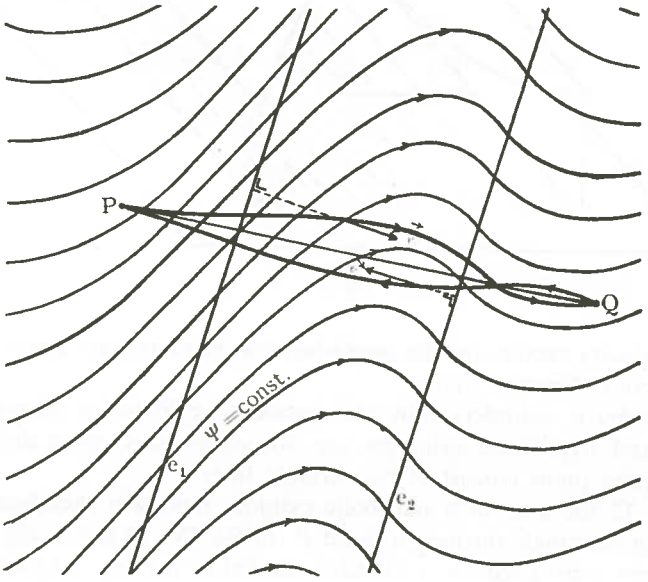

Fig. IV, 10.

The projections of these generators consist of the straight lines, which connect the points of inflection of the stream-lines.

Since the vector $\vec{u}$ is constant along these lines both in direction and magnitude,

ξ must be constant for navigation along these lines. *So these straight lines are single-heading trajectories.* But they are also extremals, for the navigation equation of Zermelo is satisfied by

$$\frac{d \tan \xi}{dt} = 0.$$

So the straight lines, which connect the points of inflection of the stream-lines are also single-heading extremals (e_1 and e_2 in fig. IV, 10).

If the generators of the cylinder are parallel to the (x_1, x_2)-plane, the corresponding field of flow will be rectilinear. (fig. IV, 11).

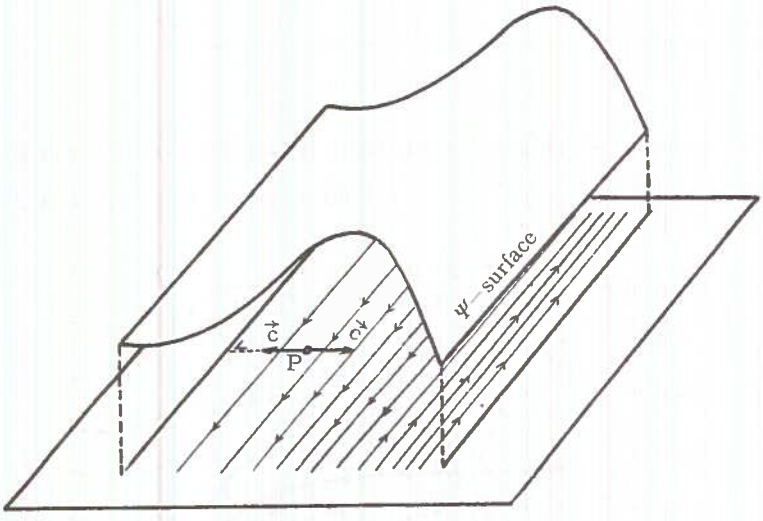

Fig. IV, 11.

The true velocity vectors for the single-heading extremals are again at right angles to the projecting directive plane.

Of the quadratic cylinders only the parabolic cylinder is admissible, because the elliptic and hyperbolic cylinders are not one-valued, since their intersections with a projecting plane consist of *two* straight lines.

In fig. IV, 12 the case of a parabolic cylinder has been sketched with the two single-heading extremals through a point P. In fig. IV, 13 the single-heading extremals have been constucted for a cylinder parallel to the (x_1, x_2)-plane.

If the field of flow also possesses a velocity-potential φ, in other words, if the field possesses a stream-function ψ and velocity-potential φ, the zero-shear lines must be perpendicular to each other. That means that the projecting directive planes also must be perpendicular to each other. Therefore this case can only occur in B (fig. IV, 8).

It may be noted that the uniform rectilinear fields of flow also belong to the

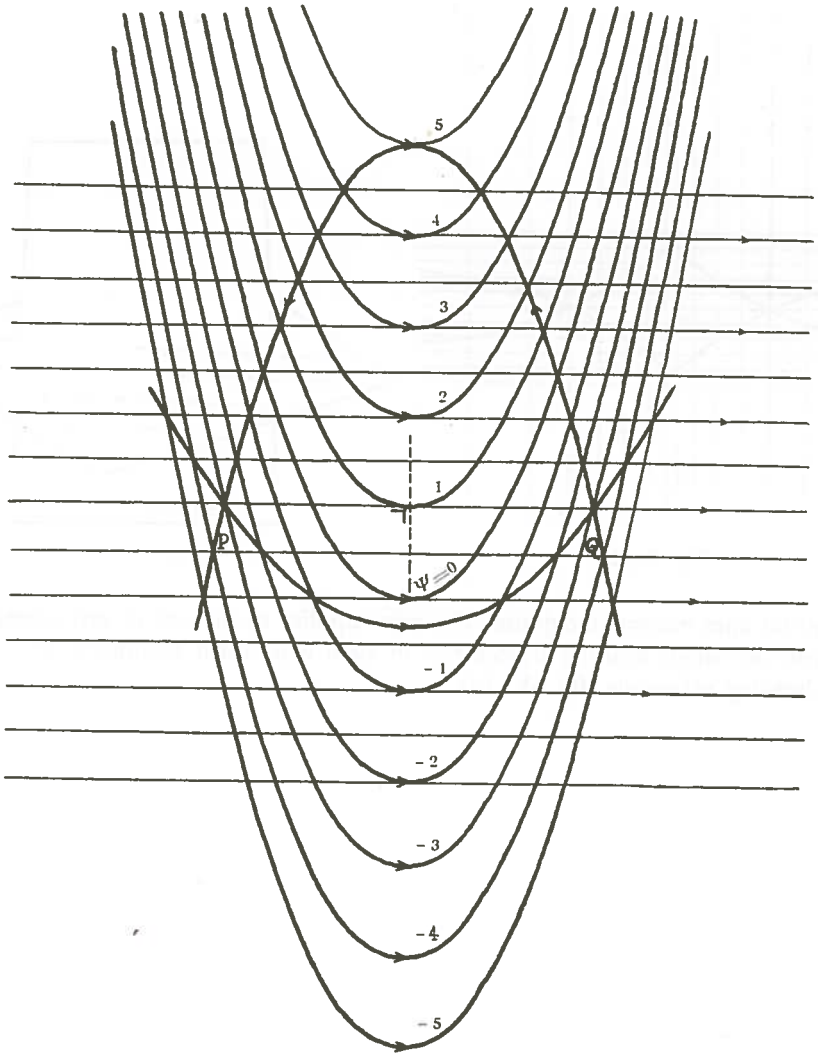

Fig. IV, 12.

category of these fields. The corresponding ψ-surface is a *plane* and all straight lines may be regarded as asymptotic lines. Therefore the sets of projections of

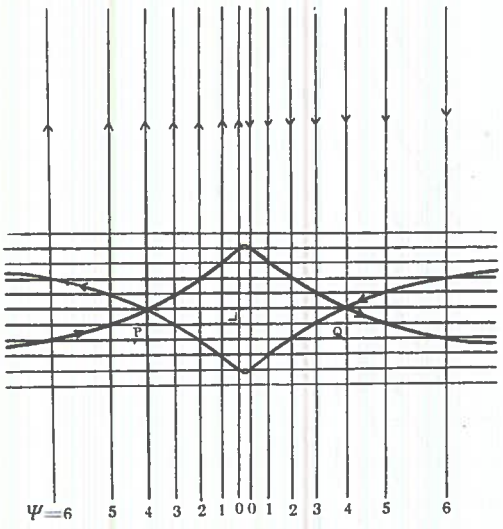

Fig. IV, 13.

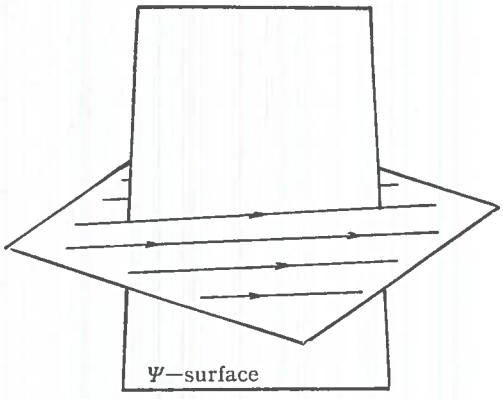

Fig. IV, 14.

asymptotic lines become indefinite. The same applies to the sets of zero-shear lines. Therefore *all* single-heading trajectories in such a uniform rectilinear field will be single-heading extremals (fig. IV, 14).

PART V

APPLICATION IN AVIATION METEOROLOGY

Introduction

In this part special attention is paid to the application of the theoretical considerations given in the four previous parts.

The navigational use of meteorological information in aviation is still continuing to expand. Especially during the last decades practical use of altimetry and pressure pattern techniques have increased the safety and economy of long range flights. The development of these methods is also still in progress. It seems of great value to describe some techniques which enable meteorologists and navigators to improve pre-flight, in-flight and post-flight operational activities.

The theoretical aspects of aeronavigation can be put into use with success if the navigation is not restricted by any operational limitations and if separation of air traffic in horizontal dimensions is allowed. By determining the most suitable flight path it is now possible to improve comfort, safety and economy of most flights. As a consequence *aeronavigation* has been recognized by traffic control authorities as an acceptable reason for deviating flights from direct routes in overland and overseas operations.

1. General

The different techniques involving a more scientifique solution of routes and compilation of the accessary flight plan are derived from the theoretical aspects given in part I, II and III. Some precautions must be taken, however, in interpreting the results. There investigations were based on a *stationary* field of flow in a plane, while the true velocity c, from now on called *true air speed*, was assumed to be constant. In reality the field of flow is non-stationary and it has to be studied on a curved surface, i.e. the geoid. Moreover, the true air speed varies between certain limits dependent on the long range cruising system, the flight level and temperature distribution. The field of flow is represented by means of different types of upper air charts. For instance in aequatorial regions the wind distribution is represented in constant level charts by means of stream-lines and isovels or isotachs. It is generally agreed however to use pressure contour charts in extra-tropical and polar regions. These charts represent the instantaneous conditions on a surface of constant pressure. Their physical properties are properly known: for instance the direction of the windvector $\vec{u}$ is determined as a first approximation by the tangent to the contour lines and the magnitude by the slope of the pressure surface according to the geostrophic windequation:

$$u = \frac{g}{2\omega \sin \varphi} \frac{dz}{dn}$$

where g is the acceleration of gravity, ω is the angular velocity of the rotating earth, φ is the latitude, n the distance normal to the contours and z the geopotential of the pressure surface.

Wind speeds in pressure contour charts may also be given by isotachs.

One of the outstanding advantages of the pressure contour chart is that the flight nearly takes place in a constant pressure surface as the flight level of the aircraft is adjusted with a pressure altimeter.

In practice the pressure contour charts of *selected* constant pressure surfaces are used, for instance the 850, 700, 500, 300 and 200 mb charts corresponding roughly to heights of 1500, 3000, 5500, 9000 and 12000 m. For aeronautical purposes it is often not allowed to neglect the change of the field of flow with time. Since in long range flights 10 to 15 hours of flight time are common, the "fixed time" pressure contour and constant level charts give an erroneous picture of the circumstances along the route. To eliminate partly the errors "composite" pressure contour charts or "composite" constant level charts may be introduced, which give a "continuous" representation of the wind distribution in such a way that the situation in an arbitrary point of the route is nearby the expected situation at the time the aircraft will be at that point. In composite charts the wind distribution is determined by stream-lines and isotachs and if certain conditions are fulfilled the wind can approximately be determined by means of contours and the geostrophic wind-equation. Unless stated otherwise, the techniques to be described however are demonstrated in fixed time pressure contour charts.

I. *Chart projections to be used.*

The projection of the earth's surface on a plane necessarily introduces deformations. Consequently a simultaneous conservation of conformity and equivalence is impossible. Primarily for meteorological and navigational procedures a conservation of angles is necessary (bearing, heading, wind-direction etc.). Moreover it is preferable to maintain the equivalence as well as possible, in other words it is recommended that the scale factor only varies between narrow limits. That is why it is customary to use conformal maps which are almost equivalent, especially in the working areas The best known charts which fulfill these conditions are: for equatorial region the cylindrical Mercator projection, for extra-tropical regions the Lambert conformal conic projection (with standard paralleles at 30 and 60 degrees North) and for polar regions the polar stereographic projection. If a great number of flights is concentrated in a relative narrow band between two stations the most suitable chart to be used is the oblique Mercator projection (Kahn's projection). In order to have a handy chart for the application of the techniques to be described, a scale of chart is recommended between 1 : 10.10^6 and 1 : 15.10^6. In this publication the different construction methods are demonstrated in Lambert conformal charts with standard parallels at 30 and 60 degrees North and scale 1 : 10.10^6.

II. *Grid navigation.*

In 1942 flightlieutenant K.C. Maclure developed the system of grid navigation, which was introduced to avoid the singularity of the longitude-latitude lattice near the north pole. He was able to put the system to test in 1945 during the navigational exploration pole flight with the R.A.F. aircraft "Aries".

Grid navigation is defined as navigation with respect to a set of parallel lines which is superposed on a chart with a given projection. The scale of the chart in the superposed part can be considered constant. This means that the superposition should be carried out on a conformal map which is as equivalent as possible. The parallel lines are called *grid meridians*, one of the meridians, a *standard meridian*, is taken as line of reference in respect to the original chart projection. The orientation of the *grid* is determined by the choice of the standard meridian. For instance the standard meridian can be chosen parallel to one of the edges of the chart. If the chart projection contains straight meridians, for instance the Lambert conic projection or the stereographic projection, the standard meridian can coincide with one of the straight meridians. As an example chart IV shows a grid on the Lambert chart for the North Atlantic region in which the Greenwich meridian is accepted as standard meridian. The direction of the parallel grid meridians determines *grid north.*

Angles are referred to the grid meridians and grid north. For instance the true heading referred to the meridians of the projection chart and true north now changes into *grid heading* referred to the grid meridians and grid north.

The magnetic heading being the sum of true heading in one of the terminalpoints of a segment and variation in the midpoint of a segment becomes the sum of grid heading in one of the terminalpoints of the segment and the *grid variation* or *grivation* in the midpoint of the segment.

Since the grid overlay on a map can be considered as a transformation certain auxiliary lines should be transformed simultaneously. For instance the lines of equal *magnetic variation*, or *isogonals* which are loci of points for which the angle between a geographic meridian and the magnetic meridian is constant, should be transformed into lines of equal angle of grid variation or *isogrivs*, which are loci of points for which the angle between the grid meridian and the magnetic meridian is constant. According to the transformation the grivation in any point is the algebraic sum of the angle of variation and the angle between a grid meridian and a chart meridian, or convergence in that point. In virtue of this property the isogrivs can be found by adding graphically the isogonals and lines of equal convergence (after having normalized both sets of lines properly).

Although originally grid navigation was used for polar regions the system can be introduced with success also elsewhere, mainly because of two reasons:

1) Introduction of a grid considerably simplifies the interpretation of the theory, since it is easy to adjust a rectangular coordinate system to the grid.
2) At a given point of the chart angles can be measured by parallel displacement of a protractor until one of the standard meridians passes the midpoint of the protractor. (See fig. V, 1).

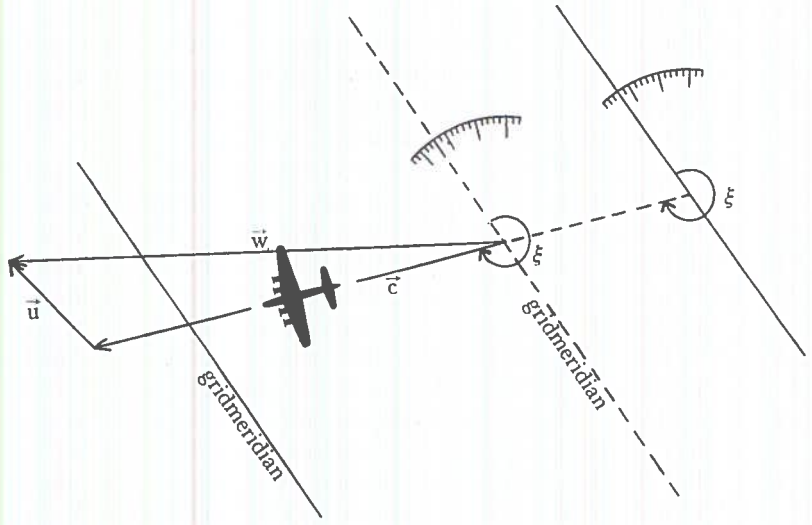

Fig. V, 1.

Moreover it is possible by means of a computor to compile some quantities of a flightplan in conjunction with the construction of any flight track. If the steering agency is a magnetic compass the flightplan for any track will contain elements like grid heading and grivation in stead of true heading and variation.

III. *Construction of special types of pressure pattern trajectories.*

At present pre-flight planning is based on techniques which make use of all kinds of templates in order to compute flight times along various tracks. After having examined a few routes, the most suitable one is selected. However, to find the most favourable route for a given system of navigation, a greater number of routes should be studied and such a task is laborious and time consuming. The construction of the complete figure as described in part I, 6 associated with any system of navigation gives a better survey of the behaviour of such routes.

From the foregoing paragraphs it is evident that the theory developed in part I can be transferred in practice without great deviation from the results stated there, *if the navigational procedures are based on composite analyses or composite prognostic analyses of upper air circulation on charts with a conformal and almost equivalent projection overlaid with a grid.*

If necessary the true air speed is assumed to be constant. The true air speed regularly surpasses the wind speed. Therefore, according to I, 3 the airflow can be considered as an unlimited manoeuvrable field of flow. Moreover it is supposed if not otherwise stated, that the flight altitude is maintained constant throughout the flight. The systems of navigation defined in part I, 5 can be introduced without alterations.

The systems should only refer to the superposed grid of the chart. Systems, such as stream navigation, potential navigation and evolute navigation can easily be realized and under certain conditions be adapted to purely technical navigation systems.

The structure of the airflow is rather complicated and it is well-nigh impossible to express the airflow mathematically. The construction of flight tracks can therefore be carried out only approximately by means of graphical methods of integration. Owing to this limitation any track will be subdivided into a number of segments, for instance segments of equal length, segments of an equal number of degrees and hourly segments.

Consequently each track should be considered as a *multiple* composite track. In practice flights are made along prescribed routes, e.g. great circle, rhumbline, Lindy line and composite tracks with one or two turning points. Sometimes the heading is given as a function of time, for instance in single heading navigation (change of heading with time is equal to zero).

The construction of a trajectory for a given system of navigation as defined in I, 5 can be accomplished by constructing the post-time fronts W associated with the point of departure P and the pre-time fronts W_1 associated with the point of destination Q. The appropriate trajectory through P and Q is a section of the locus of points for which the sum value $W + W_1$ is equal to the sum value $W + W_1$ in point P or, which comes to the same, the sum value $W + W_1$ in point Q.

IV. *The minimum flight path computor.*

As the construction of pressure pattern trajectories by methods described in part I, II and III is laborious without aids, a computor has been designed by F. C. Bik, captain of the K.L.M., Royal Dutch Airlines and the author (14).

This computor enables the navigator to construct the minimum flight path (see part V, 2) and to determine the quantities that form part of the accessory flightplan.

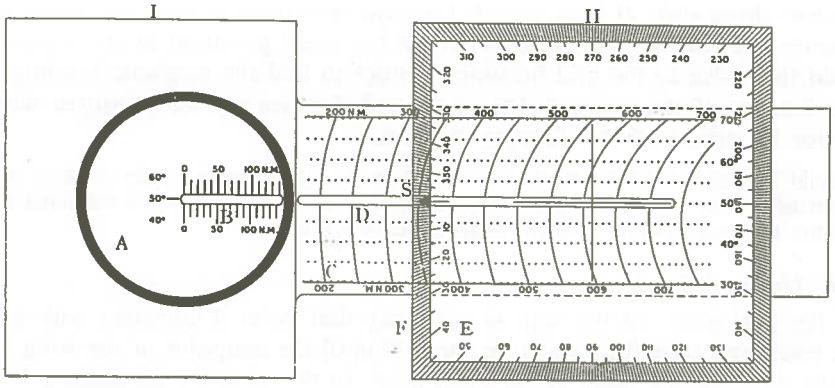

Fig. V, 2.

The computor may also be used successfully however for navigational purposes along other flight paths.

The instrument consists of two parts (I and II) of transparent material (see fig. V, 2). Part I shows a "wind disk" A with a groove B for plotting the wind vector, which can revolve along its periphery. Slide C contains a distance diagram for various chart latitudes based on the scale factor of the projection used. The zero point of the diagram coincides with the centre of the rotating disk. In groove D the true air speed (air distance per hour) can be plotted and ground distances can be measured.

Part II consists of a protractor *E* which can be shifted along slide *C*. The edge *F* of the protractor is perpendicular to slide *D*. The intersection on the distance diagram indicates the true air speed, given in terms of distance per hour along 55 degrees latitude. This distance is projected into groove D (point *S*). The protractor may be turned 180 degrees into slide *C*, dependent on the direction eastbound or westbound as used on the chart. The principle of the computor is based on a subdivision of the track into segments per unit time, for instance hourly segments. The computor can be used mainly for three purposes, notably for constructing the unit time segments, for measuring angles (headings, bearings) and measuring distances. The use of the computor will be described for two cases.

Case A The heading is known.

First adjust the true air speed by shifting protractor *E* along slide *D* in such way that edge *F* indicates the true air speed (air distance per hour) for a given latitude. Next put the protractor on the map until point *S* coincides with a point on the map, in which the heading is defined and until groove *D* points into the direction corresponding to the given heading (fig. V, 3). After that, disk *A* is rotated till groove *B* points into the direction of the mean wind vector along the segment *MS*. In this position the endpoint *P* of the wind vector is plotted. Then *SP* is an hourly segment. In a contour chart the disk is rotated until groove *B* is parallel to a contour line. To measure the magnetic heading: keep the computor exactly in this position and move the protractor along slide *D* until one of the grid meridians crosses the centre of the protractor and read the *grid heading*. Read the mean grivation of the segment *SP* and add this value to the grid heading in order to find the magnetic heading.

The distance of the segment *MS* or ground distance can be measured with the computor by means of the distance diagram.

It should be noted that for instance on a Lambert chart the segments refer to circle elements approximately, whilst the flown segment approximates a rhumbline element; the measured distance is therefore somewhat shorter than the distance actually flown.

Case B The track is known.

Put the protractor on the map in such way that point *S* coincides with a point of the track and turn the computor about *S* until the endpoint of the wind vector coincides with another point of the given track. In this position the heading is determined as described in case A.

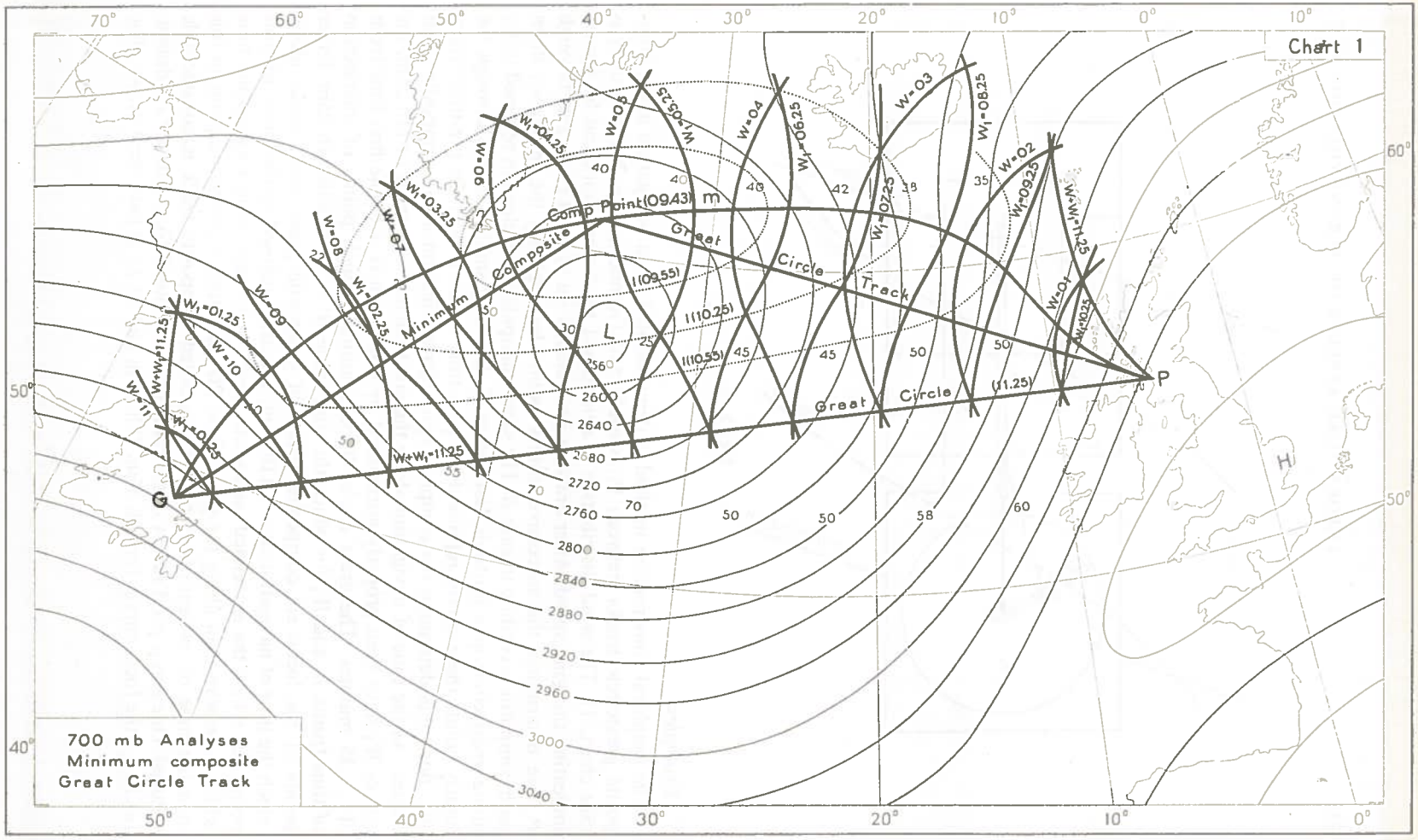
Chart 1
70°
60°
50°
40°
30°
20°
10°
0°
10°
60°
50°
40°
50°
40°
30°
20°
10°
0°
Comp Point(09.43) m
Composite
Great
Circle
Track
Minimum
Great Circle
(11.25)
P
G
L
H
(109.55)
(110.25)
(110.55)
W=.06
W=.07
W=.08
W=.09
W=.1
W=.11
W=.02
W=.03
W=.04
W=.05
W=.01
W=.025
W+W1=11.25
W1=01.25
W1=02.25
W1=03.25
W1=04.25
W1=05.25
W1=06.25
W1=07.25
W1=08.25
W1=09.25
2560
2600
2640
2680
2720
2760
2800
2840
2880
2920
2960
3000
3040
700 mb Analyses
Minimum composite
Great Circle Track

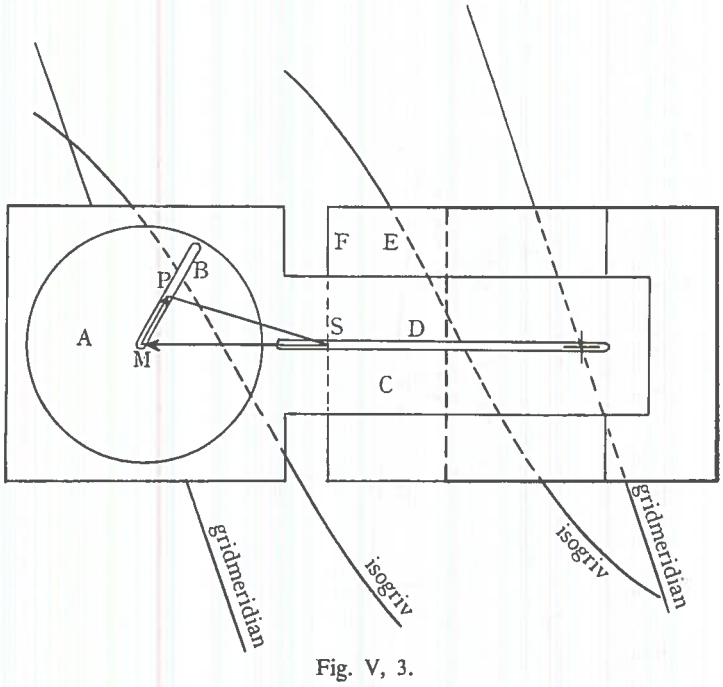

Fig. V, 3.

V. *Examples.*

The graphical construction method is demonstrated for a navigation along composite greatcircle tracks between P(restwick) and G(ander), in a 700 mb analysis (See chart. 1). The wind distribution is determined by the contours and by figures indicating the wind speed. After drawing an arbitrary set of great circle arcs through *P*, one determines the successive hourly points by applying the minimum flight path computor according to case *B*. The same manipulation is done in reversed order along great circle arcs through destination *G*. Drawing smooth curves through the hourly points these curves represent the post-time fronts *W* and the pre-time fronts W_1. Both sets determine the complete figure for navigation along composite great circles. As the time of navigation along the great circle *PG* is equal to 11h 25m, the curves W_1 have been properly normalized by starting in *G* with the first time front $W_1 = 25$ minutes. The great circle *PG* is running through points of intersection of time fronts *W* and W_1 for which the sum value $W + W_1$ equals 11h 25m. Other points of the locus are composite points of composite great circle tracks along which the time of navigation also is 11h 25m. The area enclosed by the locus contains points for which the associated composite great circle tracks yield a navigation time which is *smaller* than along the great circle *PG*. Selecting a composite point in this area the time of navigation along the associated composite track is considerable reduced. One gets a good survey of the times of navigation if focal curves *l* are drawn. In chart I the focal curves for 10h 55m, 10h 25 m and 9h 55 m have been drawn. The

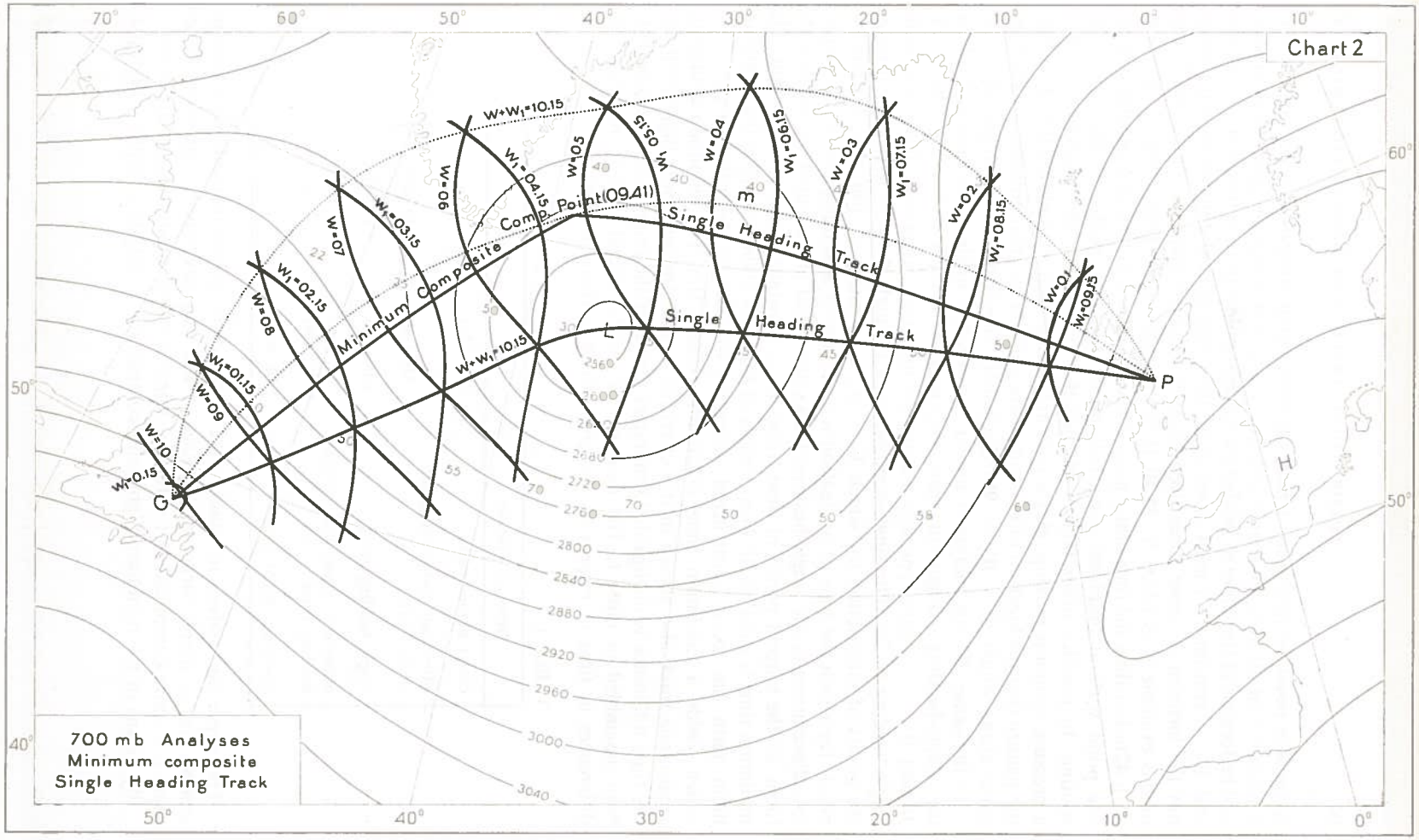
Chart 2
W+W1=10.15
W=06
W1=04.15
W=05
W1=05.15
W=04
W1=06.15
W=03
W1=07.15
W=02
W1=08.15
W=01
W1=09.15
W=07
W1=03.15
W1=02.15
W=08
W1=01.15
W=09
W=10
W1=0.15
Comp. Point(09.41)
Minimum Composite
Single Heading Track
Single Heading Track
W+W1=10.15
G
L
m
P
H
700 mb Analyses
Minimum composite
Single Heading Track

composite point or points for which the time along composite great circle tracks is a relative or absolute minimum (relative to adjacent composite great circle tracks), will be located at the curve m joining the tangent points of time fronts W = constant and W_1 = constant. In most cases more than one critical composite point exists, but the location in some cases needs a more detailed analysis. The critical point in this example is at 61.00 N, 36.50 W with a navigation time of 9h 43 m, which is 1h 42m less than the time along great circle PG. The selection of a suitable composite point without graphical construction methods is a matter of experience and routine. In practice other factors like weather conditions, the direction in which a pressure system is moving, play a part in locating such a point, but it is clear from the picture that the location of the composite point in an area, bounded by the focal curve along which $W + W_1$ = 9h 55m hardly effects the total navigation time.

In the same 700 mb analysis a similar construction method has been carried out for single-heading navigation from Prestwick to Gander (Chart 2). The curves W and W_1 = constant represent a complete figure for navigation along composite single-heading tracks. The single-heading track through P and G is running through the points of intersection for which $W + W_1$ = constant = 10h 15m. The critical points for which the time of navigation is a relative or absolute minimum in respect to adjacent composite single-heading tracks are found at the curve m, which is the locus of the tangent points of time fronts W = constant and W_1 = constant. The minimum time is equal to 9h 41m. Finally in the same 700mb analysis the minimum flight path has been constructed according to methods described in part V, 2, which yields a minimum time of 9h 40m (Chart. III). The minimum composite great circle track also shown in this chart fits in with the minimum flight path and the time difference is negligable (3 minutes). Some of the important time data have been assembled in table I. The figures $\triangle T$ in the second column represent the differences in time in respect to the great circle navigation time.

TABLE I.

Prestwick-Gander	T	ΔT
Great circle track	11h 25m	—
Minimum composite great circle track	9h 43m	1h 42m
single heading track	10h 15m	1h 10m
minimum composite single heading track	9h 41m	1h 44m
minimum flight path	9h 40m	1h 45m

The upper air analysis in which some of the construction methods were demonstrated, has a simple structure because of the well developed depression. When there is a more complicated structure of upper air flow similar results are found.

By means of the minimum flight path computor it is easy to compile a flightplan

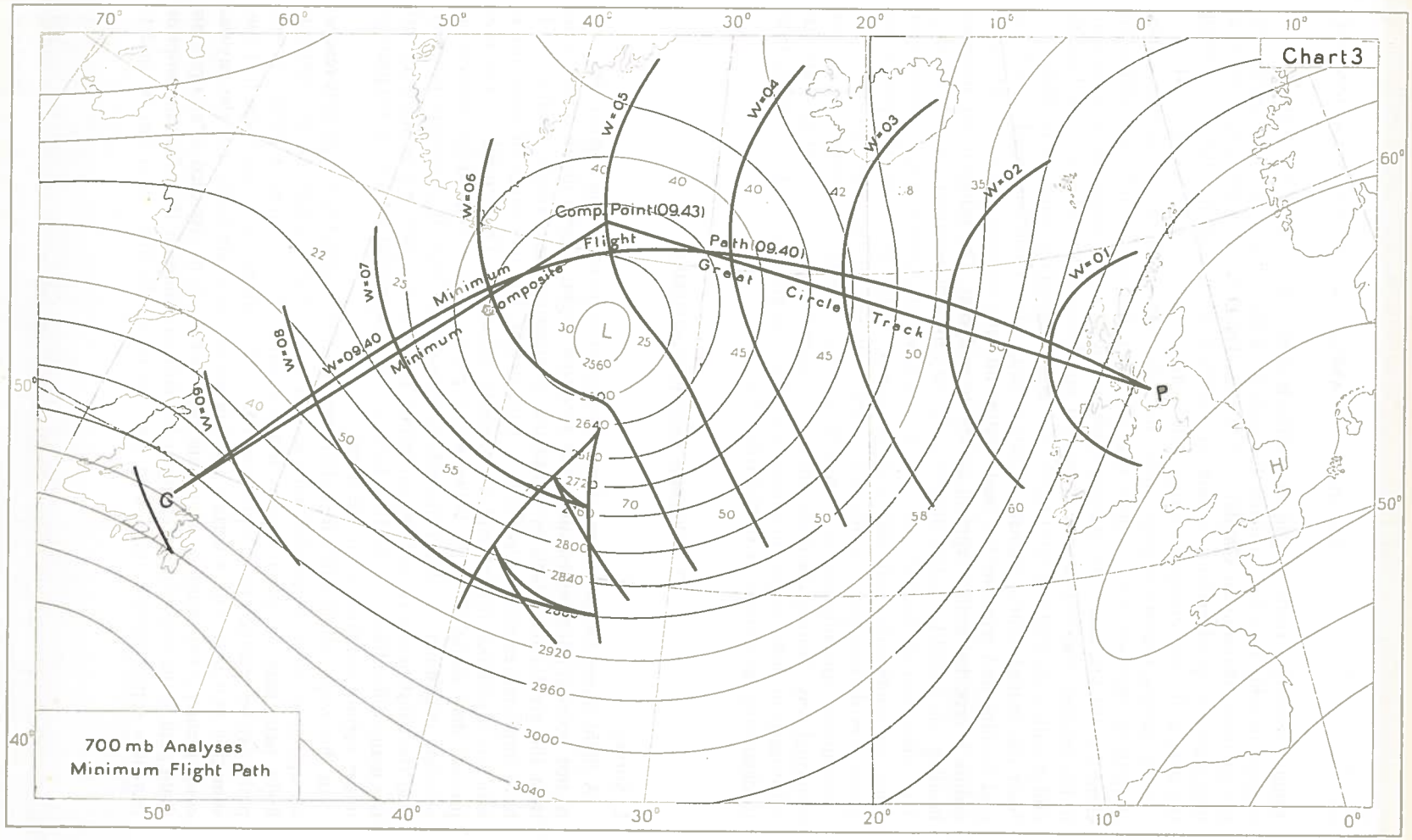
Chart 3
70°
60°
50°
40°
30°
20°
10°
0°
10°
60°
50°
40°
W=09
W=08
W=07
W=06
W=05
W=04
W=03
W=02
W=01
W=09.40
Minimum
Composite
Flight
Path (09.40)
Great
Circle
Track
Comp. Point (09.43)
Minimum
C
P
L
H
2560
2640
2720
2800
2840
2920
2960
3000
3040
700 mb Analyses
Minimum Flight Path

along a *prescribed* route, if grid navigation is used. An example of a flight analysis is given in table II, which contains the data for a flight along the great circle westbound from Shannon to Gander with a Douglas D C 6B, operating a constant indicated air speed cruising system at 10.000 ft flight altitude. Before sampling the data a 700 mb composite prognostic chart is constructed. (See chart 4).

After having drawn the great circle, the minimum flight path computor is used starting in Shannon with a mean true air speed during the first hour (including climb) of 191 kts, read from cruising tables or graphs. After adjusting the computor in the manner described in case B the first hourly segment is plotted, grid heading and grivation are read and substituted into the corresponding column of the flightplan. Next the second hourly segment is determined, using a true air speed of 209 kts, grid heading and grivation are read, written into the columns and so on. This procedure is repeated until a segment covers the endpoint. The values of the magnetic heading are found by adding algebraically the values of grivation and grid heading. The other data of the flightplan like distance, accumulated distance, accumulated time, air temperature, altitude, true air speed, indicated air speed, break horse power, revolutions per minute, brake mean effective power, fuel flow per hour, accumulated consumption, gross weight are inserted into the columns in the conventional way. During the flight the fuel consumed, fuel aboard and gain loss are substituted in order to get an impression of the progress of the flight and in order to determine the deviations of flightplan data.

2. **Minimum flight path navigation**

I. Survey.

A flight along the geometric shortest route, that means along a great circle arc is not necessary the fastest and most economic flight. Flights along other routes than the great circle, such as rhumbline, composite track, single heading track, have improved economic profits to a large extent, but the choice of these routes lean on experience rather than on scientific principles. Theoretically it has been proved that along all paths between two points there is one which provides an absolute maximum benefit. This path is three-dimensional. It is obvious however, that the construction of and the navigation along such a path will as yet meet with too many difficulties. For the time being a two dimensional solution to the problem under certain conditions can be found.

In this respect flight paths are to be constructed along which some quantity reaches an optimum value. Dependent on the final result that is aimed at, the optimum flight path may be given various interpretations. For instance a minimum fuel path may be regarded as an optimum flight path if along such a path the fuel consumption that goes with a certain cruising system, is a minimum, and the payload consequently a maximum. A minimum flight path may be regarded as an optimum flight path, if the time of travel along such a path is a minimum. If the fuel consumption increases approximately linear with time the minimum flight path can be said to

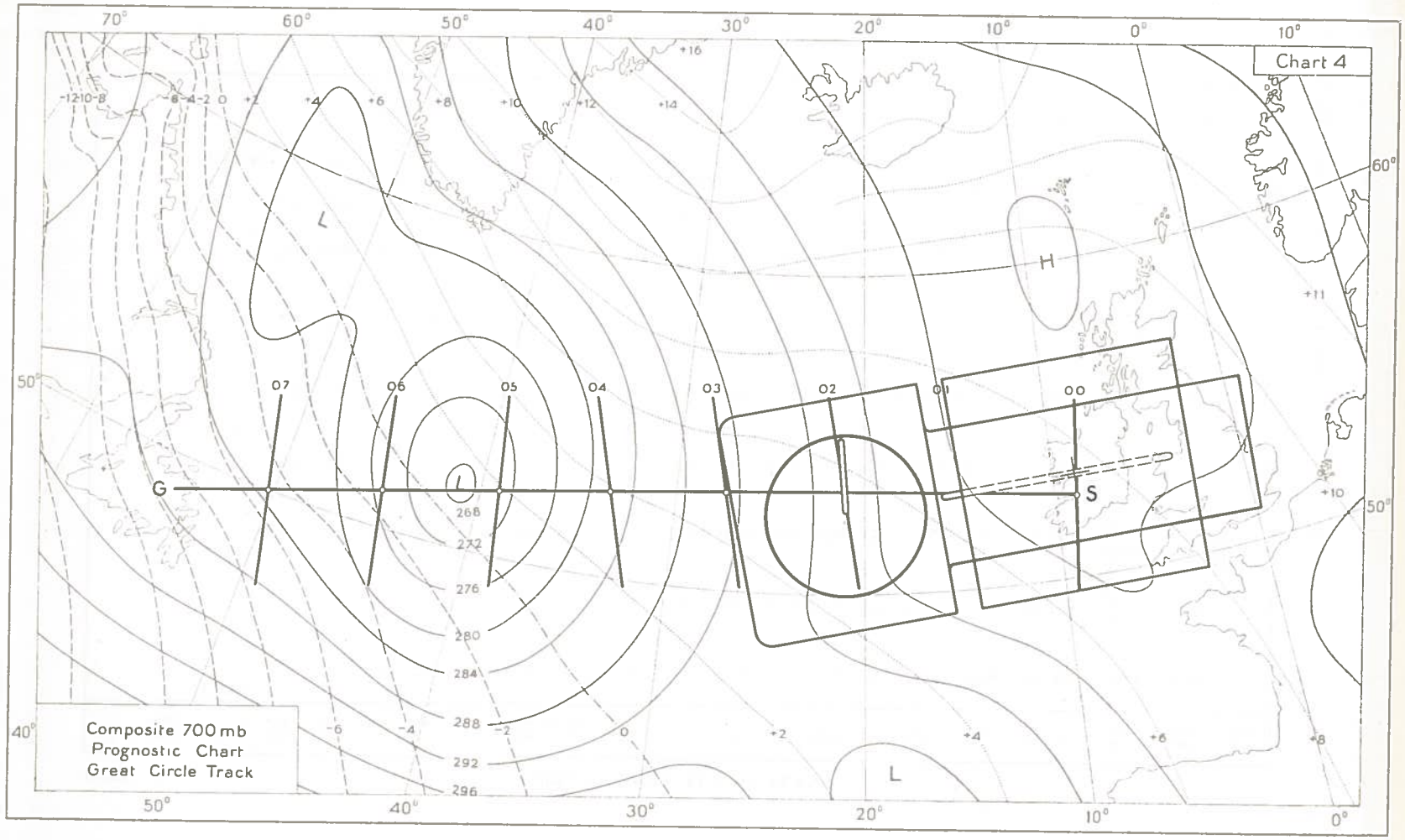
Chart 4
Composite 700 mb
Prognostic Chart
Great Circle Track
G
S
L
H
L
07
06
05
04
03
02
01
00
268
272
276
280
284
288
292
296
70°
60°
50°
40°
30°
20°
10°
0°
10°
60°
50°
40°

TABLE II. GREAT CIRCLE FLIGHT PLAN

GMT	after / behind	from / to	dist. gs	acc. dist.	acc. time	grid head.	griv.	magn. head.	air temp. °C	Alt.	TAS	IAS	BHP	RPM	BMEP	F.Fl/ hr	acc. cons.	gross wt	fuel consd.	fuel aboard	gain / loss
		EINN 1	217	217	01	283	+7	290	— 3	10°	208	First Flying Hour					2700	104.000	2660	30.000	
		1 2	227	444	02	276	+6	282	— 3		224	190	1120	2050	155	2050	4750	101.300	2050 4710	27.340	+40
		2 3	227	671	03	276	+5	281	— 5		224	190	1095	2000	155	1930	6680	99.250	1940 6650	25.290	
		3 4	220	891	04	277	+4	281	— 8		224	190	1070	1950	155	1880	8560	97.320	1890 8540	23.350	+20
		4 5	214	1105	05	278	+3	281	— 8		224	190	1070	1950	155	1880	10440	95.440	1880 10420	21.460	+20
		5 6	222	1327	06	291	0	291	—10		224	190	1045	1900	155	1830	12270	93.560	1810 12230	19.580	+40
		6 7	219	1546	07	293	—3	290	—14		224	190	1045	1900	155	1830	14100	31.730	1810 14040	17.770	+60
		8 CYQX	175 216	175 1721	00.48	293	—7	286	—18		224	190	1025	1850	155	1430	15530	89.900	1450 15490	15.960	+40
					07.48													88.470		14.510	

approximate the minimum fuel path. In this part the minimum flight path will be taken as the primary factor for any economical longe range flight. Up to now a number of construction methods have been published which are very laborious because the use of dividers, slide rules, protractors and so on is involved. The minimum flight path computor puts all these tools into one device and a working method has been developed which enables a rapid and practical construction of the path and compilation of the accessory flightplan.

The theory on which the construction method is based has been described in part III. With reference to this theory an explanation will precede the new method by following the historical development. In 1872 Francis Galton devised an empiric method for the construction of the most favourable route for sailing ships (8). On the principles thereof Giblett, in 1924, based his method for air ships (4). Another interpretation was given by Bessemoulin and Pône in 1949, adding an important feature which made it possible to draw the minimum flight path through the points of departure and of destination (9). All these methods ultimately relate to the concept of time fronts and extremals described in parts III, 5 and III, 6. The time fronts were called "isodic lines" by Galton and "isochrones par sol" by Bessemoulin and Pône. Other methods are developed which refer to the simplified form of the navigation equation of Zermelo III, 9. Two of them, one by J. S. Sawyer (15) and one by I. I. Gringorten (16) make use of the shear term $\frac{\partial u_1}{\partial x_2}$ but in view of the difficulty to measure this term these methods are laborious and cumbersome.

The method described below is an extension of the method of Bessemoulin and Pône. The properties of the extremals of parts III, 5 and III, 6 can be translated for the minimum flight path and can be summarized as follows:

I. *The minimum flight path connects the tangent points of the time fronts $W =$ constant, associated with the starting point P and the complimentary time fronts W_1, associated with the terminal Q, for which the sum of W and W_1 is constant and equal to the sumvalue at P or Q.*

II. *The time of travel along the minimum flight path from P to Q is equal to the value of W in Q or in other words equal to the value of W_1 in P.*

III. *The minimum flight path intersects the time fronts transversally. As a consequence the property holds:*

IIIa. *Along the minimum flight path the heading of the aircraft is perpendicular to the time fronts.*

IV. $$| \text{grad } W | = | \text{grad } W_1 | = \frac{1}{c_e},$$

where the effective true air speed c_e is equal to the sum of the true air speed c and the tail component of the wind.

Essentially the methods of Galton-Giblett and Bessemoulin-Pône can be regarded as contact transformations, since the time fronts are built up successively by drawing certain envelopes, which are generated by points of a previous envelope (fig. V, 4).

II. *The method of Bessemoulin and Pône.*

The time unit is chosen as one hour. The point of departure is P. About point P draw a circle V_1 with radius equal to the true air speed during the first hour (fig. V, 4). From several points on circle V_1 draw the wind displacement vectors $P_1 A_1$, $Q_1 B_1$, $R_1 C_1$ etc. The points $A_1 B_1 C_1$ are then located on the first time front $W = 01$, reached by an aircraft in one hour. Draw circles with a radius equal to the true air speed during the second hour about some points of $W = 01$, for instance $A_1 B_1$ and C_1. These circles are enveloped by a curve V_2. From some points of V_2 the wind displacement vectors for the second hour are plotted, notably $P_2 A_2$, $Q_2 B_2$, $R_2 C_2$ etc. The points $A_2 B_2 C_2$ etc. will be located on a curve $W = 02$, which can

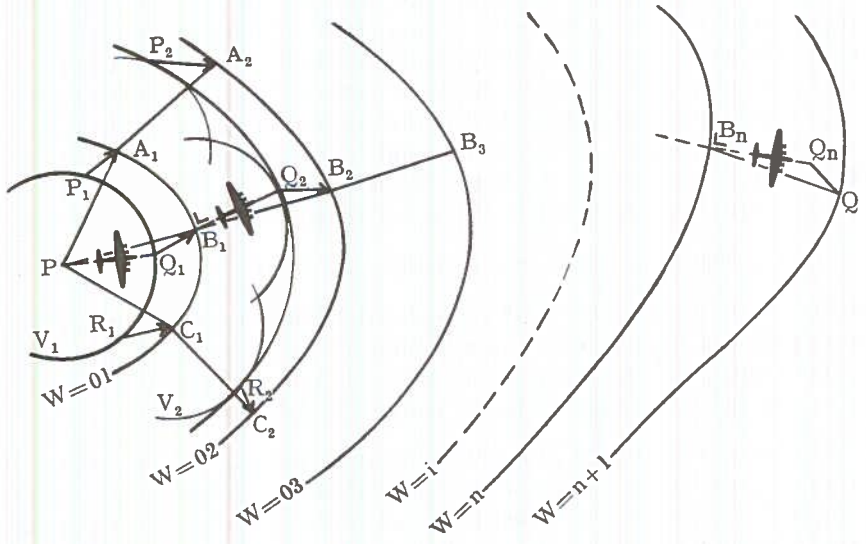

Fig. V, 4.

be reached by the aircraft after the second hour. This process may be repeated as required. For reasons of simplicity the destination Q is located on the time front $W = n + 1$. $PA_1A_2 \ldots A_n$; $PB_1B_2 \ldots B_n$; $PC_1C_2C_3 \ldots C_n$ are flight tracks which approximate minimum flight paths through P. The circles with radius equal to the true air speed of the aircraft are tangent to the envelopes V_1 V_2 etc.; that means that the true air speed vector, or heading of the aircraft is perpendicular to the time fronts $W = 01, 02, 03, \ldots n$. This property was already proved in part III.

In order to find the minimum flight path which is passing the destination Q, the construction is started in point Q by applying the procedure in reversed direction. From Q plot the wind displacement vector in opposite direction QQ_n. Drop from Q_n the perpendicular on time front $W = n$. The foot B_n of this perpendicular is a point of $W = n$ on the required track. Repeat this method to find B_1 on $W = 01$

and until the point of departure P is finally reached. The minimim flight path between P and Q is the track $PB_1B_2B_3 \ldots B_nQ$; the associated true air speed vectors (headings) PQ_1, $B_1\,Q_2$ are perpendicular to the time fronts ($W = 0$) $W = 01$, $W = 02$ etc.

III. *The method of Galton and Giblett.*

This method can be described in a similar way (fig. V, 5). After drawing the indicatrix $W = 01$ (chapter III, 9) for the point of departure P, the indicatrices V_i for several points of $W = 01$ can be drawn. These indicatrices V_i determine an envelope, which is time front $W = 02$. For several points of time front $W = 02$ the process is repeated and so on.

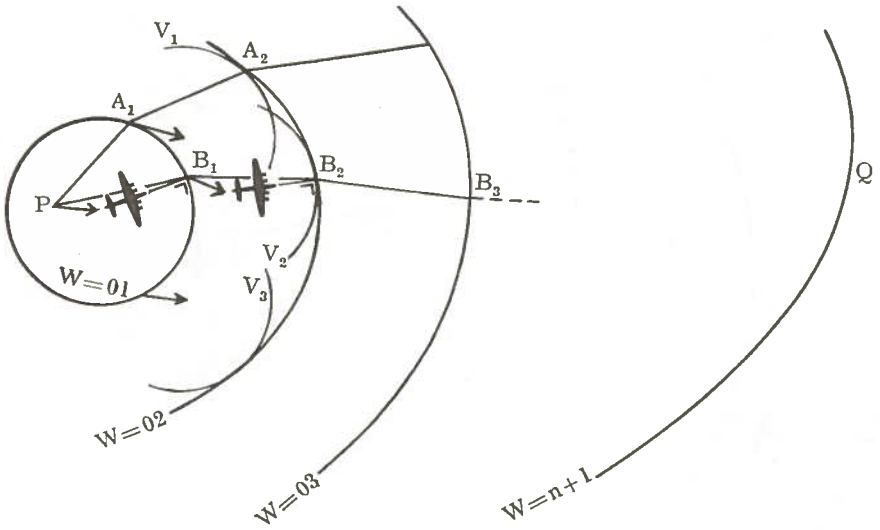

Fig. V, 5.

Both methods described are more or less complimentary. They differ in as much as the heading in the method of Bessemoulin and Pône is perpendicular to the *previous* time fronts and in the method of Galton-Giblett is perpendicular to the *following* time fronts. Taking the limit for the time $\triangle\ W \rightarrow 0$ both methods merge into each other.

It is clear from the properties mentioned in V. 2 I, II, III, IIIa and IV that the construction of time fronts and minimum flight paths can also be performed by not starting the contact transformation from the point of departure but by starting the contact transformation from the point of destination (fig. V, 6). Let Q be the destination and let the time unit again be one hour. Draw about Q a circle V with radius equal to the true air speed. From several points on circle V draw the wind displacement vectors P_1A_n, Q_1B_n and R_1C_n in *opposite* direction. The points $A_n\,B_n\,C_n$ are then located on the first *complementary* time front $W_1 = 01$, on which the aircraft will be before reaching Q in one hour. Next draw the circles with radius equal

to the true air speed about some points of time front $W_1 = 01$, for instance the points $A_n\, B_n$ and C_n. These circles are enveloped by a curve V_1. From any point on V_1 the displacement vectors P_2A_{n-1}, Q_2B_{n-1}, R_2C_{n-1} are plotted in opposite direction. The points A_{n-1}, B_{n-1}, C_{n-1} are then located on the complimentary time front $W_1 = 02$, on which the aircraft will be before reaching destination Q in two hours. This process may be repeated until point of departure P is contained within the set of time fronts $W = 01, 02 \ldots n + 1$. For simplicity P is just located on time front $W_1 = n + 1$. The tracks $QA_n\, A_{n-1} \ldots$, $QB_n\, B_{n-1} \ldots$ $QC_n\, C_{n-1} \ldots$ are flight tracks which approximate minimum flight paths through destination Q. In order to find the minimum flight path through P and Q plot the wind displacement vector

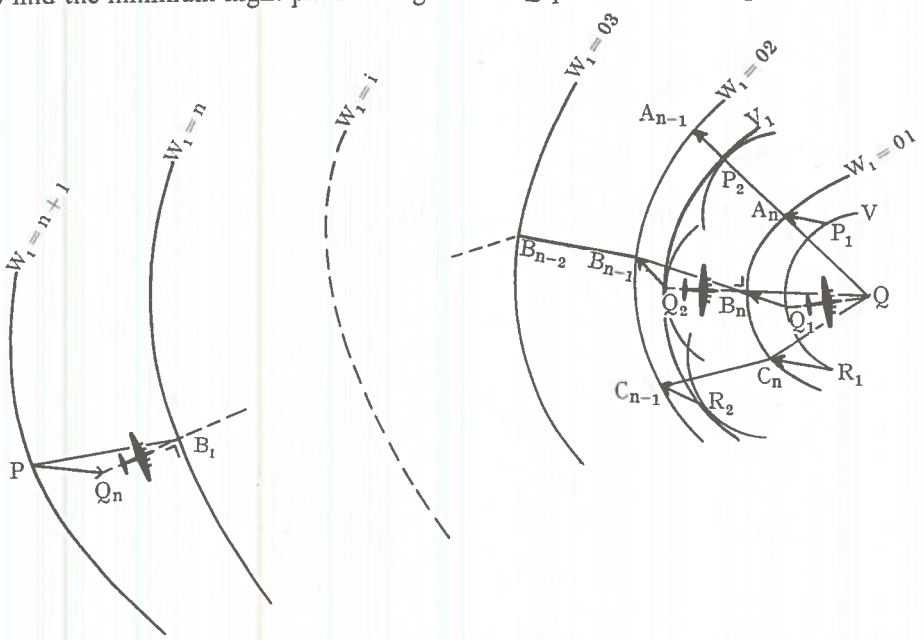

Fig. V, 6.

PQ_n. From Q_n drop the perpendicular on time front $W_1 = n$. The foot B_1 on this time front is a point on the required track. Plot from B_1 again the wind displacement vector B_1Q_{n-1} and drop from Q_{n-1} the perpendicular $Q_{n-1}B_2$ on time front $W_1 = n - 1$ and so on, until point B_n on time front $W_1 = 01$ is found and until finally the point of destination is reached. The track $PB_1B_2 \ldots B_nQ$ is the required track. Again one can observe that the latter method differs from the method of Bessemoulin and Pône inasmuch as the headings along the track are perpendicular to the following time fronts, instead of being perpendicular to the previous time fronts.

Taking the limit for the time unit $\triangle W \to 0$ both methods yield the same minimum flight path. It was shown theoretically that the minimum flight path for $\triangle W \to 0$ connects the tangent points of the time fronts $W =$ constant and the complimentary time fronts $W_1 =$ constant for which $W + W_1$ is equal to $W + W_1$ in P or $W + W_1$

in Q. In figure V, 4, 5 and 6, $W + W_1 = n + 1$ hour. Summarizing there are three important solutions to the problem of finding the minimum flight path through point of departure P and point of destination Q.

1) *By constructing the time fronts W = constant, associated with the point of departure P and plotting the minimum flight path starting from destination Q.*
2) *By constructing the complimentary time fronts W_1 = constant associated with destination Q and plotting the minimum flight path starting from the point of departure P.*
3) *By constructing the time fronts W = constant, associated with point of departure P, the complimentary time fronts W_1 = constant, associated with destination Q and connecting the tangent points of time fronts for which $W + W_1$ is equal to the sum value in P or Q.*

Which of these methods is to be preferred depends on the priority of factors which play a part in pre-flight planning. The first method is suitable to have a good survey of times of navigation along minimum flight paths which are planned from the same point of departure to different places of destination. Such a consideration may be important in respect to the terminal weather conditions. The second method is suitable for having a good survey of times of navigation along minimum flight paths which are planned from different points of departure to the same destination. This procedure is worth while in case a company is operating several longe range flights, for instance transatlantic flights from different aerodromes. The third method can be issued if both factors mentioned above should be studied. Apart from this a detailed analysis is obtained for comparison of the times of navigation along *composite* minimum flight paths by means of focal curves.

Minimum flight path navigation is most suitable for areas where navigation is not restricted by airways etc.

Transoceanic flights lend themselves extremely well to these procedures since the navigation on board an aircraft is mainly expressed in units per hour, preferable from the moment of take-off (ground speed, fuel flow, altimetry, position and weather reports). It is self-evident to design a technique of flight planning which fits in with the hourly time base of the construction and which also fits in with the hourly navigational administration en route (flight log).

The minimum flight path may serve as a flight log, also by plotting the hourly positions in the chart which gives a better impression and a more accurate picture of the progress of the flight (pictural "how goes it"). The collection of data required for flight planning is also simplified by the hourly zones of the flight path. The intended flightplan track is omitted, because the track as given for the determination of the aircraft heading, is no longer of importance. Zonal information as wind direction and wind speed, effective component and wind correction angle are not needed, because these data are inserted in the upper air chart.

It will be clear from this summary that the first method of construction (time fronts associated with the starting point and minimum flight path from destination) should be preferred above the two other methods.

a. *Construction of time fronts* (fig. V, 7).

Read from cruising tables and graphs the true air speed for the first hour, which is a weighed mean value of the air speed during the first hour with climb included. Adjust this value on the computor for the correct latitude and put the computor into the upper air chart in such way, that point S in groove D is located at the starting point P. Rotate wind disk A until groove B coincides

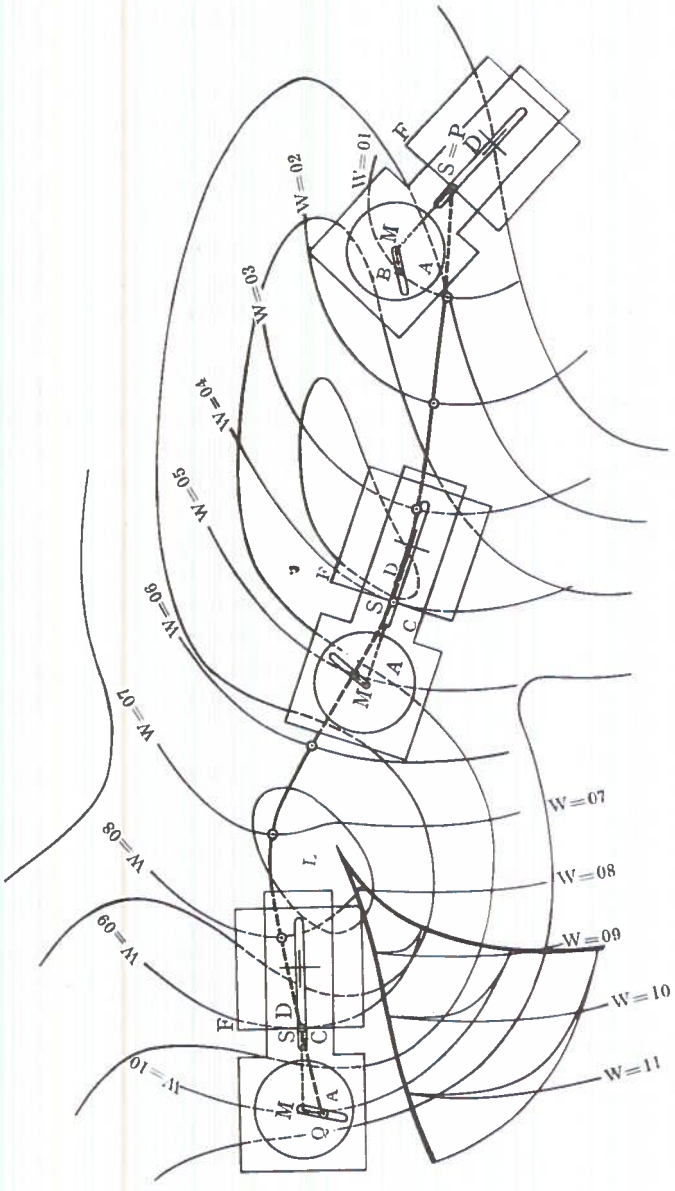

Fig. V, 7.

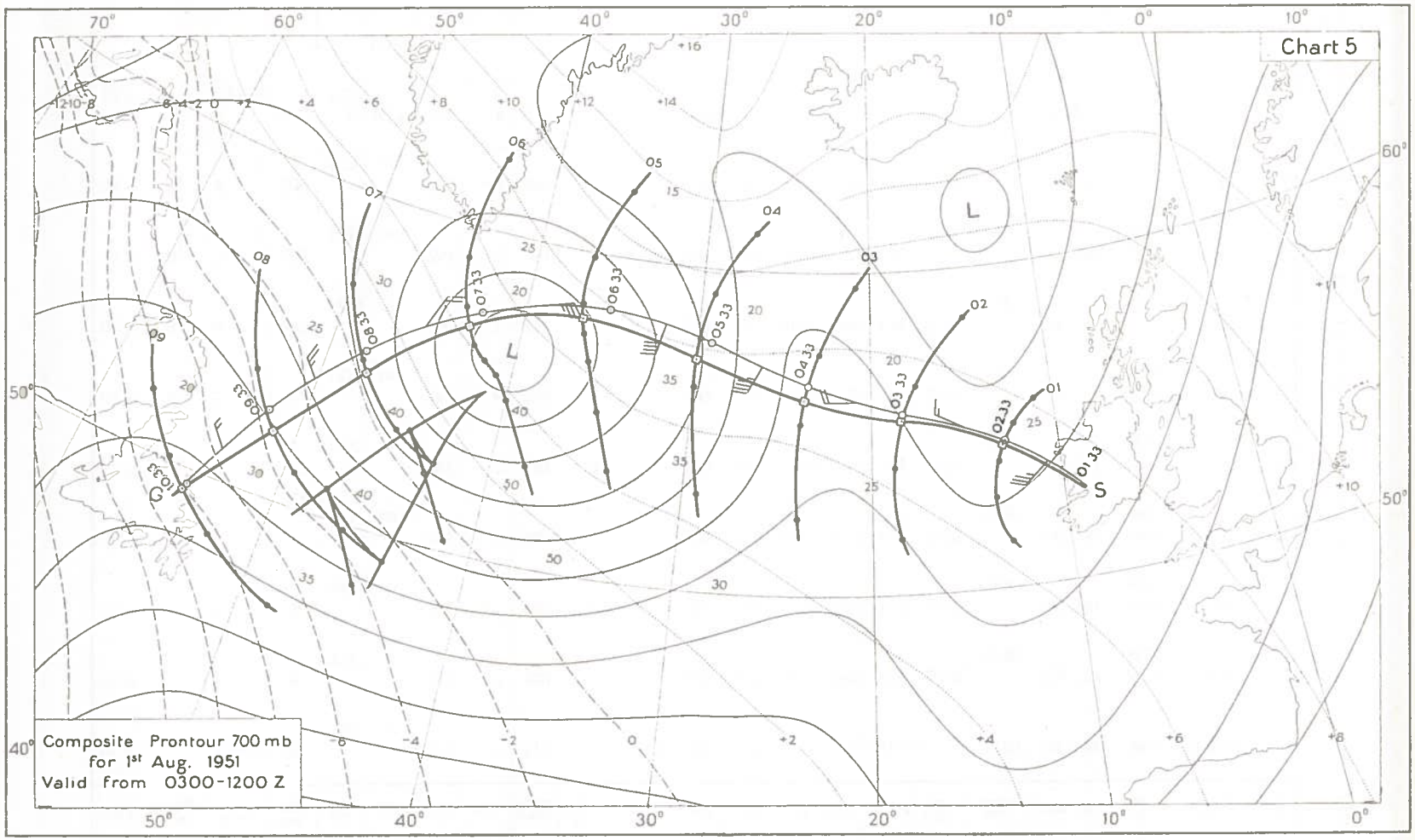
Chart 5
Composite Prontour 700 mb
for 1st Aug. 1951
Valid from 0300-1200 Z
70°
60°
50°
40°
30°
20°
10°
0°
L
L
L
S
01
02
03
04
05
06
07
08
09
01 33
02 33
03 33
04 33
05 33
06 33
07 33
08 33
09 33
10 33

TABLE III. **MINIMUM FLIGHT PATH PLAN**

GMT	ahead / behind	from / to	dist. / gs	acc. dist.	acc. time	grid head	griv.	magn head.	air temp. °C.	Alt.	TAS	IAS	BHP	RPM	BMEP	F.Fl/ hr	acc. cons.	gross wt	fuel consd.	fuel aboard	gain / loss
01.33	—	EINN 1	180	180	01	305	+7	312	—5	10.000	191	First Flying Hour					2630	107.000	2600	24.200	
02.33	—	1 2	191	371	02	302	+7	309	—3		209	205	1155	1900	144	2010	4640	104.370	2020 4620	21.600	+20
03.33	—	2 3	187	558	03	301	+7	308	0		209	205	1130	1875	142	1960	6600	102.360	1980 6600	19.580	
04.33	—	3 4	217	775	04	298	+7	305	0		209	205	1105	1875	140	1920	8520	100.400	1900 8500	17.600	+20
05.33	B_{10}	4 5	227	1002	05	295	+7	302	—2		209	205	1080	1850	138	1870	10390	98.480	1880 10380	15.700	+10
0.633	B_{13}	5 6	215	1217	06	282	+6	288	—4		209	205	1060	1825	137	1840	12230	96.610	1860 12240	13.820	—10
07.33	B_{10}	6 7	207	1424	07	270	+2	272	—5		209	205	1040	1800	136	1810	14040	94.770	1830 14070	11.960	—30
08.33	B_5	7 8	205	1629	08	263	—2	261	—6		209	205	1020	1775	136	1770	15810	92.960	1800 15870	10.130	—60
09.33	B_5	8 9	200	1829	09	262	—6	256	—5		209	205	1005	1775	134	1740	17550	91.190	1760 17630	8.330	—80
10.33 10.36	B_2	9 CYQX	13/200	13 1842	00.03	258	—8	250	—5	↓	209	205				90	17640	89.450	100 17730	6.570	—90
					09.03													89.360		6.470	

with the mean direction of the isohypses for the first hour and plot in this groove the average wind vector.

The wind speed is read in the chart from the figures which indicate these speeds. Turn the computor about point $S = P$ and plot the wind vector again. In this way a number of points is found for the first time front $W = 01$. Next read the true air speed from cruising tables and graphs for the second hour. This speed is a function of cruising system, temperature, height and weight. Adjust the air speed to the computor and shift the computor until S is located somewhere on the time front $W = 01$ and until edge F is tangent to the time front.

In this position rotate again wind disk A and plot the wind vector. Repeat this plotting for a number of points on $W = 01$. The plotted points are then located on time front $W = 02$. This procedure is continued for the successive time fronts $W = 03 \ldots$, until the system of time fronts covers the destination Q.

b. *Plotting the minimum flight path.*

Starting in destination Q plot the average wind displacement vector of the last hourly zone in opposite direction by means of the wind disk A. Move the computor until the plotted point appears in groove D of slide C. Next shift and rotate slide C until the edge F is tangent to the previous time front and plot this tangent point on the chart. The tangent point is a point of the required track. From this point the same manipulation is carried out and repeated until point of departure P is reached. An important element in the method is the possibility to measure the heading simultaneously with the plotting of the minimum flight path.

c. *Determination of grid- and magnetic heading, distances etc.*

Apart from the contourlines the upper air charts also contain grid meridians and isogrivs. If the system of time fronts have been drawn and the plotting of the track is taking place, grid heading, grivation and magnetic heading are determined simultaneously as soon as an hourly segment has been obtained.

After shifting and rotating slide C until edge F is tangent to a previous time front, the computor is kept in this position and the protractor E is moved over slide C until the centre M is located on the grid meridian. Then read from the grid meridian the grid heading and interpolate the grivation in the midpoint of the segment. The sum of grid heading and grivation is the magnetic heading. The ground distances of the hourly segments between the points of intersection of the minimum flight path and time fronts can be measured with the distance diagram of the computor.

If terminal Q is not exactly located on the last time front but between two time fronts, interpolation must be applied. In this case plot a fraction of the wind vector, which fraction is determined by the flight time between Q and the last time front before Q. If for instance Q is located halfway between the time fronts, a displacement equal to half the wind velocity is plotted and the construction is applied accordingly. The setting of the computor remains unchanged for the second and following hours because the change of true air speed at flight altitude is negligible in most cases. Other flightplan data like break horse power, brake mean effective power, revolutions per minute, fuel flow, gross weight etc. are obtained in conventional way by means of the cruising tables and graphs.

Chart 5 gives an example of a flight from Shannon (Ireland) to Gander (New-Foundland) as it was actually performed on August 1st 1951 using a constant indicated air speed cruising system of 205 kts. Table III on the opposite page gives the accessory flightplan data for the minimum flight path. The planned time of departure was set at 01.00 gmt. The composite prognostic 700 mb chart valid from 03.00 until 12.00 gmt shows a deep low at 56.30 N 40.00 W, valid for 09.00 gmt and a second low at 62.00 N 13.00 W, valid for 04.00 gmt. The time front for the first flying hour was constructed with a mean true air speed of 191 kts (temperature at 700 mb —5°C).

The other time fronts were found with a mean true air speed of 209 kts (mean temperature at 700 mb —3° C) at 10.000 feet flight level.

The setting of the true air speed of 209 kts on the minimum flight path computor was taken at 55°N. The minimum flight path was running on top of the low. The pre-computed minimum flight path time is 9h 03m.

The flight time from Shannon to Goosebay should be 9h 15m. The total distance measured is 1842 n.m., which is 126 n.m. longer than the great circle distance Shannon-Gander. The flightplan time along the great circle, which was found by the method described in V. 1. V was 9h 55m, 52 minutes more than the flight time along the minimum flight path. For the air traffic clearance a composite pressure pattern flight was mentioned with turning point at 58.00 N 40.00 W.

The information for air traffic control such as the crossing of 13°, 20°, 30°, 40° and 50° W was found by interpolation between the time fronts and gave respectively 01.00, 02.30, 04.00, 05.30 and 07.35 hrs after take-off. The take-off time was 01.33 gmt. This time was used as the hourly time for position and weather reports. On the chart the actual flight track is shown and the winds aloft, obtained with altimetry and radio means.

The total distance covered was 1890 n.m., 48 n.m. more than the intended track and 174 n.m. more than the great circle distance. The total time from Shannon to Gander range station was 9h 05m, giving a wind component of 0 kts and a time difference with the intended minimum flight path time of 2 minutes.

In spite of the small deviation of the actual track from the intended track the headings of the initial flightplan were sustained in order to apply the rule: "Stick to your headings", except during the last flying hour where a correction angle of 10 degrees was applied, determined by measuring the angle between the actual position of 09h 33m and the *intended* position on the minimum flight path at the same time.

Gander was reached without further corrections. A reanalysis on the actual map showed indeed that the flown track was a very close approximation of the actual minimum flight path (More details are given in (14)).

IV. *Other construction methods.*

It is obvious from the gradient property III, 15 that the construction of time fronts and ultimately of the minimum flight path can be accomplished by using the equation

$$| \text{grad } W | = \frac{1}{c_e}.$$

Let the time unit be again one hour and let $W = i$ be a given time front. The distance between two successive fronts at any point of the line $W = i$ is then equal to the sum of true air speed and tail wind (taking a head wind as a negative tail wind).

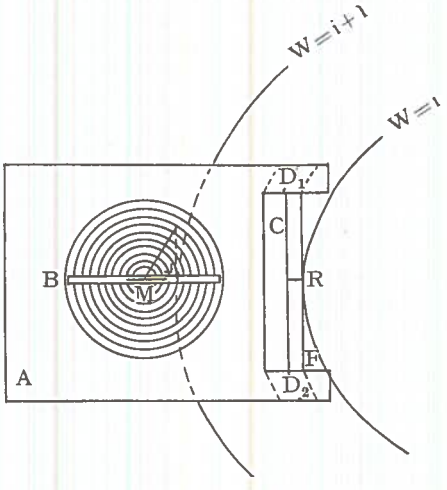

Fig. V, 8.

Therefore a good approximation of the construction of a time front can be achieved if at a given point R of time front $W = i$ a distance is put equal to the sum value mentioned above. In order to accomplish this procedure a template of transparent material can be used consisting of a plate A with groove B and a small bar C, which can move along two slides D_1 and D_2 (fig. V, 8).

On plate A a set of concentric circles is drawn centred about point M which

is also the midpoint of groove B. The radii of the circles correspond to 10, 20, 30 n.m. distances on the chart for a certain mean latitude, dominating the working area. The edge F of bar C is normal to the groove and the distance from the edge to the midpoint indicates the true air speed, which is readable from two distance diagrams on slides D_1 and D_2. Adjusting the template to the true air speed, one places the template on the chart so that the edge is tangent to the time front $W = i$ in a point R. In this position the average wind vector is indicated within the set of concentric circles and a normal is dropped onto groove B. The foot is plotted on the map and this foot is approximately located on time front $W = i + 1$. This procedure is repeated for a number of points R located on the given time front. Since the point of departure P can be considered as a degenerated time front $W = 0$ the construction is also valid there. The construction can be completed by applying the methods described

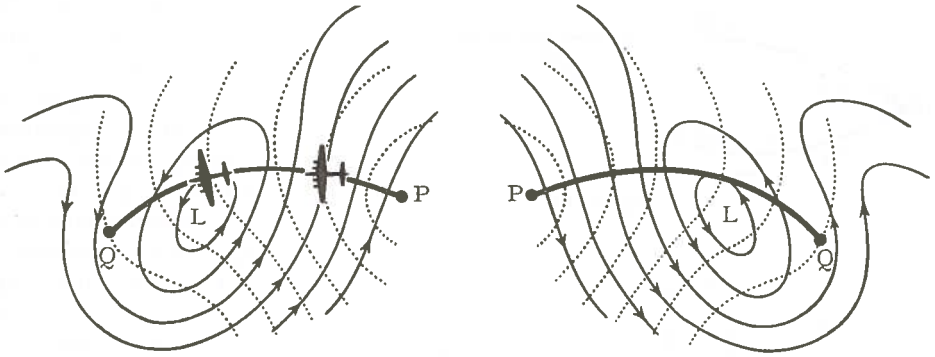

Fig. V, 9.

earlier. This method is suitable for getting qualitatively a good impression of the minimum flight path by means of a simple device.

The construction of the minimum flight path by using the time fronts associated with the point of departure or using complimentary time fronts associated with destination can be interchanged. This is demonstrated in fig. V, 9. The upper air chart is turned upside down on a light table. At the same time the direction of the wind is inverted. That means that for instance a low is interpreted again as a low. In this case the construction of the minimum flight path by using the time fronts associated with the point of departure P is changed into a construction using the complimentary time fronts associated with P and the construction using the complimentory time fronts associated with destination Q is changed into a construction using the time fronts associated with Q. This inversion can be very useful in order to simplify construction techniques.

V. *Time front patterns.*

As was stated in part III the structure of the system of time fronts can be rather

complicated and, like in optics, give rise to refraction, diffraction, reflection and induction of caustics.

This may cause the possibility to find two or more minimum flight paths between two points P and Q. The property of the minimum flight path to yield a minimum flight time in that case must be interpreted in respect to admissable trajectories which run in a *neighbourhood* of the flight path.

Let e_1 and e_2 be two minimum flight paths through P and Q which are not running in *each other's neighbourhood* (fig. V, 10).

Suppose that the *conjugated* points P and $\bar{P}$ are located beyond Q. Then e_1 yields a *relative* minimum flight time T_1 in respect to admissable trajectories which run in the neighbourhood E_1. Similarly e_2 yields a relative minimum flight time T_2 in respect to admissable trajectories running in the neighbourhood E_2. If there are no other minimum flight paths between P and Q, one of them, say e_2 yields an *absolute* minimum flight time, except if Q is lying on a double line m, which is the locus of double points of the system of time fronts associated with P.

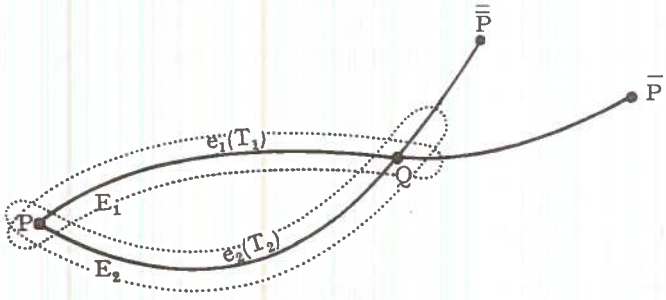

Fig. V, 10.

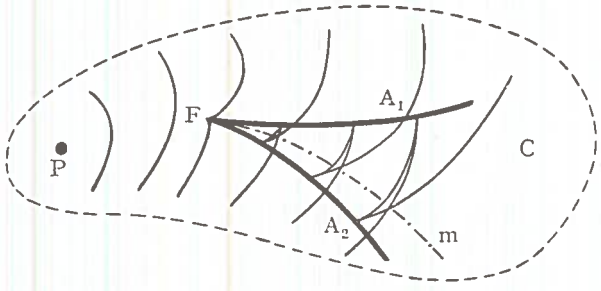

Fig. V, 11.

In that case $T_1 = T_2$, so e_1 and e_2 are equivalent, concerning flight time. Some of the patterns will be studied more in detail.

A. *Induction of a caustic.*

Fig. III, 9 shows the induction of a caustic occuring frequently in practice. The caustic possesses a cusp or focus in point F (see also fig. V, 11).

The picture may be interpreted as the projection onto the $(x_1 ; x_2)$ plane of the regression line and conic point of the integral conoïd W associated with point of departure P in $(W ; x_1 ; x_2)$ phase space. The time front passing through focus F shows a nodal point. The following time fronts possess cusps at the branches A_1 and A_2 of the caustic and double points which are located on the double line m. According to Lindenberg the family of the minimum flight paths through P which

are associated with this pattern of time fronts consists of two groups, each of which form a *field* of minimum flight paths (fig. V, 12). The minimum flight paths of the first group G_1, are tangent to branch A_1. The minimum flight paths of the second group G_2 are tangent to branch A_2. Both groups are separated from each other by the minimum flight path which runs from P to focus F.

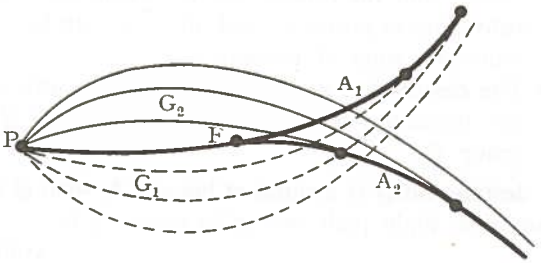

Fig. V, 12.

In upper air charts the time front pattern with caustics often occurs, especially in two cases:

1) *At the rear of a closed vortex associated with a depression or anticyclone.*
2) *In a region with a strong windshear (frontal zone, jetstream).*

Both cases have been demonstrated in fig. V, 13, Fig. V, 13a shows the caustic and focus F at the rear of a "low" L. Fig. V, 13b shows the caustic curve and focus F in a frontal zone with a strong windshear.

Special attention should be paid to the location of point of destination in respect to the time front pattern. For instance in a closed area C (fig. V, 11) one can distinguish four possibilities.

1) destination Q is located at a double line m. There are two equivalent minimum flight paths, one belonging to group G_1 and one belonging to group G_2 which both yield the same time of navigation.
2) Destination Q is located within the sector bounded by the double line m and branch A_1 of the caustic. There are two minimum flight paths, one belonging to

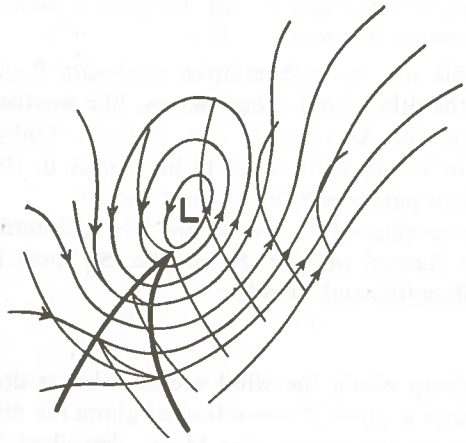

Fig. V, 13,a.

Fig. V, 13,b.

group G_1 and one belonging to group G_2, the second of which yields an absolute minimum time of navigation.

3) Destination Q is located within the sector bounded by the branch A_2 of the caustic and the double line m. Again there are two minimum flight paths, one belonging to group G_1 and one to group G_2, the first of which yields an absolute minimum time of navigation.
4) The destination is located beyond the sector bounded by the caustic. There is *one* minimum flight path through P and Q belonging either to group G_1 or group G_2.

If destination Q is located at branch A_1 then Q is the conjugated point of P on the minimum flight path belonging to group G_1. If Q is located at branch A_2, Q is the conjugated point of P on the minimum flight path belonging to group G_2. If Q coincides with focus F, Q is the conjugated point of P on the minimum flight path between P and F, which belongs neither to group G_1 nor to group G_2.

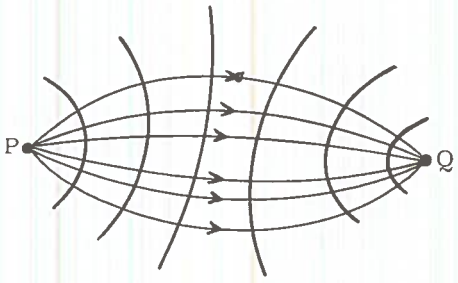

Fig. V, 14.

It is interesting to note that the caustic may degenerate into a point or focus (fig. V, 14). In that case there is an infinite number of minimum flight paths through P and Q each giving the same time of navigation.

The construction of this pattern causes no difficulties in practice. To find a point of the branches A_1 or A_2 the minimum flight path computor is to be moved along the previous time front in such way that the edge F of the protractor is gliding along the front. At the same time one looks at the movement of the midpoint of the wind disk. At the moment that this midpoint comes to a standstill the point which causes a cusp of the next time front has been reached. This point is located at one of the branches of the caustic. The same procedure is repeated for the next time fronts.

If destination Q is located at the double line m both relative minimum flight paths are equivalent concerning time. On the other hand other factors, like weather conditions, may be different along both paths. As soon as two or three double points of m have been found, it is easy to locate destination Q in respect to the pattern and to conclude which minimum flight path yields the greatest benefit.

In chart V, the induction of the caustic takes place at the rear of the "low", situated at 56.30N 40.00W. Destination Gander is located outside the caustic. So there is only one minimum flight path between Shannon and Gander.

B. *Refraction pattern.*

If a line exists in the upper air chart along which the wind vector $\vec{u}$ has a discontinuity the minimum flight paths through a point P are refracted along the discontinuity line. The refraction is governed by the law of von Mises, described in part III, 10. For aircraft flying at a low altitude such a line of discontinuity

exists along the intersection of a frontal surface and a constant pressure surface. A similar line of discontinuity may be introduced if an aircraft for any reason changes from one altitude to another for instance with the purpose to avoid an area of bad weather or to fly over a mountainous area. In such a case the charts should contain two or more analyses, which are separated along a discontinuity line, for instance a 700 and 500 mb analysis, separated along the boundary of a region of bad weather (fig. V, 15).

In order to construct a refracted minimum flight path the concept of the complete figure of time fronts and minimum flight paths again can be introduced. It will be obvious that the time fronts are refracted also along the discontinuity line. In preparing the complete figure graphically no difficulties arise. Chart 6 shows a section of a surface map with a depression some hundred miles west of Scotland moving east slowly. Interpreting this chart as to represent the air circulation just above the friction layer the occlusion may be interpreted to represent the line of discontinuity. The time fronts and minimum flight path have been constructed from point of departure at Schiphol airport to destination Prestwick, valid for a flight at low altitude with a constant true air speed of 100 knots.

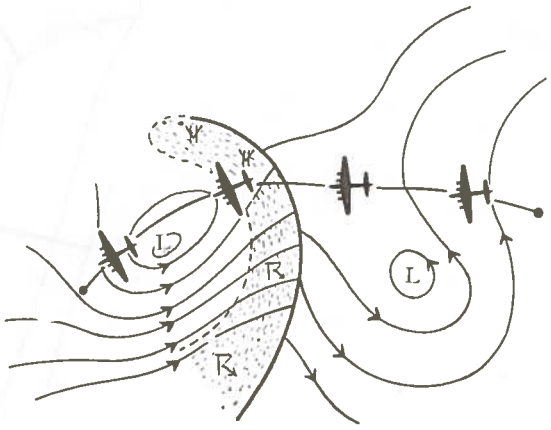

Fig. V, 15.

C. *Diffraction pattern.*

It may occur that in aviation the operations are restricted by mountain ridges, bad weather zônes, forbidden flight regions etc After the region has been delineated the problem arises to find the track along which the time of navigation is a minimum. It was shown in part III, 12, that the minimum flight path now consists of sections of minimum flight paths which are tangent to the boundary of the region and parts of the boundary itself. The pattern of time fronts shows much resemblance to the diffraction of all kind of waves around an obstacle. Fig. V, 16 shows this pattern, with point of departure P, around the convex region B. The minimum flight path e_1 through P is tangent to the boundary g in point R_1. Another minimum flight path e_2 through P is tangent to the boundary g in point R_2. Up to the tangent points R_1 and R_2 the time fronts have been indicated by full lines. After that they have been represented partly by full lines, partly by dotted lines on each side of the minimum flights paths e_1 and e_2. The dotted portions have no real physical meaning. G being the area bounded by e_1 and e_2 and g, an arbitrary point Q, located within G cannot be reached along a member of the family of minimum flight paths associated with P.

Supposing e_1' and e_2' are minimum flight paths through Q which are tangent to

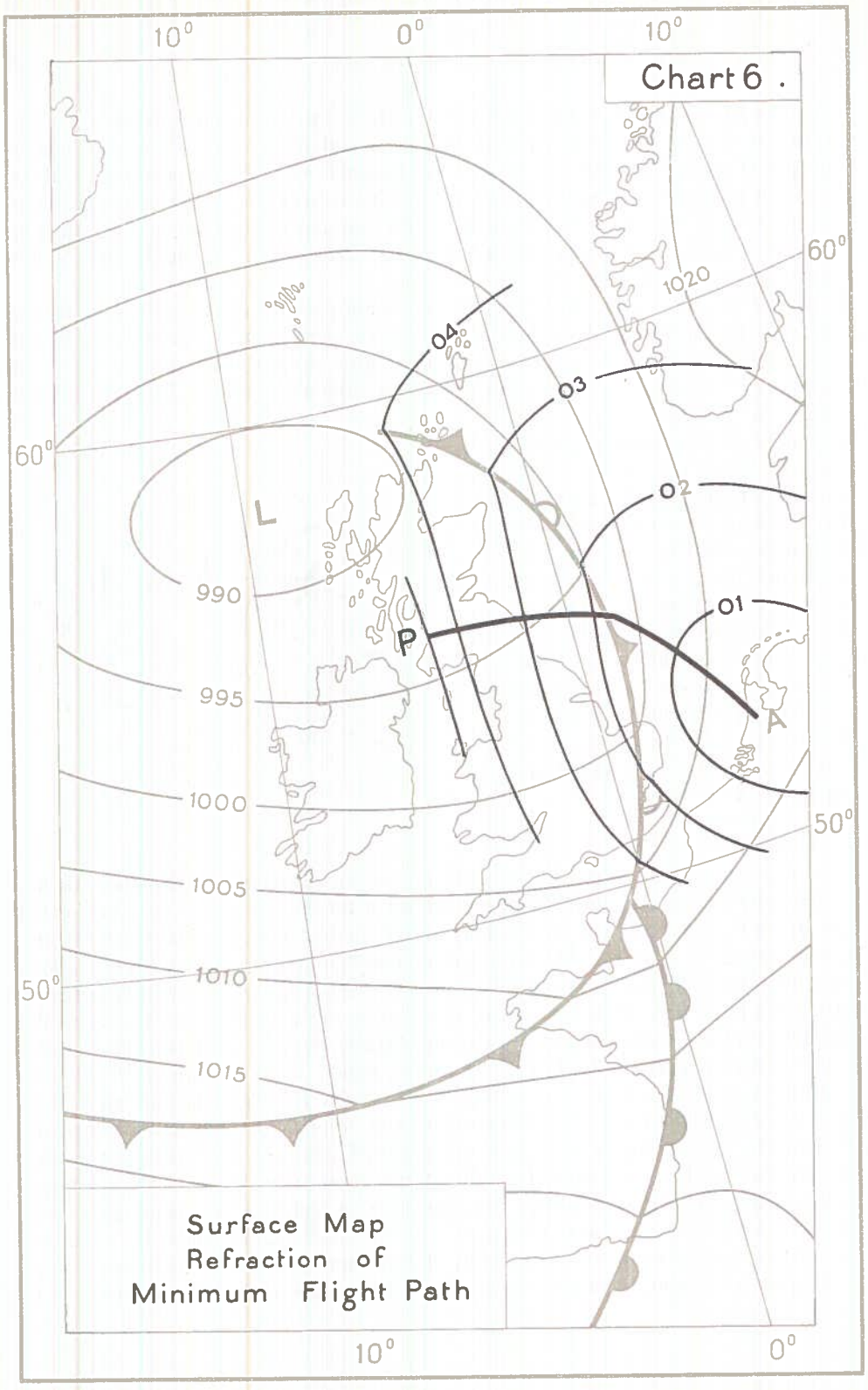
Chart 6 .
10°
0°
10°
60°
60°
50°
50°
10°
0°
1020
04
03
02
01
L
990
995
1000
1005
1010
1015
P
A
Surface Map
Refraction of
Minimum Flight Path

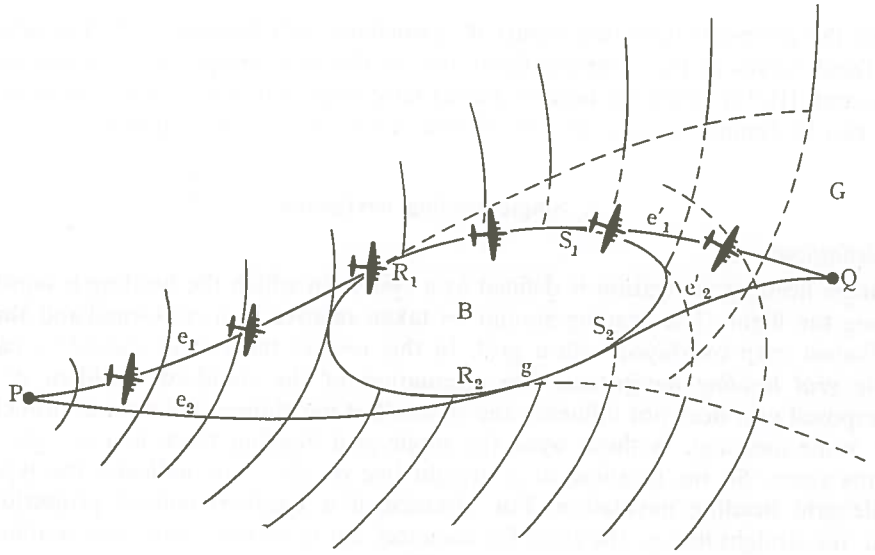

Fig. V, 16.

g in the points S_1 and S_2, one of the minimizing tracks between P and Q consists of the arc PR_1 along e_1, the arc R_1S_1 of the boundary g and the arc S_1Q along e_1'. Another minimizing track consists of the arc PR_2 along e_2, the arc R_2S_2 along g and the arc S_2Q along e_2'.

It should be noted however, that along the arcs R_1S_1 and R_2S_2 along g the boundary condition III of part III, 12 must be fulfilled. This is difficult to test. The diffraction pattern demonstrates that more than one minimum flight path through two given points may occur.

D. *Reflection pattern.*

Supposing that for operational or other reasons the aircraft must call at an arbitrary point on a boundary g, the problem arises along which track between two points the time of navigation is a minimum. The problem bears much resemblance to the reflection of light upon a mirror. As a result of the reflection on g of the minimum flight path (see part III, 11) the time fronts will be reflected as shown in fig. V, 17. The condition for reflection however is rather complicated. Therefore it is easier to construct the time fronts W associated with points of departure

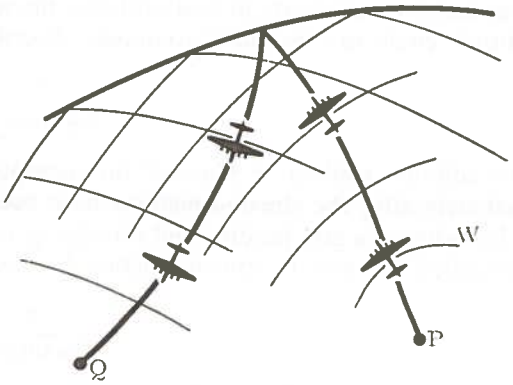

Fig. V, 17.

P and the complimentary time fronts W_1 associated with destination Q. Considering the focal curves of the complete figure one of the focal curves must be tangent to g (see part III, 11). After the tangent points have been determined, the broken extremal can be found by using the set of time fronts W and W_1 separately.

3. Single-heading navigation.

I. *Definitions.*

Single-heading navigation is defined as a system in which the heading is constant during the flight. The heading should be taken relative to a conformal and almost equivalent map overlayed with a grid. In this respect the system should be called *single grid heading navigation.* The orientation of the standard meridian of the superposed grid does not influence the system but the choice of the projection chart has some meaning. Without wind the single grid heading track is a straight line on the chart. So the meaning of a straight line on the chart indicates the type of single grid heading navigation. For instance, if a Lambert conical projection is used, the straight line on the chart for distances not more than 2000 n.m. is approximately coincident with the great circle. The single grid heading navigation then may be called great circle heading navigation. Using a Mercator chart the straight line represents a rhumbline. Then the single grid heading navigation may be called rhumbline heading navigation. In practice the invariant grid heading should be corrected by applying the grivation in order to navigate with a magnetic compass.

Single grid heading navigation necessarily introduces a variable magnetic heading navigation. Flying a constant magnetic heading the single heading navigation is called a *single magnetic heading navigation.*

II. *Construction of single heading tracks.*

In literature different methods have been described in order to construct single heading tracks (2) (17). These methods are based on the formula of Bellamy (see part II, 2). However, the proposed methods are laborious and approximative. Using pressure contour charts in mid latitudes the air current in a narrow strip about a latitude circle can be fairly accurately described by means of the stream-function

$$\psi = \frac{g}{2\omega \sin \varphi_m} z$$

The addition method of Maxwell for superposed vector fields can be applied immediately after the stream-functions have been properly normalized.

Introducing a grid heading and classifying a single heading navigation as a stream navigation the pseudo stream-function becomes:

$$\psi' = \frac{g}{2\omega \sin \varphi_m} z',$$

z' being any auxiliarly height.

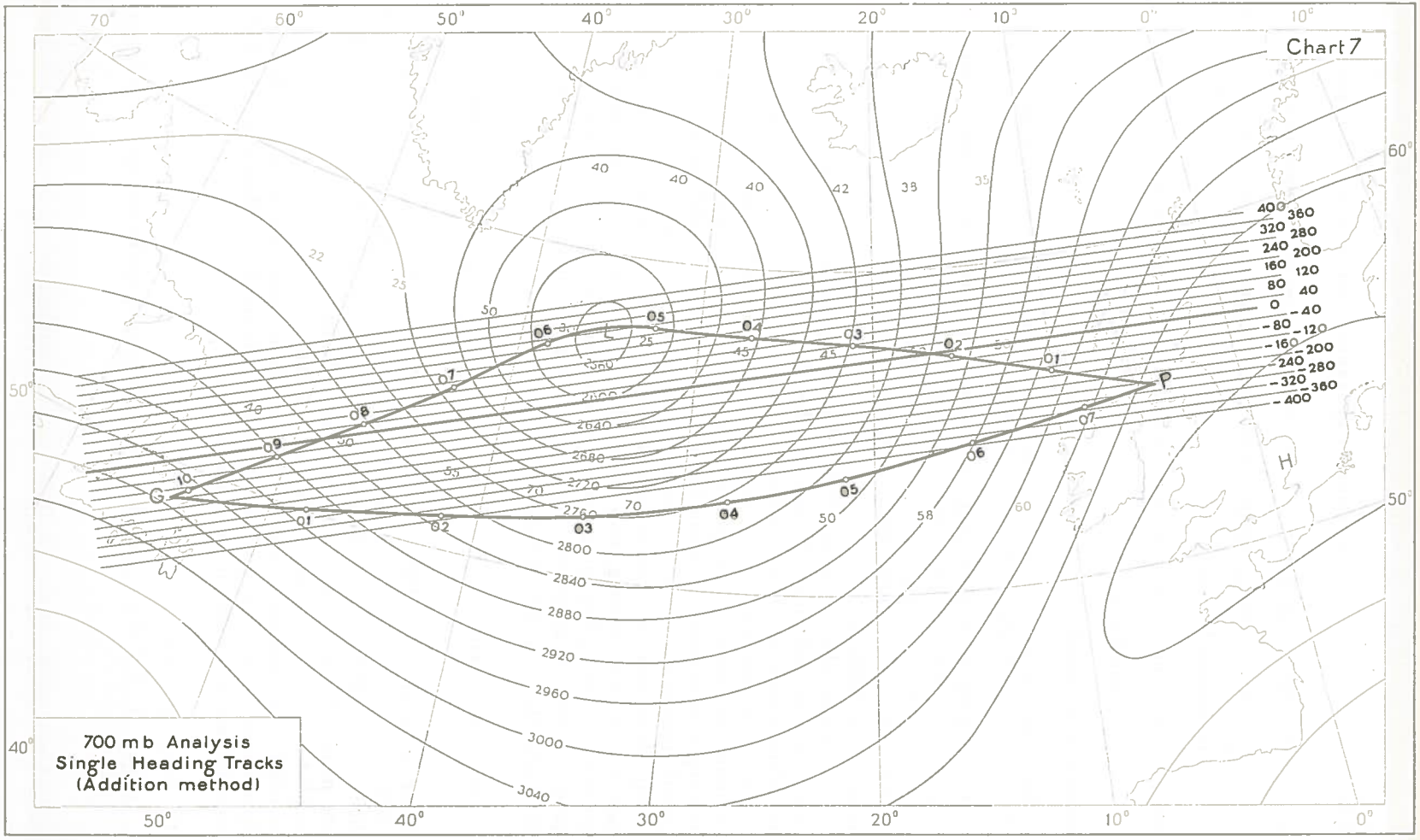
Chart 7
700 mb Analysis
Single Heading Tracks
(Addition method)
70°
60°
50°
40°
30°
20°
10°
0°
L
H
G
P
2560
2600
2640
2680
2720
2760
2800
2840
2880
2920
2960
3000
3040
400 360
320 280
240 200
160 120
80 40
0 -40
-80 -120
-160 -200
-240 -280
-320 -360
-400

c being the true air speed, assumed to be invariant along the track, then approximately $c = \frac{\triangle \psi'}{\triangle n}$, with $\triangle \psi'$ being the increment of the pseudo stream-function ψ' and $\triangle n$ being the distance between two adjacent stream-lines ψ'. Since $\triangle \psi = \frac{-g}{2\omega \sin \varphi_m} \triangle z$, the normalization is expressed by the condition $\triangle \psi' = \triangle \psi$. The distance between two adjacent parallel lines then becomes $\triangle n = \frac{-g}{2\omega \sin \varphi_m} \triangle z$, where $\triangle z$ is the increment of geopotential in the pressure contour chart.

The distance Δn may easily be determined by using a geostrophical wind scale measuring the distance Δn for a fictitious wind velocity of c knots.

After $\triangle n$ has been determined, one draws the parallel lines with mutual distance $\triangle n$ on a transparent sheet of paper and one labels the function ψ' with increment $\triangle \psi' = \triangle \psi$. For different values c of true air speed corresponding sets of equidistant straight lines may be drawn. The construction of the single grid heading track now proceeds as follows:

The auxiliary chart is put on a light table and the pressure contour chart is placed upon the sheet and rotated in such way that the sum value $\psi + \psi'$ in the point of departure is equal to the sum value $\psi + \psi'$ in the point of destination. Both charts being in the right position one to another the single grid heading track can now be drawn by connecting the points of intersection of the ψ and ψ'-lines. The grid heading is determined by measuring the angle between the grid meridians and the parallel lines of the ψ'-field. The method is demonstrated in chart 7 which represents a 700 mb analysis, the same as used in charts 1, 2 and 3. A single grid heading flight has been planned starting from Prestwick with destination Gander, with a true air speed of 200 kts. The corresponding transparent sheet with parallel lines has been prepared with an increment $\triangle \psi' = \triangle \psi = 4$ decametres for $\varphi = 52°$. Select an arbitrary straight ψ'-line passing through Prestwick:

$$\psi = kz = 3090\, k, \quad \psi' = -250\, k, \quad k = \frac{g}{2\omega \sin 52°}, \quad \psi + \psi' = 2840\, k.$$

Since in Gander $\psi = 2990\, k$, the value of ψ' in Gander must be $\psi' = (2840 - 2990\, k = -150\, k$. Therefore the 700 mb chart should be turned until the straight line $\psi' = -150\, k$ is passing through Gander. In this position the curve connecting the points of intersection of contour lines and pseudo stream-lines represents the single-heading track asked for. The single-heading track corresponds with the track in chart 2, constructed by means of the complete figure. The same procedure can be followed for a single grid heading flight from Gander to Prestwick. The construction can be carried out in a few minutes.

III. *Some applications.*

In part II, 2 it was shown that all single heading tracks through the points of

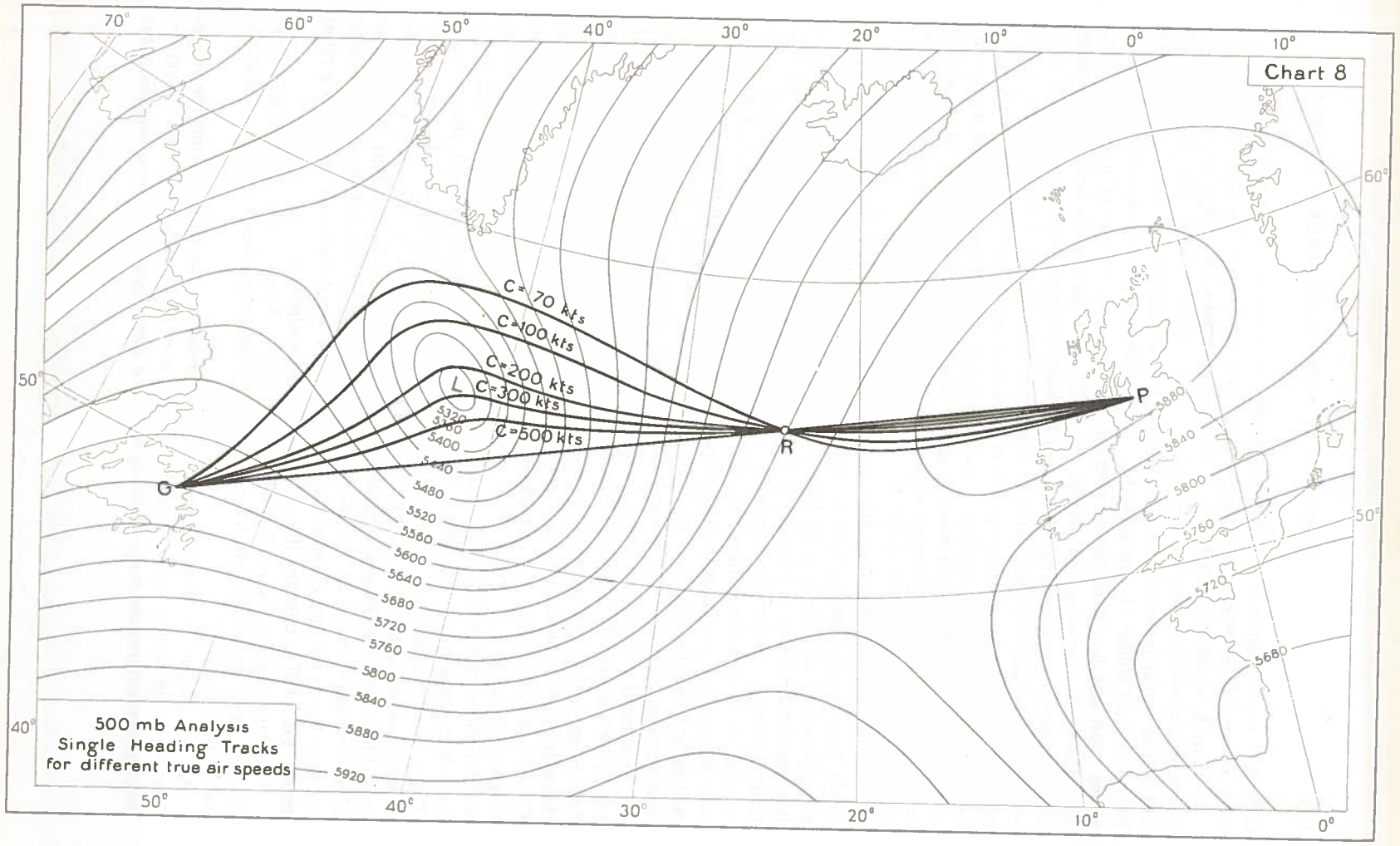
Chart 8
70°
60°
50°
40°
30°
20°
10°
0°
10°
60°
50°
40°
C = 70 kts
C=100 kts
C=200 kts
C=300 kts
C=500 kts
L
G
R
P
5320
5360
5400
5440
5480
5520
5560
5600
5640
5680
5720
5760
5800
5840
5880
5920
5880
5840
5800
5760
5720
5680
500 mb Analysis
Single Heading Tracks
for different true air speeds

departure and destination for different values of the true air speed intersect each other in some fixed points, provided the addition method can be applied.

In chart 8, a 500 mb chart, the single-heading tracks have been constructed by means of the addition method for true air speed values of 500, 300, 200, 100 and 70 kts. The tracks intersect each other in point R, located an the great circle through Prestwick and Gander. The total number of concentration points is according to theory at the most one less than the number of maxima and minima of a contour line, provided such a contour line passes the point of departure als well as the point of destination. In general it can also be stated roughly that the number of concentration points is at the most one less than the number of axes of ridges and troughs, which intersect a straight line through points of departure and of destination. Chart 8 shows two axes which fulfil the condition, one associated with a trough and one associated with a ridge. So in this case there is maximally *one* concentration point. It should be clear that the single heading tracks from Gander to Prestwick eastbound also intersect the concentration point R.

A similar addition method may be applied to find the track associated with a single true heading navigation or rhumbline navigation. Drawing the rhumbline through points of departure and destination, (for instance Prestwick and Gander) this line can be taken as a base line of a set of parallel equidistant rhumblines. The same distance $\triangle n$ for the increment $\triangle \psi'$, as used in great circle navigation, can be used to draw a set of lines "parallel" to the baseline. After the set of lines has been drawn on a transparent sheet of paper the function ψ' with increment $\triangle \psi'$ can be labelled and the addition method can be applied without any difficulty, taking into account, that the navigation behaves like a stream navigation (fig. I, 15). It can be noted that for instance on a Lambert conformal projection with standard parallels at 30° and 60° N, the rhumbline which is used as baseline of the auxiliary field of flow is approximately identical for *east- and westbound flights* with a latitude circle through point of departure. As a matter of fact each latitude circle is a rhumbline. Chart 9 shows another 500 mb contour chart. With a true air speed of 150 kts the single grid heading or great circle navigation tracks and the single true heading or rhumbline navigation tracks both from Prestwick to Gander and vice versa have been constructed by means of the addition method described above. Point R is a concentration point located at the great circle Prestwick Gander. The maximum number of concentration points is again one since there are two axes of troughs and ridges crossing the great circle between both places. By accident there is also a concentration point R_1 for the rhumbline navigation located at the rhumbline through Prestwick and Gander but theoretically it is not necessary that such a point exists, except if a contour line is passing both endpoints.

The figures along the track indicate time marks. From these figures it is evident that the great circle navigation track is in both directions faster than the rhumbline navigation track.

As was stated in part IV some practical rules can be derived from the single-heading navigation in order to study the minimum flight path navigation. In certain circulation patterns the single-heading track is a close approximation of the minimum

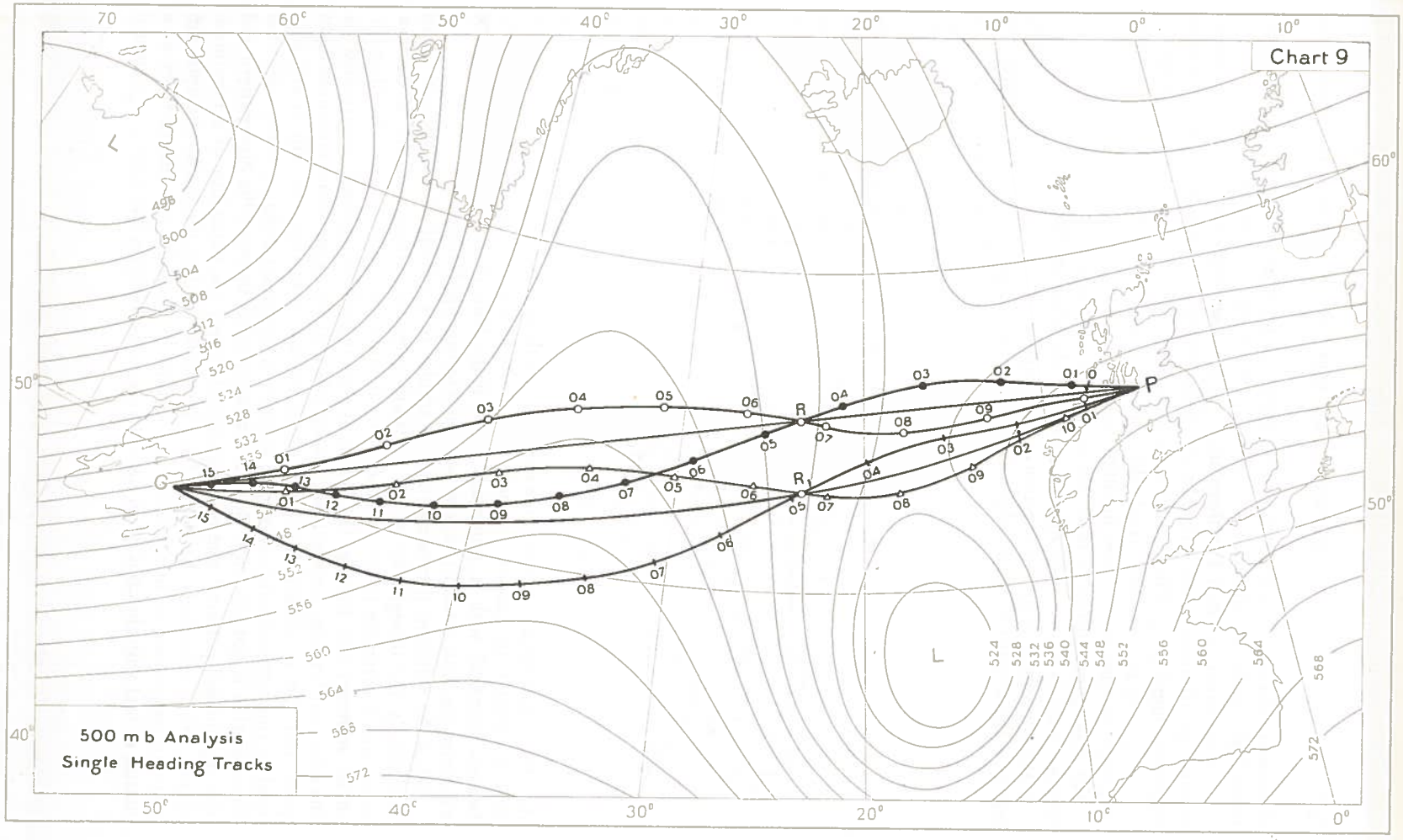
Chart 9
500 m b Analysis
Single Heading Tracks
70
60°
50°
40°
30°
20°
10°
0°
10°
60°
50°
40°
L
L
G
R
R
P
498
500
504
508
512
516
520
524
528
532
536
540
544
548
552
556
560
564
568
572

flight path and even in a few cases each single-heading track is identical with a minimum flight path, for instance in a uniform rectilinear air current.

As was shown in part IV, there are in general *four* single heading tracks passing through an arbitrary point, which have a three pointic contact with a corresponding minimum flight path. These tracks are determined by the optimum headings ξ_1, $\xi_1 + \pi$, ξ_2 and $\xi_2 + \pi$. As a result the following rule may be given for short flight distances, shorter than a few hundred miles:

For short flight distances there are in general four directions in which the single heading track is a very close approximation of the minimum flight path.

If the concept of a stream-function ψ is accepted, these points are found in those parts of the countour chart, where the corresponding points at the ψ-surface are hyperbolic points. In parts of the contour chart where the corresponding points at the ψ-surface are elliptic points, the optimum headings become imaginary and in that case the rule has no significance. In exceptional cases the optimum headings ξ_1 and ξ_2 become equal, the rule then applies to *two* directions only and finally it is possible that in certain points ξ becomes indefinite which means that the rule applies to all directions. It was shown in part IV that in special air currents some selected single-heading tracks at the same time become identical with a minimum flight path. One of these patterns should be examined more in detail in view of some interesting applications.

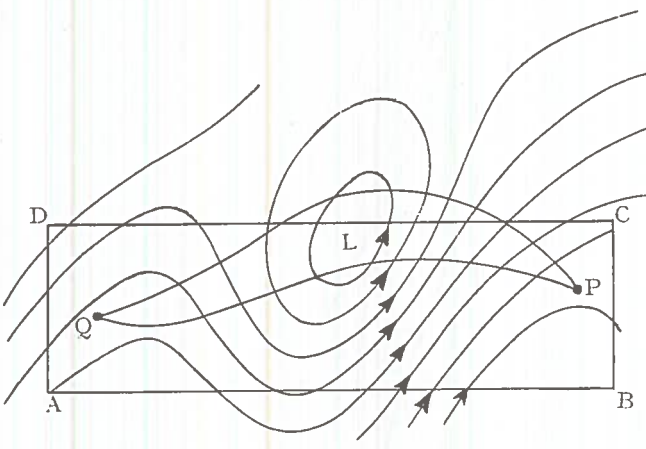

Fig. V, 18.

When the standard pressure surface is similar to a cylindrical surface and when accordingly the topography of the constant pressure surface consists of contour lines, which originate from a contour line by shifting it parallel into the direction of an arbitrary axis (see fig. IV, 10), then the single-heading track, determined by the optimum heading perpendicular to the axis is at the same time a minimum flight path and the single-heading track which deviate from this one, will in any case tend to run approximately along the associated minimum flight path provided that the deviation is not too wide. So if a similarity exists between the flow pattern and the "cylindrical pattern" one can immediately study the behaviour of a mimimum flight path qualitatively by considering the single-heading track with the optimum heading perpendicular to the axis. The airflow in constant pressure surfaces as a matter of fact with the concept of meandering, often behaves like such a "cylindrical

airflow" with axis of troughs and ridges as projections of the cylinder generators. When the structure of the airflow is more complicated, then it is still possible to recognize some areas where the airflow looks like a cylindrical airflow, and the minimum flight paths which run in such areas, still tend to run approximately along the single-heading track. This track is qualitatively easy to identify, for instance by the addition method or roughly by routine only. In figure V, 18 for instance there are two minimum flight paths, one running on top of the low *L*, the other one, which is located in rectangular *ABCD* tends to run along the single heading track, because in this rectangular the airflow looks fairly well like a cylindrical airflow. Such speculations may be very useful in practice to have a qualitative idea of the behaviour of the minimum flight path. After examining the upper air charts in this way it will be understood that the construction of the minimum flight path meets with less difficulty in as much the time fronts need not be drawn over a wide area, and in special cases it may be recommended to fly along the single-heading track, if both tracks hardly deviate from each other.

REFERENCES

(1) Koschmieder, H., Dynamische Meteorologie, 2. Aufl., pp. 191 seq.
(2) Gringorten, I. I. 1948. The theory and computation of single-heading flights. Bull. Amer. Meteor. Soc., pp. 343—351.
(3) Frank, P., 1933. Die schnellste Flugverbindung zwischen zwei punkten, Z. Angew. Math. Mech; **13,** pp. 88—91.
(4) Giblett, M. A., 1924. Notes on meteorology and the navigation of airships, Met. Mag. **59,** p. 1.
(5) Zermelo, E., 1931. Ueber das Navigationsproblem bei ruhender oder veränderlicher windverteilung, Z. Angew. Math. Mech., Vol. **1,** pp. 114—124.
(6) Carathéodory, C., 1935. Variationsrechnung und partielle Differentialgleichungen II Teil, pp. 234—242.
(7) See (6) 298—300 pp. 249—251.
(8) Galton, F., 1866. On the conversion of wind charts into passage charts. Rep. Brit. Association, Nottingham.
(9) Bessemoulin, I., Pône, R. 1949. Determination de routes aeriennes a durée minimum. J. Sci. Meteorologie, **1,** pp. 101—121.
(10) Landé, A. 1928. Optik, Mechanik und Wellenbewegung. Kap. 8 in: Handbuch der Physik XX Band. Berlin.
(11) Kneser, A. 1925. Lehrbuch der Variationsrechnung Vieweg Braunschweig 2. Aufl., pp.157.
(12) See (11) 289—291 pp. 243—245.
(13) Von Mises, R. 1931. Zum Navigationsproblem der Luftfahrt. Z. Angew. Math. Mech., **11** pp. 373.
(14) Bik, F. C., de Jong, H. M. 1953. A report on the theory and application of the Minimum Flight Path. Royal Dutch Airlines, K.L.M. Holland.
(15) Sawyer, J. S., 1949. Theoretical Aspects of pressure pattern flying. Met Reports, Vol. **1,** No. 3. British Air Ministery, Met. off., London.
(16) Gringorten, I. I., 1948. Minimal-flight paths Navigation Vol. **1,** pp. 194—202.
(17) U.S. Air Forces Headquarters Air Warning Service 1953. Meteorological Aspects of Pressure Pattern Flight. Washington.